STUDIES OF SOME MAGNETO-OPTICAL PROPERTIES OF FERROMAGNETIC FILMS

Jennifer Mary Pearce B.Sc.

A thesis submitted to the

University of London

for the degree of Doctor of Philosophy

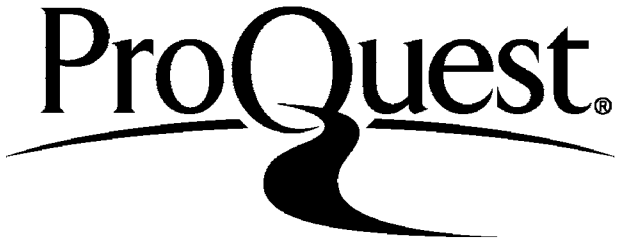

Abstract

This thesis deals with the detection and measurement of the Faraday and Voigt effects in monocrystalline (110) films of ferromagnetic nickel. The Faraday and Voigt rotations were measured as a function of four parameters: applied field, specimen thickness, wavelength and polarization azimuth of the incident light.

Nickel films were grown epitaxially on a monocrystalline copper layer deposited on rock salt. The specimens were selected, using optical and electron microscopy, to be as near as possible to the theoretical ideal of pure, parallel-sided, monocrystalline films. The thickness of each specimen was measured using a multiple beam Fizeau fringe technique.

The magneto-optical rotations were measured using a photo-electric polarimeter, accurate to $\frac{1}{6}'$ of arc, which is described later in the thesis.

The saturation dispersion and azimuthal behaviour of the Faraday and Voigt effects are discussed and compared with available theory.

Acknowledgements

This work was carried out in the Physics Department of Royal Holloway College, University of London, under the supervision of Dr. R. F. Miller whose help, advice and encouragement were invaluable.

I would also like to thank all my friends and colleagues, both at Royal Holloway College and Surrey University, especially:

Mr. R. May for help in specimen preparation.

Mr. G. Hayward for making various pieces of apparatus.

Dr. M. C. Jones for many useful discussions on theoretical aspects of the work.

Miss N. Draper and Miss M. Nicholson for typing the thesis.

The project was supported by the Science Research Council to whom I am indebted for financial support.

Finally, I would like to thank my parents for their continued support and encouragement.

Contents

		Page
Abstract		2
Acknowledgements		3
Contents		4
Introduction		7
CHAPTER 1:	Theory of the Faraday and Voigt effects	9
CHAPTER 2:	History of experimental development	26
CHAPTER 3:	Preparation of the films	37
	3.1 Introduction	37
	3.2 Substrate	37
	3.3 Deposition of the film	38
	(i) Vacuum chamber	38
	(ii) Procedure	40
	3.4 Removal of the film from substrate	42
CHAPTER 4:	Investigation of the films	44
	4.1 Electron microscopy	44
	4.2 The structure of (110) films	51
	4.3 Optical microscopy	58

CHAPTER 5:	The polarimeter		61
	5.1	Introduction	61
	5.2	The principle of the polarimeter	63
	5.3	Experimental arrangement	65
	5.4	Optical components	65
	5.5	The electromagnet	73
	5.6	The photomultiplier	78
	5.7	Electrical system	80
	5.8	Method of measurement	82
CHAPTER 6:	Determination of film thickness		85
	6.1	Introduction	85
	6.2	The multiple beam Fizeau fringe technique	86
	6.3	Measurement of film thickness	88
CHAPTER 7:	Results and discussion		91
	7.1	Introduction	91
	7.2	Faraday rotation in quartz	91
	7.3	Faraday rotation in nickel	92
	7.4	Discussion on dispersion	98
	7.5	Anisotropy of Faraday effect	103
	7.6	Discussion of curves in group A	112
	7.7	Voigt rotation	122

7.8	Voigt effect in quartz	122
7.9	Voigt effect in nickel	123
7.10	Discussion on dispersion of Voigt effect	129
7.11	The Voigt effect in zero applied magnetic field	130
7.12	Final conclusions	135
7.13	Suggestions for further work	138

References 139

Introduction

When a plane polarized electromagnetic wave is incident upon a body in a magnetic field, the reflected and transmitted beams are found to be elliptically polarized. The ellipticity introduced at or near normal incidence is extremely small, so that the transmission case is generally referred to as a rotation of the plane of polarization. When the magnetic field is parallel to the direction of propagation of the wave, this phenomenon is known as the Faraday effect. When the field is perpendicular to the direction of propagation, the phenomenon is called the Voigt effect.

The Faraday rotation was first observed in 1845 but the much smaller Voigt effect was not discovered until much later, in 1898. In spite of the fact that the Faraday effect was discovered over a century ago, there have been very few accurate measurements made on ferromagnetic materials in the visible range of the spectrum. There is no record in the literature of any measurement of Voigt rotation in ferromagnetics at optical frequencies.

The work in this thesis describes the measurements of Faraday and Voigt rotations in monocrystalline nickel films. The first chapter gives an outline of the way in which the theoretical treatment of magneto-optical effects has developed from the purely classical approach, to more sophisticated quantum mechanical

techniques. Chapter 2 gives a review of existing experimental results of Faraday rotation in ferromagnetic films. The preparation and investigation of the specimens to be used are described in Chapters 3 and 4. The experimental arrangement for measuring the Faraday and Voigt rotations of the specimens is explained in Chapter 5. Another variable is involved in calculating the specific rotations of the individual specimens and this is the thickness of the film. This was measured using a multiple beam Fizeau fringe technique which is described in Chapter 6. Finally, in Chapter 7, the results are discussed and compared with available theory.

CHAPTER 1

Theory of the Faraday and Voigt effects

As long ago as 1834, Faraday tried to find a connection between magnetism and light but with no result. In spite of initial failure he continued to believe that there was a relationship to be found and continued his experiments until, finally, in 1845 he discovered that a magnetic field did have an effect on a polarized beam of light passing through a glass block. This effect (the Faraday effect) consisted of a rotation of the plane of polarization of the light when the block of glass was situated between the pole pieces of an excited electromagnet.

He observed that:

1. the rotation was proportional to the length of substance traversed by the light beam;
2. the rotation was proportional to the strength of the magnetic field acting along the direction of propagation;
3. the magneto-optical rotation combined algebraically with any optical activity already present in the substance;
4. the sign of the rotation depended upon the direction of the field.

Faraday performed similar experiments with many more transparent solids and liquids and found that when the effect was present, the above observations held true. He was unable to detect any rotation in gases, but this was later measured by Kundt and Röntgen in 1879.

It was found that most substances produced a positive rotation but the sign of the effect did not depend upon whether a substance was para- or dia-magnetic. Negative diamagnetics are rare, however.

In 1854, Verdet stated a formula to express Faraday's results for the magneto-optic rotation θ_λ, of light of wavelength λ,

$$\theta_\lambda \propto \text{magnetic field intensity } H \times \text{path length } L \text{ in the specimen}$$

$$\text{i.e. } \theta_\lambda = V.H.L. \qquad (1.1)$$

where V is the Verdet constant.

Kundt, in 1884, proved experimentally that, for ferromagnetics, the rotation was proportional to the intensity of magnetization J, as well as the path length L, until saturation was approached,

$$\text{i.e. } \theta_\lambda = K.J.L. \qquad (1.2)$$

The Verdet formula is a particular case of the Kundt equation. K and V are usually expressed in units of minutes/gauss cm.

These formulae described the rotation which resulted from certain physical conditions but they gave no indication of the mechanism causing the rotation.

Fresnel (1825) gave a phenomenological description of optical activity, that is, that rotation of a plane polarized beam arises from a difference between the velocities of right- and left-handed circularly polarized components. Righi (1878) and Becquerel (1879) showed that right- and left-handed circularly polarized light travelled with different velocities in a magnetized medium, and Brace in 1901 showed that plane polarized light could be resolved into two circular components of opposite sense, on entering a magnetized medium.

This gave the relationship

$$\theta_\lambda = \frac{\pi HL}{\lambda}(n'' - n') \qquad (1.3)$$

where n'' and n' are the refractive indices of the medium, for right- and left-handed circularly polarized light respectively. Therefore, the Verdet constant

$$V = \frac{\pi}{\lambda}(n'' - n') \quad . \qquad (1.4)$$

In an attempt to account for the difference between n'' and n', Drude (1912) produced two theories based on different sets of assumptions:

1. 'Molecular currents' were assumed and the centres of the corresponding electronic orbits were supposed to be set into vibration by the light waves passing through the medium. From this theory an expression was obtained which indicated magnetic rotations of opposite sign on either side of an absorption band. This attempt was discarded because of lack of experimental evidence.

2. This theory was based on the Hall effect. It was supposed that quasi-elastically bound electrons were set into vibration by the light waves and that they were then subject to a force arising from a magnetic field, at right angles to the field and their velocity, and equal to $e\ v\ H$ where

   e = charge (e.m.u.)

   v = velocity of electron, and

   H = applied magnetic field (oersteds).

Essentially, the field modifies the frequency of the forced circular vibrations set up by the light waves.

Stoner (1926), using the Larmor precession formula to obtain the modification in frequency, and classical dispersion theory for the refractive index n, obtained similar expressions for V, to those

of Drude. That is

$$n^2 = 1 + \sum_m \frac{N_m \frac{4\pi e^2}{m\omega_m^2}}{1 - \frac{\omega^2}{\omega_m^2}} \qquad (1.5)$$

where $\omega_m = 2\pi\nu_m$ and ν_m = natural frequency corresponding to an absorption line of the set of electrons of which there are N_m per unit volume. This equation only applies to regions sufficiently far from ν_m that absorption can be neglected.

Using equation (1.4) which may be written as

$$V = \frac{2\pi}{\lambda} \delta n \qquad (1.6)$$

since $\delta n = n'' - n = n - n'$, Stoner went on to prove that

$$V = - \frac{\pi e}{m\lambda} \cdot \frac{dn}{d\omega} \qquad (1.7)$$

or

$$V = \frac{e}{2mc} \cdot \lambda \cdot \frac{dn}{d\lambda} \qquad (1.8)$$

where

m = mass of electron

n = refractive index of the medium

$\omega = 2\pi\nu = \frac{2\pi c}{\lambda}$

From this

$$V = -\frac{\pi c}{2ne\lambda^2} \sum_m N_m \left(\frac{\frac{4\pi e^2}{m\omega_m^2}}{1 - \frac{\omega^2}{\omega_m^2}} \right)^2 \qquad (1.9)$$

which is in the form of an equation

$$V = \frac{1}{n} \left(\frac{A}{\lambda^2} + \frac{B_m \lambda^2}{\lambda^2 - \lambda_m^2} \right) \qquad (1.10)$$

with

$$B_m = -N_m \frac{e^3 \lambda_m^4}{2\pi m^2 c^4} \qquad (1.11)$$

Hence the Hall effect theory led to the conclusion that the rotation should be positive increasing to a maximum on either side of an absorption band. It led to formulae which cover the experimental results for a number of substances over a wide range of wavelengths.

This theory is of interest because of the development of the classical theory of dispersion. However, it was inadequate in that it did not account for the negative rotations which were found.

With the introduction of the quantum theory, many new approaches to the problem appeared and were developed. In 1936 Schütz introduced

the general formula

$$V = \frac{1}{s_o} \sum_{ss'} \left\{ \frac{a(s's)\nu^2}{(\overset{o}{\nu}{}^2_{(s's)} - \nu^2)^2} + \frac{b(s's)\nu^2}{(\overset{o}{\nu}{}^2_{(s's)} - \nu^2)} + \frac{c(s's)}{T} \frac{\nu^2}{\overset{o}{\nu}{}^2_{(s's)} - \nu^2} \right\} e^{-\frac{\overset{o}{w}_s}{kT}} \qquad (1.12)$$

where

$$s_o = \sum_s e^{-\frac{\overset{o}{w}_s}{kT}}$$

ν = frequency of incident light

T = absolute temperature

k = Boltzmann's constant

$\overset{o}{\nu}_{(s's)}$ = natural frequency of electron

$a(s's)$, $b(s's)$, $c(s's)$ = constants

$\overset{o}{w}_s$ = energy of state s .

This was developed using the following process:

1. calculation of the electric moment induced in the atom by the electric light vector;
2. insertion of this moment into Maxwell's electromagnetic theory to give the refractive indices.

3. calculation of the effects of absorption in the medium.

The theories mentioned thus far generally accounted for the magnitude and dispersion characteristics of magneto-optic rotations observed in dielectrics and most other non-ferromagnetic materials. They did not adequately describe the magneto-optic behaviour of ferromagnetics, especially with regard to the extremely large Faraday rotations observed.

Early attempts to explain these phenomena consisted of using the work which Becquerel did on the difference between the refractive indices for right- and left-circularly polarized light, under the action of an external magnetic field, together with the assumption that in ferromagnetics there was an effective internal magnetic field of considerably higher order than the external field. In fact, Voigt (1908) found that the effective field necessary to produce the observed rotations was of the order of 10^6 - 10^7 oersteds, that is, the order of magnitude of the so-called Weiss field which was postulated to account for ferromagnetism.

It was impossible to explain the origin of such a strong magnetic field. The effective magnetic field for a charge inside a magnetized medium was, according to Wannier (1947)

$$H + 2\pi (1 + p)J \qquad (1.13)$$

where p = parameter depending on the motion of the electron, varying between 0 and 1. Heisenberg (1928) explained the Weiss field in terms of quantum mechanical forces of interaction, or exchange forces, between the spins of neighbouring electrons responsible for the atomic magnetic moments. Although such an interaction energy could be thought of as an equivalent effective field, as far as the alignment of elementary magnets was concerned, it could not affect the motion of the electrons as an equivalent magnetic field. It is the motion of the charges, giving rise to electrical currents, which affects the optical properties.

The answer to this problem was provided by Hulme (1932) who introduced the spin orbit interaction. This was the energy of interaction of the magnetic moment of an electron $\underset{\sim}{\mu}$ with the magnetic field it experienced as it moved with momentum $\underset{\sim}{p}$ through the electric field $-\underset{\sim}{\nabla}V$ inside the medium, and it had the form

$$\underset{\sim}{\mu} \times \underset{\sim}{\nabla}V \cdot \underset{\sim}{p} \qquad (1.14)$$

Such an interaction provided a relation between the momentum $\underset{\sim}{p}$ and the magnetic moment $\underset{\sim}{\mu}$ of the electron and it was therefore plausible that this might be responsible for the connection between optical and ferromagnetic properties.

Hulme calculated the two indices of refraction using the Heisenberg model of a ferromagnetic, and the Kramers-Heisenberg

dispersion formula. He accounted for the difference between the indices of refraction for right- and left-circularly polarized beams by considering the splitting of the energy eigenvalues due to the spin-orbit interaction. However, he neglected the effect of the spin-orbit interaction on the wave functions. Kittel (1951) showed that this change of wave functions produced a difference in the two indices of refraction of the desired order of magnitude. This was important, since it was shown that in ferromagnetics the orbital angular momentum was quenched and hence there was no splitting of the eigenvalues due to spin-orbit interaction.

Hulme also neglected absorption, thus finding only real indices of refraction. Hence, although the formula agreed with experiment in order of magnitude and (to some extent) dispersion, the sign of the theoretical rotation for iron was negative instead of positive.

The rotation was given by

$$K = \frac{2\pi(n^2 - 1)(n^2 + 2)}{3nc} \frac{\omega h \nu^2}{W^2 - h^2 \nu^2} \cdot \frac{J}{J_\infty} \qquad (1.15)$$

J, J_∞ = magnetization, saturation magnetization

W = excitation energy of an atom or crystal

ω = spin orbit exchange energy at magnetic saturation of the crystal

$W + \omega \frac{J}{J_\infty}$ = excitation energy of an atom in a crystal with regard to the spin-orbit exchange energy for a change of orbital moments by one quantum

n = refractive index.

This formula gave a rotation of $-400{,}000^\circ/cm$ for iron instead of the observed $+300{,}000 - 400{,}000^\circ/cm$.

Darwin (1935) developed a general theory of magneto-optics by assigning to the medium a refractive tensor which took the place of the usual complex index of refraction or the two different complex indices of refraction for light of right- or left-handed circular polarization. This gave

$$\theta_\lambda = \tfrac{1}{2} KL \Re (n'' - n') \qquad (1.16)$$

where $\Re(n'' - n')$ = real part of the difference between the complex refractive indices for right- and left-handed circularly polarized light.

Argyres (1955) also used the idea of a refractive tensor. He included the absorption effects and hence showed that if the extinction coefficient for iron was assumed to be zero, then the Faraday rotation changed sign. Similarly, the Faraday elliptical polarization and Kerr rotation vanished unless there was a difference

between the extinction coefficients of right- and left-circularly polarized light. Argyres used band theory to describe both dispersion and absorption. He considered the effect of spin orbit interaction on the magneto-optical phenomena and calculated the polarizability and conductivity tensors. The coherent scattered radiation was also computed using the semi-classical theory of radiation.

The expression found by Argyres for the Faraday rotation was

$$\theta = \frac{1}{2}\left(\frac{\omega L}{c}\right) \Re(n'' - n') \qquad (1.17)$$

where

ω = angular frequency of the light beam

L = thickness of medium

and

$\Re(n'' - n')$ = real part of the difference between the complex refractive indices for right- and left-circularly polarized light.

Also

$$(n'' - n') = -4\pi\left(\frac{\sigma_1}{\omega} + ij\right)$$

where

σ_1 = polarizability

j = conductivity

n = real index of refraction

k = extinction coefficient

i = $\sqrt{-1}$

He also produced an expression for the polarizability of the form

$$\sigma_1 = -\frac{4ec}{m}\left[\sum_{m>n}\left(\frac{Q_{mn}}{\omega_{mn}^2 - \omega^2}\right)_{av}\right] J \qquad (1.18)$$

where J = magnetization of specimen.

From this equation it could be seen that σ_1 depended on the angular frequency through the expression $(\omega_{mn}^2 - \omega^2)$, therefore it was possible for the calculated Faraday rotation to change sign, which has been observed, below a certain frequency. This will be verified later.

To obtain numerical estimates of the order of magnitude of these effects, it was necessary to approximate the structure of the wave functions and the wave bands. Argyres did this and obtained values which agreed in order of magnitude and in sign with experimental

results for the rotations and ellipticities in magnetically saturated polycrystalline materials at optical frequencies.

The theory which was used in the previous work took only partial account of the boundaries of the magnetic film, i.e. the Faraday rotation for a distance L in an infinite magnetic material. D. O. Smith (1964) produced an expression comparable with equation (1.17)

$$\theta = \tfrac{1}{2}\,\delta(p + q)$$

where δ = phase shift through the distance L and p and q were the complex off-diagonal elements of the skew symmetric dielectric and skew symmetric permeability tensors, respectively. He then added boundary conditions and calculated that for light travelling from medium j through the magnetic film and into medium k

$$\theta = \frac{\delta}{(a_+ - ib_+\delta)}\left(mp - \frac{m_j m_k}{m}\,q\right)$$

where

$$a_+ = m_j + m_k$$

$$b_+ = \frac{m_j m_k}{m} + m$$

$\delta \ll \tfrac{1}{2}\pi$ phase shift through the film

and

m = wave impedances in various media

The impedance of a polarized plane wave in a stratified medium is defined at any point as the ratio of the tangential component of the field vectors at that point. The reciprocal impedance or admittance is the index of refraction in a bounded medium.

Donovan and Medcalf (1964) extended the quantum mechanical theory of interband magneto-optical phenomena in ferromagnetics first developed by Argyres. A theory was developed which could be applied to the anisotropic manifestations of the Faraday effect in ferromagnetic materials with cubic symmetry. The perturbation calculation of Argyres was carried out to the second order in spin orbit coupling. It was found that for propagation in face-centred cubic crystals along the [100] and [111] directions, the Faraday rotation should be the same. However, Heavens and Miller (1962) found values of 7.9×10^4 for [100] and 9.7×10^4 deg. cm^{-1} for [111] in monocrystalline nickel using $\lambda = 5460$ Å .

For other directions of propagation, the Faraday rotation was predicted to be dependent on the orientation of the initial plane of polarization with respect to the crystal axes. The effect should be most pronounced for propagation along [110] type directions, and Medcalf (1965) obtained an expression for the Faraday rotation of the form

$$\theta_F = \tfrac{1}{2} \bar{\beta} z_o (1 + 0.05 \beta_3 \sin 2\phi) \qquad (1.19)$$

where

z_o = specimen thickness ($\ll 2 \times 10^{-4}$ cm)

ϕ = angle between the incident electric vector and a cubic axis

$\bar{\beta}$ = numerical constant having an approximate value of 3.1×10^3 cm^{-1} (Miller and Heavens (1962)).

This equation represented a sinusoidal variation about the isotropic value as a mean, with an amplitude of 5% and stationary values at $\phi = \pm \pi/4$ and $\phi = \pm 3\pi/4$. Which sign is to be associated with the maximum value, and which with the minimum is unknown, since the sign of the parameters is arbitrary; but it is clear that maximum and minimum will be interchanged by reversing the field direction (which is indicated by the sign of the direction cosine $\beta_3 = \pm 1$).

Voigt Orientation

Medcalf also produced an expression for the Voigt effect using the same procedure as for the Faraday rotation with different boundary conditions. The Voigt orientation is characterized by propagation at right angles to the magnetization vector in the specimen.

The expression was of the form

$$\theta = \tfrac{1}{2} \bar{\alpha} z_o (f_1 \sin 2\phi - f_2 \cos 2\phi) \qquad (1.20)$$

where

ϕ = angle between the direction of the magnetization and the direction of polarization of the incident wave

f_1 and f_2 = real functions dependent on the crystal orientation

z_o = specimen thickness

$\bar{\alpha} \simeq 3.3 \times 10^2 \text{ cm}^{-1}$.

Medcalf gave a maximum value for the rotation of the transmitted wave, putting in a value for $\bar{\alpha}$, of 5000^{o}cm^{-1} . This occurred when the propagation and the magnetic field directions were both along <110>-type crystal directions.

CHAPTER 2

History of experimental development

In 1881, Hall made an attempt to measure the Faraday rotation in ferromagnetic films, using nickel sputtered in a hydrogen atmosphere. No rotation was detected, probably because his films were paramagnetic nickel hydride. The first successful measurement of the Faraday rotation in ferromagnetics was made by Kundt in 1884, on films of electrolytically deposited iron and cobalt, and the following relation characterized the results

$$\theta_\lambda = K.L.J. \qquad (2.1)$$

as shown in equation (1.2).

In 1887, Du Bois confirmed Kundt's results with his measurements on iron, cobalt and nickel films.

The first dispersion curves for ferromagnetics were produced by Lobach in 1890. He made measurements on iron, nickel and cobalt films which agreed with Kundt's observations that the dispersion was anomalous. He also noted that the results were affected by the purity of the specimens used. Figure 2.1 illustrates Lobach's results.

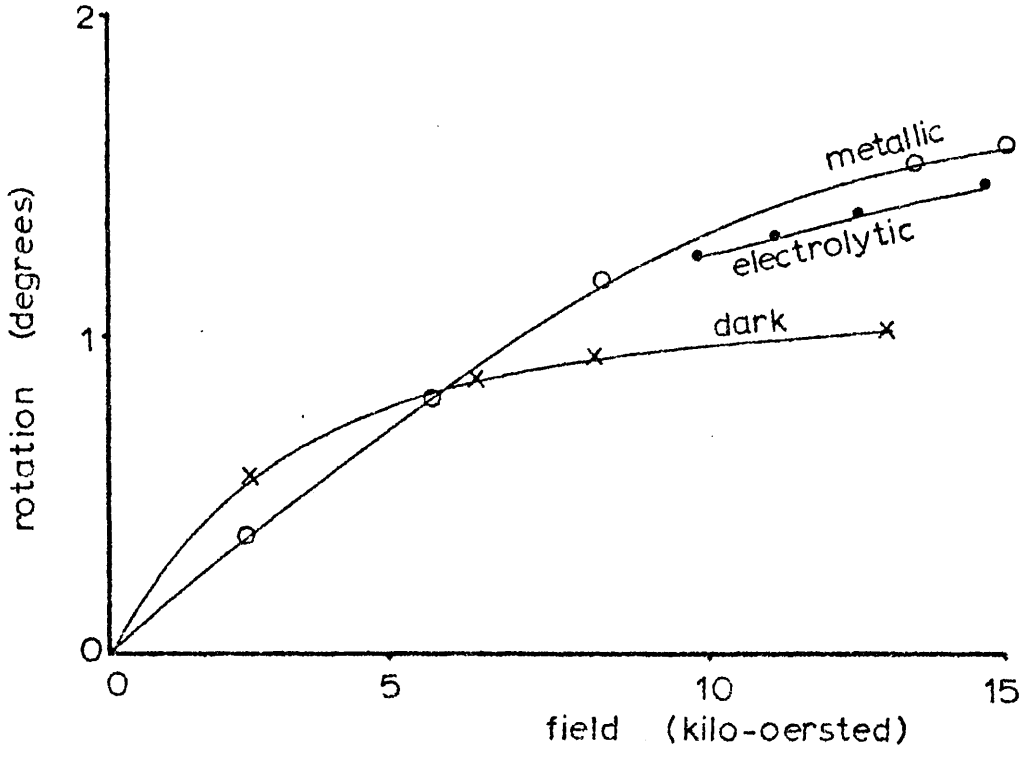

Results of Lobach

(Figure 2.1)

Hirsch (1893) showed that the temperature dependence of rotation was similar to that of magnetization, also that the rotation fell to zero at the Curie point.

In 1907, Harris made measurements using sputtered iron films and produced dispersion curves which were different from those obtained by Lobach. He also noted that the results appeared to depend on the sputtering atmosphere. The results of Skinner and Tool (1907, 1908) are shown in Figure 2.2. They also show that different results are to be expected from films of the same material produced by different methods. They used three different types of films referred to as 'dark', 'metallic' and 'electrolytic' iron. The 'dark' films were obtained by sputtering slowly in various atmospheres, the 'metallic' films were made by sputtering quickly, and the electrolytic films were obtained from a solution of ferrous ammonium nitrate. The dispersion curves for electrolytic and metallic iron were similar to Lobach's while those for dark iron were comparable with Harris's measurements. Skinner and Tool's value for saturation rotation per centimetre was two to three times higher than previous results.

Until that time, sunlight had been used as the polarimetric light source, but in 1908 Ingersoll made magneto-optic dispersion measurements using a Nernst lamp. The films were of sputtered iron and his results agreed with those of Lobach. He suggested that the

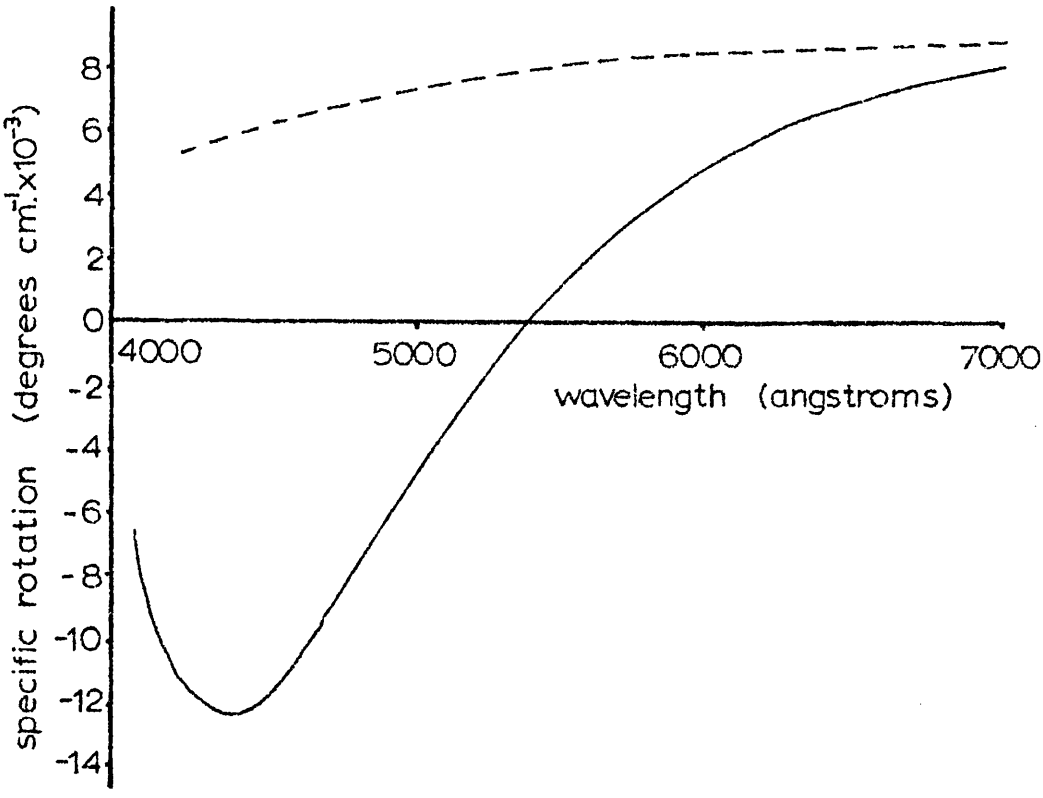

Results of Skinner and Tool

(Figure 2.2)

'dark' films of Skinner and Tool were probably oxidised and also that their thickness measurements were rather inaccurate. Ingersoll's results are shown in Figure 2.3.

In further experiments, Ingersoll (1924) showed that the occluded gases from the sputtering atmosphere could significantly affect the results, it was found that heating the films to 300°C for a certain length of time increased the Faraday rotation by a small amount in the visible and by quite a large amount in the infra-red. This work was repeated and confirmed by Poritsky in 1926.

The introduction of vacuum evaporation provided the next innovation in preparation of specimens for the measurement of Faraday rotation. In 1929, Cau made a lengthy investigation into the magneto-optic properties of iron films, evaporated in vacuo, sputtered, and deposited electrolytically. He came to the conclusion that the former method was less consistent than the latter two methods. This was probably due to the relatively primitive vacuum techniques used. Also, all his measurements were made below 10 Koe., that is, below saturation magnetization.

In 1946 and 1948, König published measurements which demonstrated the need for specimen purity and a more detailed knowledge of the specimen structure. Films of polycrystalline iron were produced by evaporation at 10^{-5} torr, the lowest operational pressure available at that time, and rotation measurements were made on the films before

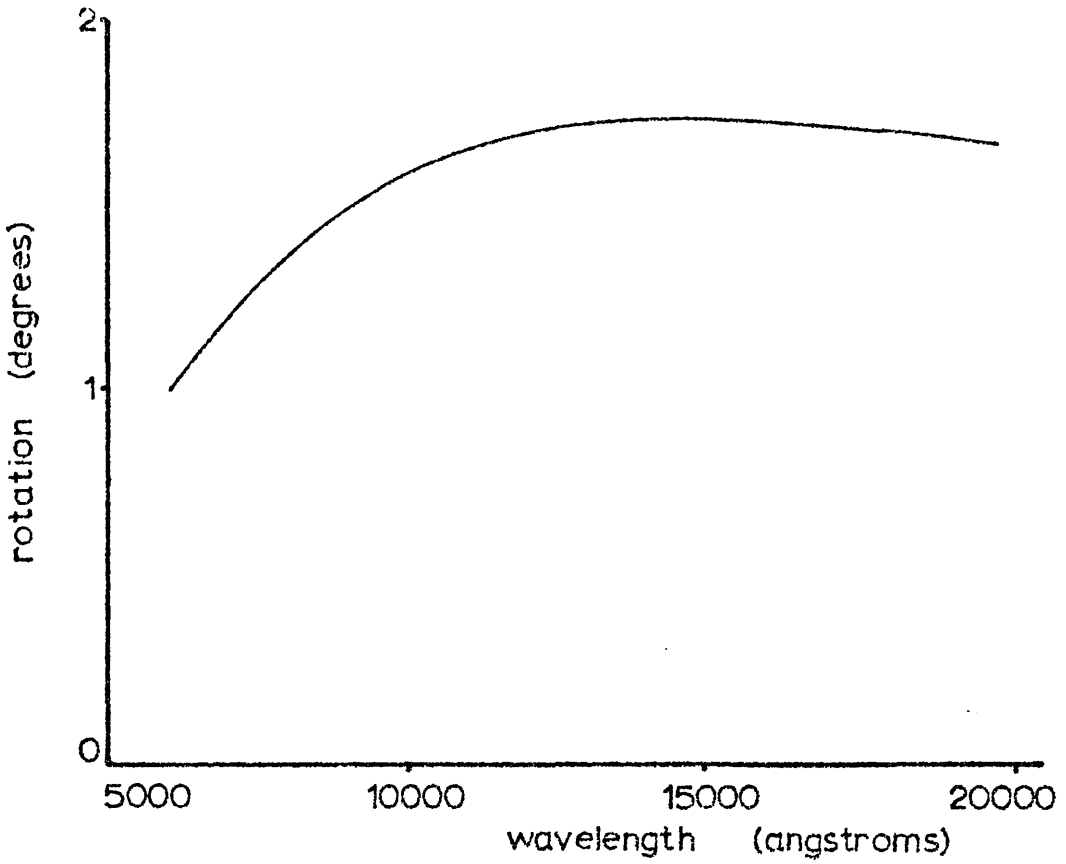

Film thickness = 5800Å
Field = 5700 Oe.

Results of Ingersoll

(Figure 2.3)

and after admitting either moist or dry air into the system. The dry air had no effect, while the moist air produced a decrease in the value of the rotation. König showed that the magneto-optic rotation in films grown on cold substrates reached saturation at values of applied magnetic field which were below that corresponding to magnetic saturation of bulk iron, but that both the saturation field, and the magnitude of the rotation increased after thermal annealing. After examination it was found that the films grown on cold substrates consisted of crystallites smaller than the theoretical minimum for ferromagnetic behaviour. It was suggested that these films were only about 50% ferromagnetic, and the rest non-ferromagnetic, hence the rotation would be proportionately lower. On annealing, aggregation occurred to produce larger crystallites, and hence more ferromagnetic material, so that the film behaved magnetically according to theory. Electron diffraction was used in the investigation of crystallite size.

In 1958, Holmes, Rosen and McLung produced cobalt films by fast evaporation at a pressure of 5×10^{-6} torr. The results obtained agreed closely with those of Du Bois.

Hellenthal (1958) investigated the observed reduction of saturation magnetization for very thin films even when grown on heated substrates. In films below 1000 Å thick this was found to be due to elastic strain in the plane of the film caused by differential thermal contraction between film and substrate.

Miller, in 1962, made the first measurements on epitaxially grown nickel. He chose electron bombardment to produce the films after investigating various methods of growth. The specimens were examined by electron microscopy so that only films approximating to the theoretical ideal were used. He made measurements of the Faraday rotation as a function of thickness, applied magnetic field and crystal orientation for light of wavelength 5461 Å in nickel films. The results are shown in Figure 2.4, and were again in agreement with those of Lobach and Du Bois.

Breuer and Jaumann, and Clemens and Jaumann, both in 1963, measured the Faraday rotation and other optical and magneto-optical constants. They used polycrystalline films of iron, cobalt and nickel prepared by evaporation onto heated glass substrates from directly heated wires, from carrier coils of tungsten and from Al_2O_3 crucibles, at a pressure of 10^{-7} torr. The measurements, which were made in air, agreed with those of Lobach and Du Bois, and they observed a resonance in the Faraday rotation of nickel at about 1.0 μ. This is shown in Figure 2.5.

In 1964, Coren and Francombe investigated the Faraday effect in polycrystalline ferromagnetics and ferrites. They obtained dispersion curves for iron and nickel, although magnetic saturation was only reached for nickel. The films were prepared by sputtering onto microscope cover slips, and were examined by electron and X-ray

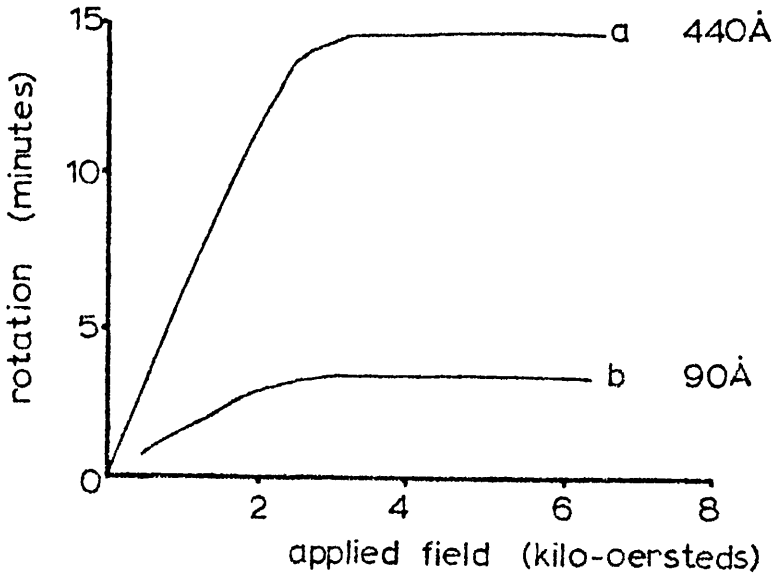

Polycrystalline films

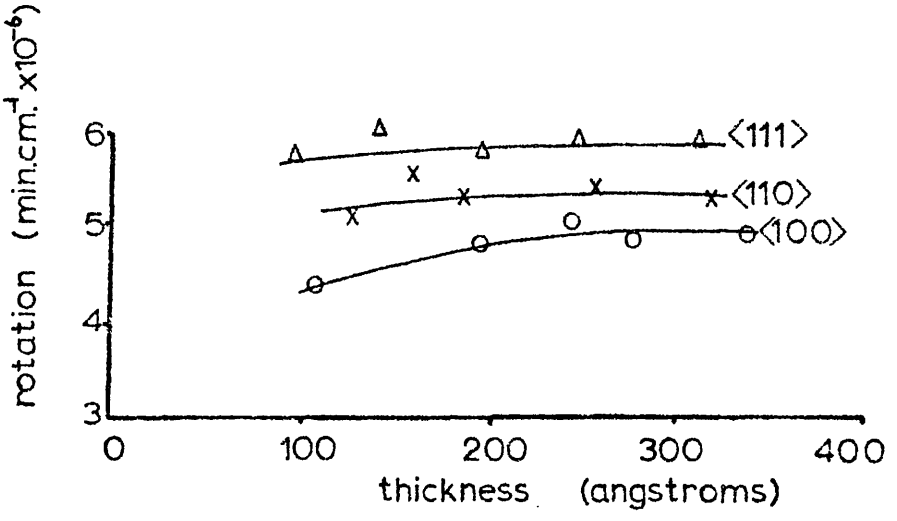

Monocrystalline films

Results of Miller

(Figure 2.4)

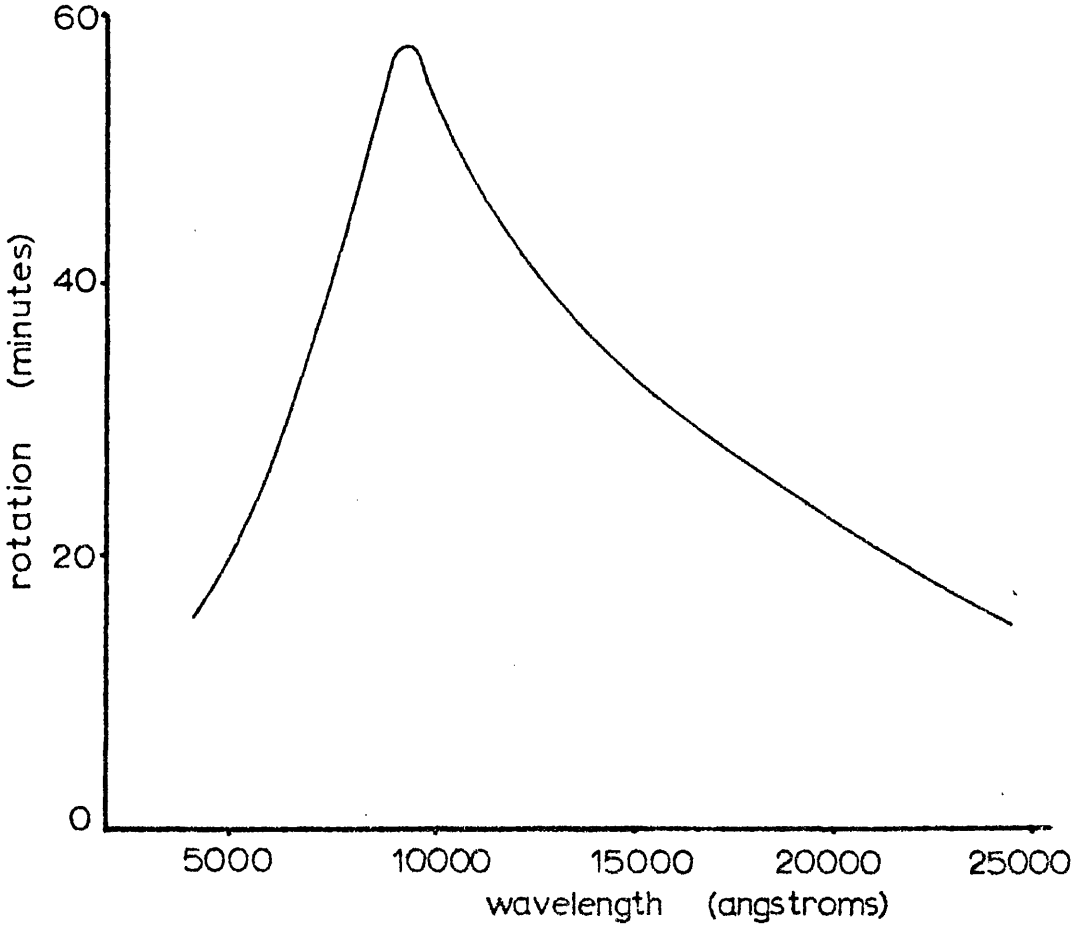

Results of Clemens and Jaumann

(Figure 2.5)

diffraction. Again, the results obtained were in agreement with those of Lobach.

It is evident from the foregoing survey that the main reason for variations and discrepancies between existing magneto-optical measurements is that differences in structure and purity exist between the various specimens used. Vacuum evaporation is generally the cleanest method of film preparation and if the material can be prepared as a single crystal layer, then the structural uncertainties of polycrystalline films can also be avoided. Furthermore, monocrystalline films possess the unique advantage that orientation dependent magneto-optical effects can be measured in transmission in the visible region.

Single crystal nickel films were therefore used in the present work, the aims of which were threefold:

1. to make measurements of the Faraday rotation throughout the whole wavelength range 2500 - 10,000 Å.

2. to investigate, for propagation along <110>, the dependence of the rotation upon the polarization azimuth, relative to the crystal axes.

3. to observe and measure the Voigt effect.

Epitaxially grown nickel films in (110) orientation proved to be suitable for all three types of measurement.

CHAPTER 3

Preparation of the films

3.1 Introduction

The phenomenon of epitaxy, in which one crystal grows in a regularly oriented fashion upon another, is a particularly effective means of producing specimens for experiments requiring very thin monocrystalline films (Heavens et al. 1961).

In this investigation, nickel vapour was condensed in vacuo, on to a suitably prepared single crystal copper substrate, so as to form a monocrystalline film in parallel orientation to the copper. The range of thicknesses employed was from 100 Å to 600 Å, the upper limit being determined by optical absorption and the lower by film continuity.

3.2 Substrate

The copper substrates were themselves formed by epitaxial growth on rock salt crystal faces. These initial substrates were prepared from artificially grown $\frac{1}{2}$" cubes of rock salt, cut by a wet string saw so as to have parallel dodecahedral faces. The upper and lower surfaces were polished on wet filter paper. The lower surface had to be smooth to ensure good thermal contact. The upper

surface was then polished by an optical polishing technique using a rotating wax lap and putty powder (Strong 1938). Excess putty powder round the edges and base of the crystal were carefully removed and polishing continued with a circular motion on a clean 'Selvyt' cloth supported on a glass plate. The surface was then rubbed on another piece of clean 'Selvyt' cloth moistened with isopropyl alcohol to remove all final traces of putty powder. The final polish was with another piece of dry 'Selvyt' cloth. The polished substrate was immediately placed on the heater in the vacuum chamber. The substrate was then annealed for one hour at 400^{o}C to remove the disorder produced in the surface layer by polishing.

3.3 Deposition of the film

(i) Vacuum chamber

The films were prepared in an Edwards 12EA coating unit. The 12" diameter glass bell jar was evacuated to a residual pressure of 10^{-6} torr by an oil diffusion pump, backed by an oil rotary pump. Pirani and Phillips gauges were used to measure the backing and chamber pressures respectively.

A schematic diagram of the evaporation chamber is shown in Figure 3.1. Insulated terminals passing through the base plate provided electrical access to the apparatus. The electron

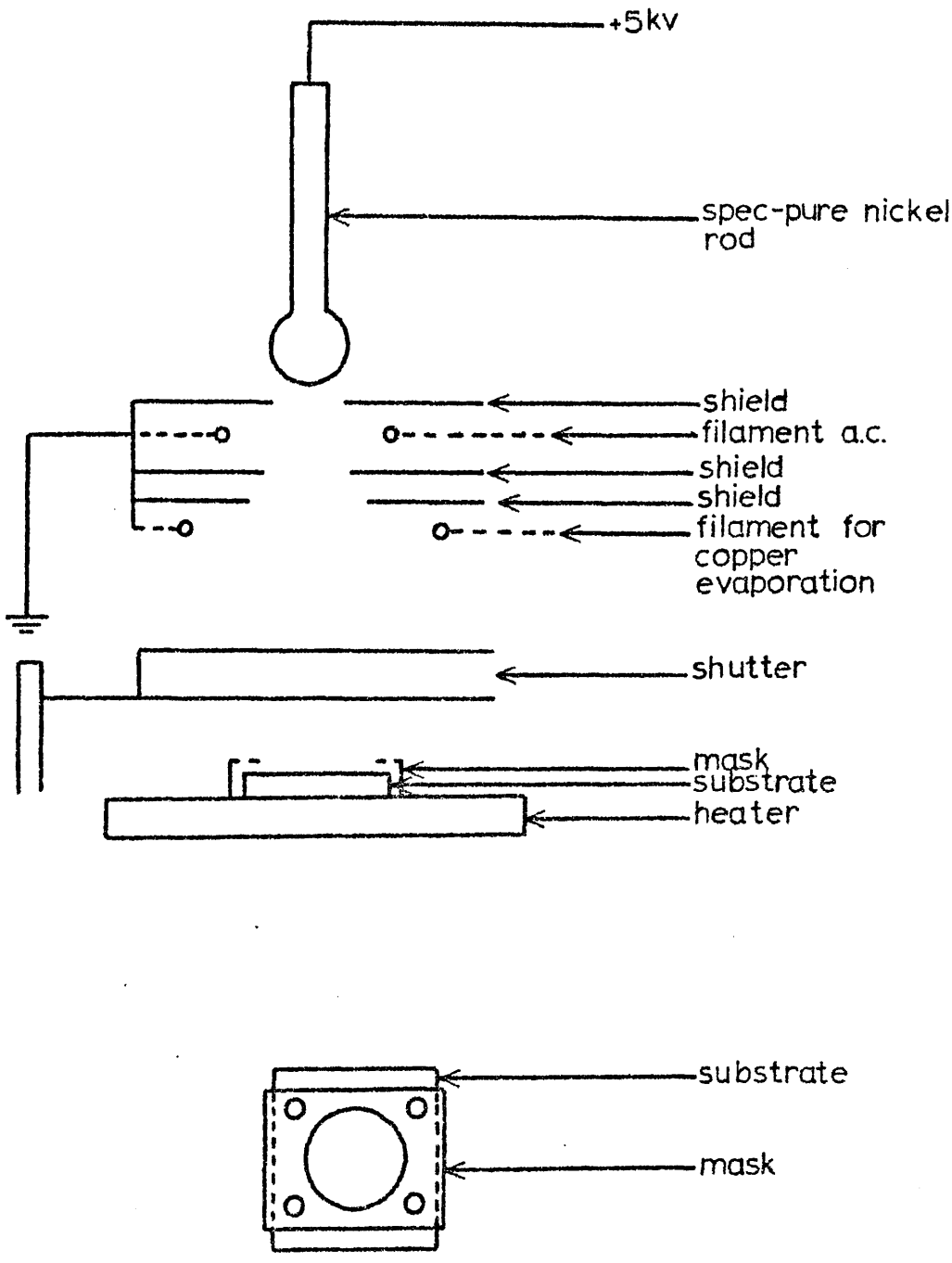

Evaporation chamber and mask

(Figure 3.1)

bombardment filament and the screens were supported by thick steel leads. An insulating glass cylinder supported the nickel rod. The filament from which copper was evaporated was just below the screen. The substrate was placed on the surface of an electrically heated stainless steel plate eight centimetres below the end of the nickel rod. A thermocouple attached to the surface of the heater plate was calibrated in terms of the actual substrate surface temperature by placing on top of a rocksalt substrate of standard thickness small amounts of crystalline substances with known melting points. The system was evacuated and the substrate temperature very slowly raised so that when the crystals melted, the thermocouple reading could be noted and calibrated at the melting points of the crystals.

A molybdenum mask was placed over the substrate to define the area of the specimen. The largest hole, 1 cm in diameter, produced the specimen for the polarimeter, the smaller holes the specimens for the electron microscope and the straight edge a specimen for thickness measurement.

A mechanical shutter was incorporated into the system to control the time of exposure of the substrate.

(ii) Procedure

The polished substrate was immediately transferred to the heater

plate. A mask was placed over the substrate. The shutter was moved across to protect the substrate and the evaporation chamber was pumped out. While evacuation of the chamber was proceeding the heater current was raised to anneal the substrate surface at 400°C. This temperature was maintained for one hour, at the end of which time the chamber had nominally reached the required pressure. The heater was again adjusted to produce the required temperature for the first deposition.

Before the substrate was placed in the chamber, 10 cm of 30 s.w.g. spec-pure copper wire had been wound round the lower filament at 4.5 cm from the substrate. When the substrate reached 330°C, (the required temperature for epitaxial deposition of the copper), the copper was melted by passing 20 amps a.c. through the tungsten filament. After a few seconds to allow for degassing, the shutter was removed and the copper evaporated over a period of about two minutes. This produced a layer of copper, 2000 Å thick, in (110) orientation on the rocksalt. The shutter was replaced.

The nickel drop was then melted by electron bombardment, which caused some outgassing of the drop. After the vacuum had been re-established, (this took only a few minutes, with the nickel drop molten), the shutter was again removed to allow a nickel film to be formed on the copper layer. After the required time, with a deposition rate of approximately 100 Å of nickel per minute, the shutter was replaced.

The films were allowed to cool to room temperature in vacuo and then removed from the system and stored in a dessicator.

3.4 Removal of film from substrate

The composite nickel/copper film was removed from the rock salt by lowering the substrate into a dish of distilled water to which a few drops of ethyl alcohol had been added to reduce surface tension. The substrate was kept nearly horizontal and the water was allowed to seep between the copper and the rocksalt, until the composite film floated freely on the surface of the water. The copper was dissolved preferentially by floating the film on a solution of 10 gm of rocksalt in 300 ml of water for about 24 hours. This solution did not attack the nickel significantly. The remaining nickel was then washed three times. This was done by picking up the nickel film on a clean glass cover slip and transferring it to a dish of distilled water, then to a second and a third, in order to remove all traces of the rocksalt solution.

At this stage, there were several pieces of nickel floating on the surface of a dish of distilled water. The large disc was picked up on a previously calibrated quartz cover slip. This piece of film had been marked before removal from the rocksalt so that the orientation of the crystal axes in the nickel was known, and could be correlated with subsequent observations. The smaller

discs were picked up on copper grids for examination by electron microscopy. Finally, the pieces of film with straight edges were collected on carefully cleaned glass slides for measurement of the film thickness by interferometry.

Throughout the removal process, care was taken to avoid bending the films and thereby setting up unwanted strains.

CHAPTER 4

Investigation of the films

4.1 Electron microscopy

The films were examined by transmission electron microscopy and diffraction to investigate the general structure and crystallographic orientation.

The instrument used was a Metropolitan Vickers E.M.3., with a magnetic focussing system consisting of a single condenser, and objective and two projector lenses. An operating voltage of 75 kV was selected, at wnich a resolution of 100 Å was generally attainable.

The magnification ranges of the microscope were calibrated by means of polystyrene latex 'B' particles.

The specimens were examined by the 'diffraction contrast' method (Hirsch et al. 1956), using a 50 μ objective aperture. Image contrast was produced by local differences in the intensities of Bragg diffracted beams. In the bright field image, where it was arranged that only the direct beam entered the objective aperture (see Figure 4.1), dark contrast resulted wherever local conditions in the crystal leads to strong diffraction away from the objective aperture.

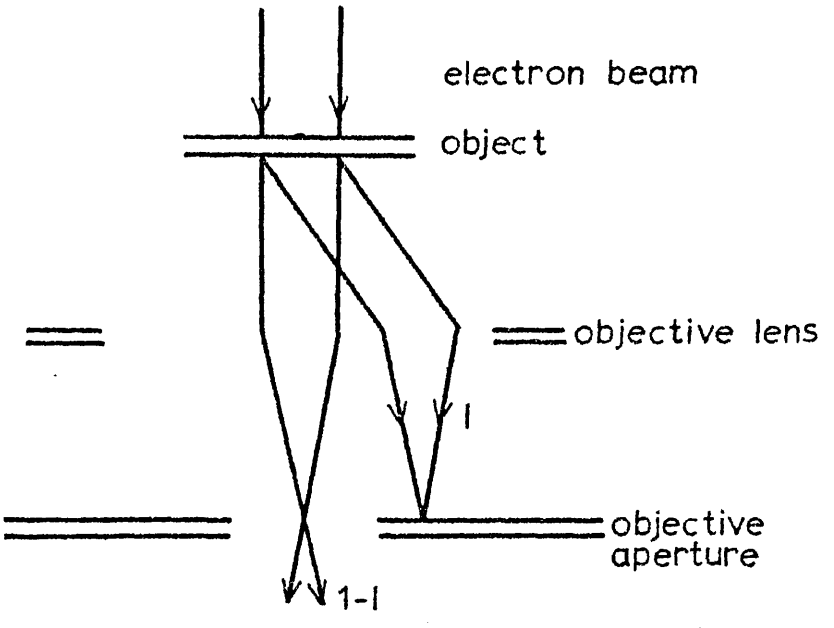

ILLUSTRATING DIFFRACTION CONTRAST

The incident electron beam is diffracted by the specimen and the diffracted beam is removed by the aperture of the objective lens. If the intensity of the incident beam is unity, and that of the diffracted beam I, then that of the transmitted beam is 1 - I. Contrast arises through local variations in the intensities of the diffracted beams.
(Hirsch et al., 1960)

(Figure 4.1)

Diffraction contrast is sensitive to changes in thickness and orientation and also to displacements of the atoms from their normal lattice positions. Dislocations are seen as lines and stacking faults give rise to a fringe pattern. By this method, a projection of the three-dimensional arrangement of the dislocations was obtained. Instruments such as the E.M.3, having a limited resolving power, are adequate for this method, as the atomic array is not actually resolved.

From the theory developed by Hirsch et al. (1960), it was possible to interpret many of the features observed with electron microscopy.

The specimens were examined after they had been cooled, stripped from the substrates and mounted on grids. These processes, although performed with great care, could have altered the nature of the specimens. However, the specimens used for the magnetic observations had been treated similarly and it was assumed that the microscope specimens were representative of the films used in the other investigation.

Electron diffraction was used to determine the orientation of the specimens. Oriented (110) films gave rise to diffraction patterns consisting of a primary array of spots generated by <111> and <11$\bar{1}$> vectors. Some of these integer spots had one or two

satellite spots situated at a distance of $\frac{1}{3}$ of $\langle 11\bar{1}\rangle$ vector in $\langle 111\rangle$ or $\langle 11\bar{1}\rangle$ type of direction.

For thicker films double diffraction effects should generate other satellites filling in the vacant positions $\frac{1}{3}$ of the way between the integer spots, in $\langle 111\rangle$ and $\langle 11\bar{1}\rangle$ type directions.

These phenomena would be compatible with the occurrence of twinning in the films on (111) and $(11\bar{1})$ type planes in the deposited crystal. The effect of twinning on the reciprocal lattice would be to produce a compound lattice consisting of the original lattice with the superposition of lattices due to any twinning. A portion of a compound lattice is illustrated in Figure 4.2 in which twinning on all four $\{111\}$ planes is accounted for.

Figure 4.3 shows typical diffraction patterns obtained from the specimens. Some have little or no twinning while others are heavily twinned on (111) and $(\bar{1}\bar{1}1)$ planes. No evidence was found of twinning on $(\bar{1}11)$ or $(1\bar{1}1)$ planes, which should take the form of bands of fringed contrast along $\langle 110\rangle$ type directions.

The diffraction patterns obtained were photographed and used in estimating the amount of twinning in the films. This was measured using an Automatic Recording Microdensitometer (Joyce Model Mk IIIc). The instrument was based on a double beam light system in which two

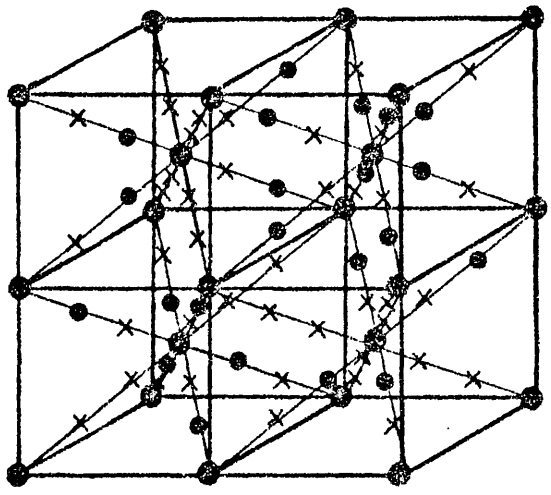

● Main f.c.c. spots

● {111} twinning spots

X Spots resulting from double diffraction at twin boundaries

The reciprocal lattice for a f.c.c. crystal, together with satellite spots which arise from {111} twinning, and those which result from double diffraction at twin boundaries.
(Pashley and Stowell, 1963)

(Figure 4.2)

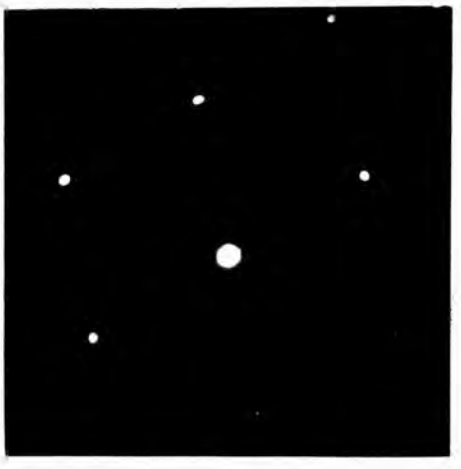

(a) no twinning

(b) little twinning

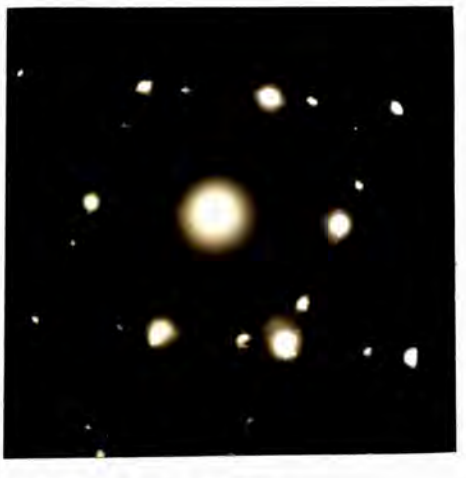

(c) heavy twinning

Electron diffration patterns

(Figure 4.3)

beams from a single light source were switched alternately to a single photomultiplier. If the two beams were of a different intensity, a signal was produced by the photomultiplier which after amplification caused a servo motor to move an optical attenuator so as to reduce the intensity difference to zero. In this way, a continuously null balancing system was obtained in which the position of the optical attenuator was made to record the density at any particular part of the specimen.

The specimen and recording tables were driven by another servo system at a speed proportional to the rate of change of density.

The image presented to the aperture was magnified. This enabled a high degree of resolution to be obtained and was a simple means for locating fine detail on the viewing screen.

The specimen table was hyperkinematically mounted and driven through a coupling ratio arm which was driven by the recording table. The specimen table was able to be disconnected to align the specimen. Control knobs provided coarse and fine motion of the specimen table in a direction perpendicular to the direction of scanning. The table could also be rotated about its centre.

The plate to be scanned was placed on the specimen table and aligned using the viewing screen and the control knobs. Several traces were obtained from each plate to ensure that the maximum

density was measured in each case. An example of the trace obtained is shown in Figure 4.4.

For relative densities, differences in the peak heights were converted into density differences from the areas under the curves.

The plates used for the density measurements were Kodak L10 and L15 which had a straight line density vs. exposure curve which went through the origin. There was found to be a slight non-linearity in the curve at higher light exposure levels, but these values were not used in this work.

4.2 The structure of (110) films

Electron micrographs of nickel films deposited directly on to rocksalt are shown in Figure 4.5a and b. (a) shows the 'lacework' structure which is typical of (100) and (111) films. This may be compared with (b), which is a (110) film, and exhibits a furrowed effect caused by elongation of the crystallites along <001> direction.

This effect is not seen in (110) films grown with an intermediate layer of copper, examples of which are shown in Figures 4.6 to 4.8. These films show a certain amount of twinning, as seen in the diffraction patterns, although less than seen by Miller (1962) in films grown directly on rocksalt. The fact that

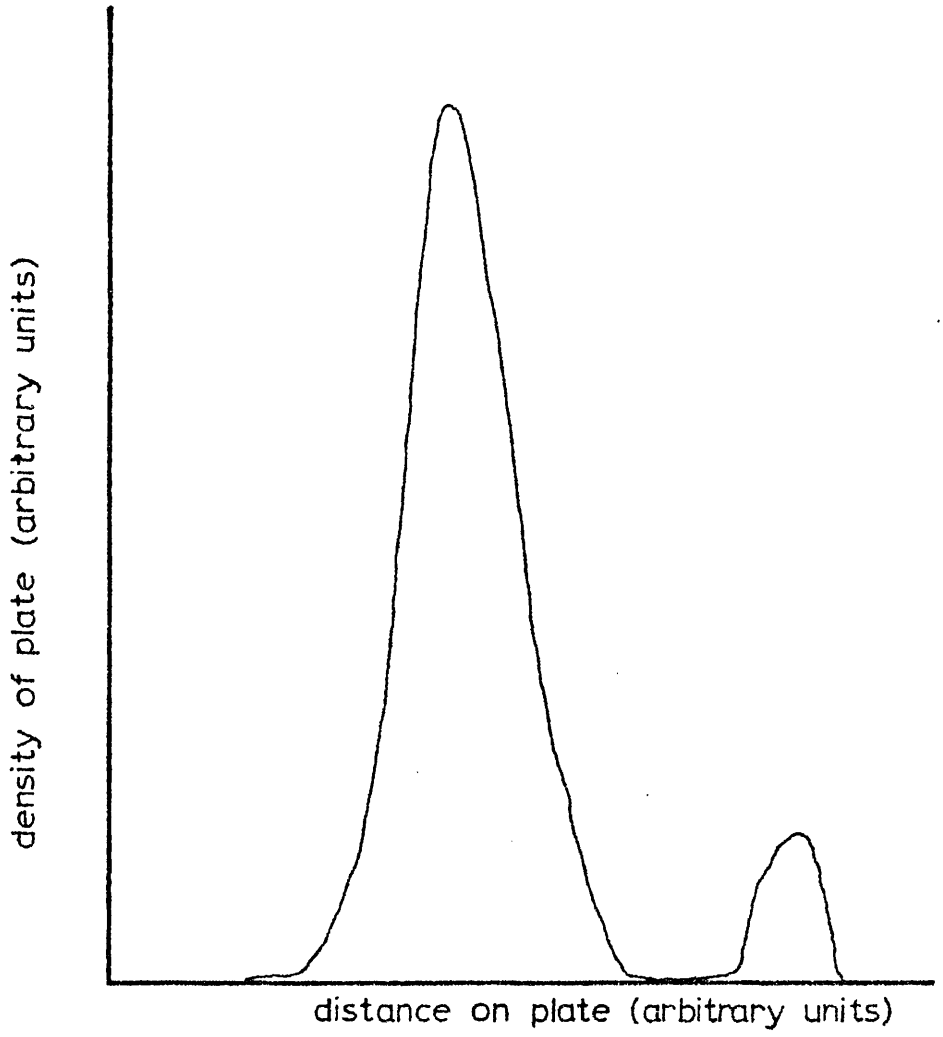

Sample microdensitometer trace

(Figure 4.4)

(a) (100) nickel film x12,000

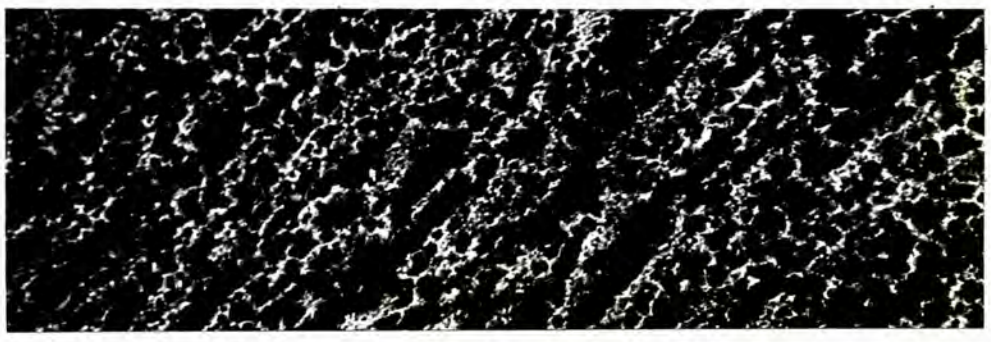

(b) (110) nickel film x36,000

Transmission electron micrographs

(Figure 4.5)

(a) (110) nickel film x48,000

(b) (110) nickel film x30,000

Transmission electron micrographs

(Figure 4.6)

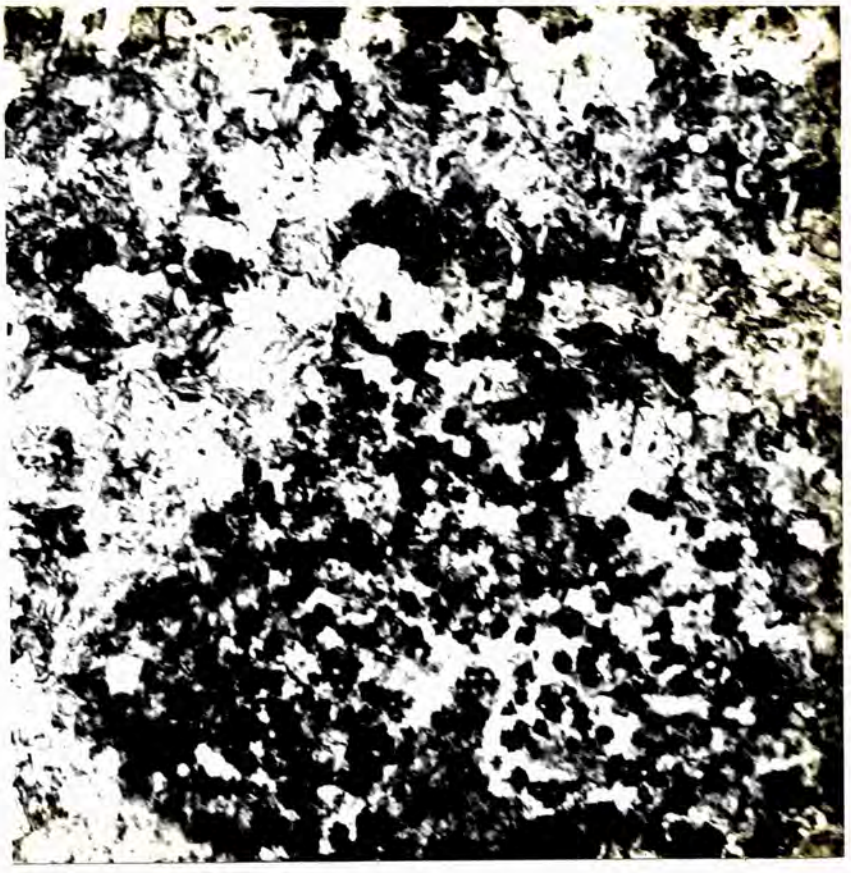

(110) nickel film x23,000

Transmission electron micrograph

(Figure 4.7)

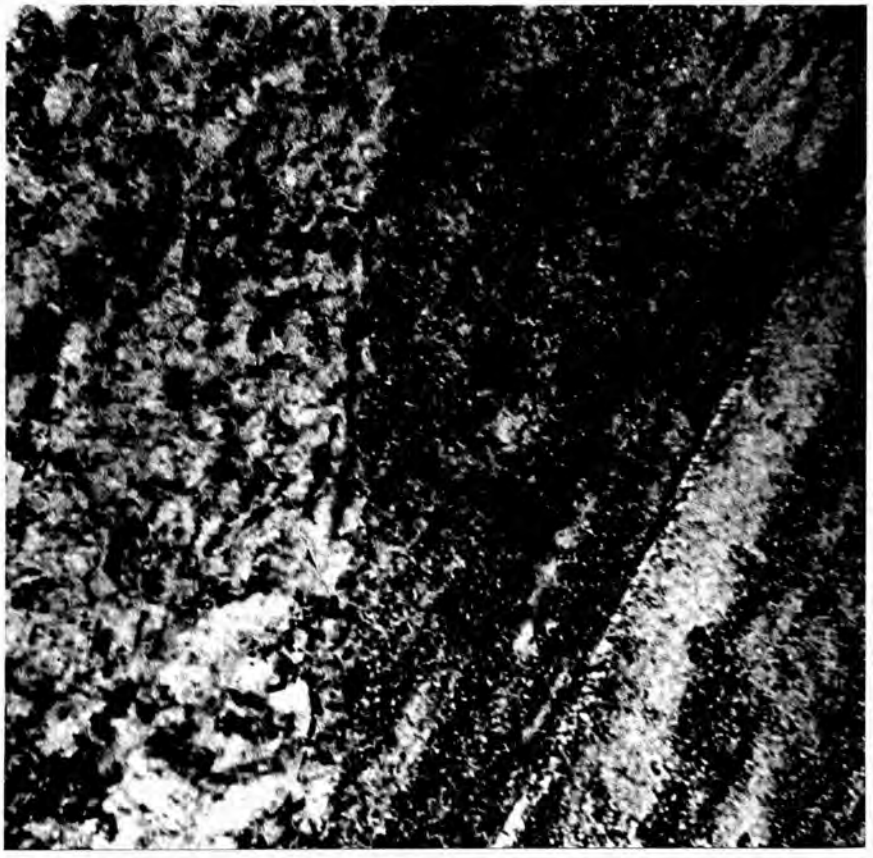

(110) nickel film ×17,000

Transmission electron micrograph

(Figure 4.8)

the twins appear on (111) and ($\bar{1}\bar{1}$1) suggests the possible origin of these faults. Several theories were put forward for the origin of the twins, possible causes being:

1. some sort of growth mechanism
2. plastic deformation due to stresses set up by differential contraction while cooling on the substrate
3. plastic deformation while stripping
4. the effects of electron bombardment in the microscope.

Considering the last possibility, this is not considered likely as no faults of this type arise during the examination of the film.

Great care was always taken, in removing the film from the substrate, not to deform the specimen by more than a few degrees. Removal was effected by allowing water to penetrate between the film and substrate in a <110> direction, thus minimising stresses in a <001> direction. Miller (1962) prepared specimens by immersing the substrate almost to the level of the film, and allowing it to dissolve completely. The film was therefore subjected to no cold working at all and again, only the usual twin features were observed. The possibility that twins on (111) and ($\bar{1}\bar{1}$1)

arise from mechanical plastic deformation can therefore be discounted.

Considering the second possibility, the film is in a state of compressive stress after cooling. This stress is not isotropic, but if twinning is to occur by deformation under this type of stress, $(\bar{1}11)$ and $(1\bar{1}1)$ should be preferred planes.

It seems most probable that twinning is introduced during the growth of the film, since the difference in energy between the twin and the normal positions in the f.c.c. lattice is quite low. Therefore during growth, atoms could fall into incorrect positions and cause a twin.

4.3 Optical microscopy

Visual examination of the film under a small bench microscope (x50) was also made to ensure that there were no small holes in the film to be used in the polarimeter.

It has been shown by Miller (1965) that in polarimetric measurements the effect of quite small holes can produce serious reductions in the observed optical rotation. The effect depends on the relative intensity of the unrotated light component which is transmitted by the holes. It was shown that for a film which would otherwise transmit 1% of the incident light, and which had holes over

1% of its area, the observed rotation was approximately half of the true rotation, assuming that all of the light transmitted by the holes reached the detector. The validity of the latter assumption depended on the size of the hole, since for small holes, there would be diffraction effects.

Figure 4.9 shows a graph of number of holes in a specimen against hole diameter. From this it may be seen that no holes with a diameter greater than 40 μm can be tolerated, some 100 holes of 10 μm diameter were allowable.

With the bench microscope used, holes down to 3 or 4 μm could be observed, the absence of smaller holes having been verified by electron microscopy. A series of circular holes from 1 mm to 3 mm diameter had been punched in pieces of black P.V.C. adhesive tape and the largest hole-free region was selected under the microscope. The tape was then stuck on the reverse side of the cover slip on which the film was mounted.

When no area was found with a sufficiently hole free region, the film was rejected.

Only films which passed all the requirements were used in this investigation. That is, only good continuous single crystal films were used. The only difference between the specimens were film thickness and percentage of twinning, both of which could be calculated.

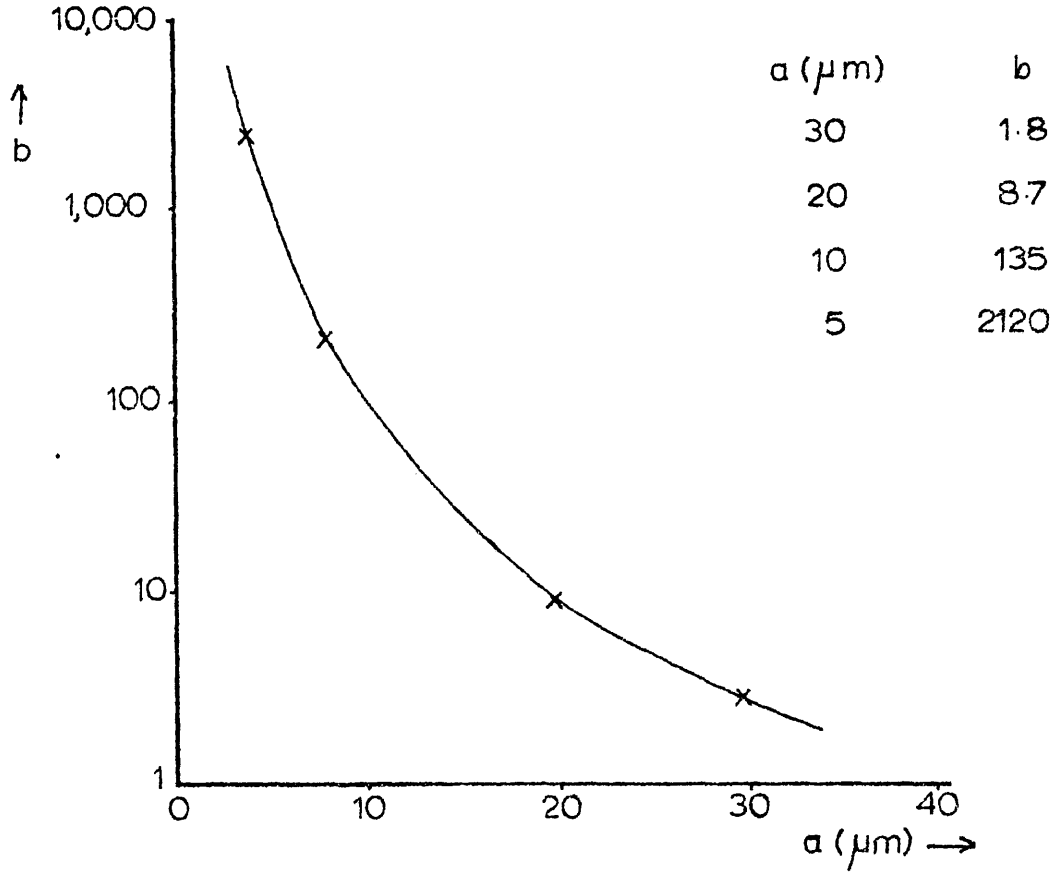

Graph of number of holes b against hole diameter a

(Figure 4.9)

CHAPTER 5

The polarimeter

5.1 Introduction

The experimental arrangement for measuring Faraday rotation in ferromagnetics has changed little since Kundt's experiments in 1884. The film is supported on a transparent substrate between the bored pole pieces of an electromagnet. Nicol prisms or polaroids are placed either side of the electromagnet and crossed to produce extinction of the light passing through the film, with the magnetic field switched on. Reversal of the magnetic field produces a 'double rotation' which is usually measured by rotating one of the polarizers so as to restore extinction.

Until 1908, sunlight was used for illumination, the wavelength dependence of Faraday rotation being determined by means of a dispersed spectrum. Ingersoll (1909) used a Nernst filament, and König (1946) used a high intensity discharge source. Higher intensity sources enabled thicker films to be used, with consequent improvement in accuracy.

In Kundt's original experiments, the magnetized specimen was placed between crossed Nicol prisms and the rotation of the analyser necessary to restore extinction was measured when the field was

reversed. Du Bois (1887), and later workers, used a Lippich half shade system to improve the setting precision. With this method an accuracy of approximately $\pm 0.02^{\circ}$ over a degree has been estimated, although the films used were highly absorbing and small apertures were necessary to ensure uniformity of the magnetic field over the film.

Ingersoll (1909, 1924) was the first to use a non-visual method of detection. In the d.c. bolometric method, illumination from a Nernstlamp was polarized by a pile of plates, and transmitted first by the specimen, then by a double image prism. The two images produced were each received on a bolometric strip. The difference between the signals was a measure of the rotation produced by the specimen.

In 1953, using a modification of this method, Ingersoll measured the Faraday rotation in gases by substituting a photomultiplier for the bolometer. The same principle was used by Holmes et al. in 1958 to measure Faraday rotation in cobalt films and by Miller in 1962 for measurements in nickel films. In 1964 Coren and Francombe measured the rotation produced by various ferromagnetic and ferrite thin films, but Breuer and Jaumann (1963) returned to the visual method for their measurements on ferromagnetics.

In 1955 Rudolph compared the visual and photoelectric methods of detection. He used a Lippich half shade system for the visual

method, and a photomultiplier detecting out-of-balance signals for the photoelectric method. The same order of precision was found for the two methods for Hg 5461 Å and Na 5893 Å with large apertures and highly transmitting specimens, and providing that the observations were made in the dark with a dark adapted eye. For small apertures and low transmitting specimens, the photoelectric method was up to an order of magnitude higher in sensitivity and eliminated eye fatigue. This method was therefore chosen for the measurements in this present work.

5.2 The principle of the polarimeter

Plane polarized light incident on a double image prism at an azimuth of 45° to the principal planes, will be transmitted as two beams of equal intensity. If the plane of polarization incident on the prism is rotated, for example by a specimen placed after the polarizer, then the intensity of one beam is increased, and that of the other beam is decreased.

Let x be the angle between the principal planes of the double image prism and the incident plane of polarization. Then, for the intensity of either beam

$$I = \text{constant } I_o \cos^2 x$$

where

I_o = intensity of incident beam

$\frac{dI}{I} = -2 \tan x \, dx$

$= -2dx$ for $x = 45^\circ$.

dI is positive for one beam and negative for the other, so that the net difference

$$\delta I = 2dI = 4Idx$$

$$\therefore \quad dx = \frac{1}{4} \frac{\delta I}{I} \text{ radians}$$

$$= \frac{45}{\pi} \frac{\delta I}{I} \text{ degrees} .$$

To obtain an accuracy of the same order as the thickness measurement (±3%), a setting precision of approximately 1' of arc is required. For a rotation of 1' it is necessary to detect a relative change of 1 in 859 in the intensity of the two beams. This is obtainable using a photomultiplier.

One of the detectors used in the present work was a trialkali photomultiplier. If the signal corresponding to a rotation of between 10-20 minutes was detected directly by the photomultiplier, a signal to noise ratio of 1 : 10 was obtained principally because of shot noise. (A 200 watt mercury iodine source with a monochromator set at 5460 Å and a film of thickness 400 Å was used

for this estimate.) Such a low signal to noise ratio is best dealt with by a phase sensitive detector system, which was set up in the following way. Light from a secondary source fell on to a part of the rotating analyser which was shielded from the main source and detector. This modulated light was detected by a photocell and the output used as a reference signal for a phase sensitive detector. The final signal was then measured in a meter unit.

5.3 Experimental arrangement

A schematic diagram of the apparatus is shown in Figure 5.1. Light from the source was focussed on the slit of the monochromator which transmitted any required wavelength within the range 2,000 - 10,000 Å.

The monochromatic light was collimated, passed through the Glan-Thompson polarizer and then through the specimen which lay between the bored pole-pieces of the electromagnet (for the case of the Faraday rotation). A Wollaston prism then divided the light into two beams which were modulated by a rotating analyser and detected by the photomultiplier.

5.4 Optical Components

Three different types of light source were used. The sources for the ultra-violet region were the 2537 Å and 3660 Å lines from a

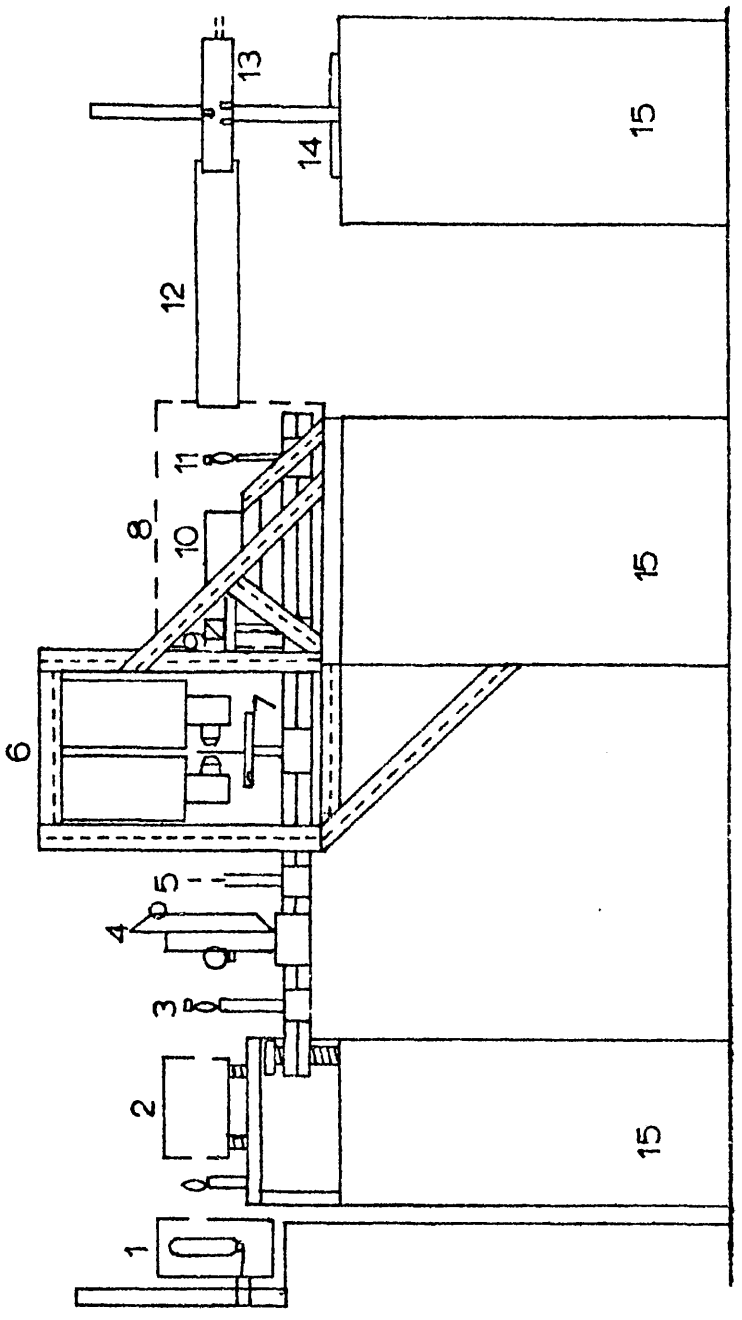

Schematic diagram of the apparatus

(Figure 5.1)

'Pen-Ray' low pressure mercury discharge. For the visible region the light source was a heated tungsten filament in iodine vapour (to prevent evaporation of the tungsten), the whole being enclosed in a quartz envelope. The lamp-housing was water-cooled to prevent thermal movement of the filament. In the infra-red region a Nernst filament was used. The control and starter system is shown in Figure 5.2.

Each source was shielded to avoid stray illumination and the light was focussed on the slit of the monochromator by means of a lens. The lenses were either glass or quartz depending upon the spectral region being investigated. The entrance and exit slits of the monochromator were in line and were set along the optic axis of the polarimeter. Diagrams of the monochromator and the optical system are shown in Figures 5.3 and 5.4.

The light from the monochromator was collimated by a lens and the parallel beam was plane polarized by passing it through a Glan Thompson polarizer. This was mounted at the axis of a circular scale with a tangent screw and vernier reading to $\frac{1}{3}'$. The fixed part of the heavy brass scale was carried by a bench stand and was adjusted so that the polarizer was normal to the polarimeter axis.

A compensating null method of measuring was used whereby the rotation of the polarizer necessary to restore balance measured the Faraday rotation directly. This meant that the polarizer had to be aligned with special care.

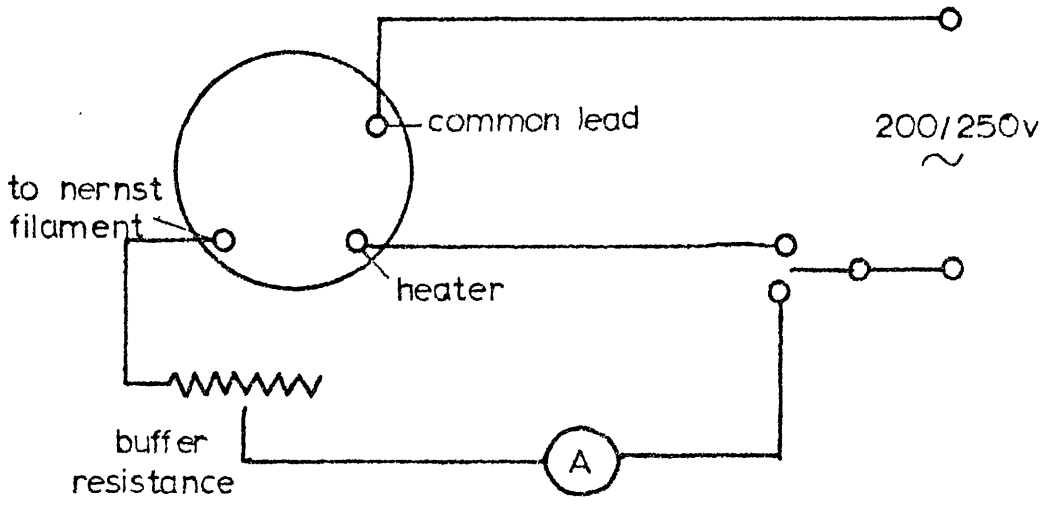

Control and starter system for Nernst filament

(Figure 5.2)

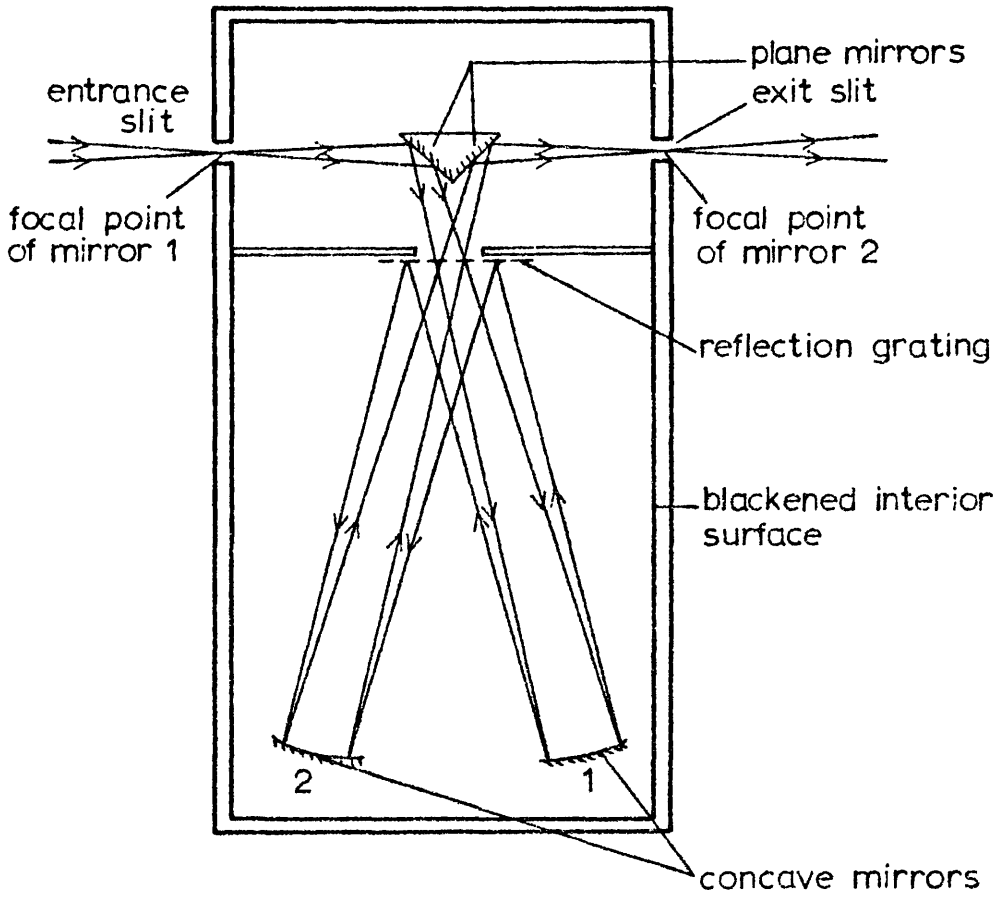

The monochromator

(Figure 5.3)

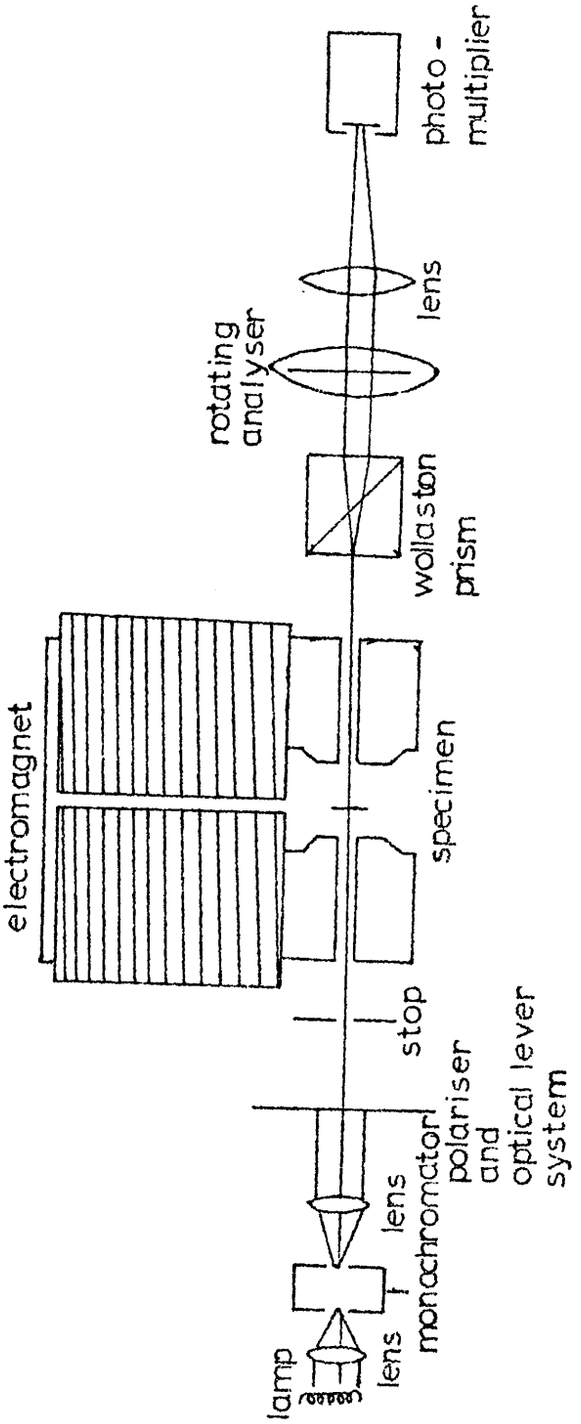

Schematic optical arrangement of polarimeter

(Figure 5.4)

Since there were a considerable number of readings to be taken and the vernier scale was rather fatiguing to use, and optical lever system was fitted to the polarizer. This also resulted in higher precision, since the deflection produced by the mirror was doubled by the system illustrated in Figure 5.5.

An iris diaphragm was placed before the electromagnet to prevent glancing reflections from the pole piece bore.

The specimens were mounted on fused quartz cover slips, 2 mm thick, in such a way that the orientation of the crystallographic axes in the specimen were known with respect to the directions of the field and light propagation.

The beam transmitted by the specimen was split into two perpendicularly polarized beams by a quartz Wollaston prism of one square inch aperture placed between the electromagnet and the analyser on a flat adjustable table. For the initial measurements, using visible light, the two parts of the prism were held together with Canada Balsam, but for the other measurements, when ultra violet and infra red transmission were required, glycerine was used as a fixative.

The two beams were then modulated by a rotating analyser which consisted of a Glan Thompson prism mounted in a polaroid disc. The prism and disc assembly was belt-driven at 38.25 cycles per second

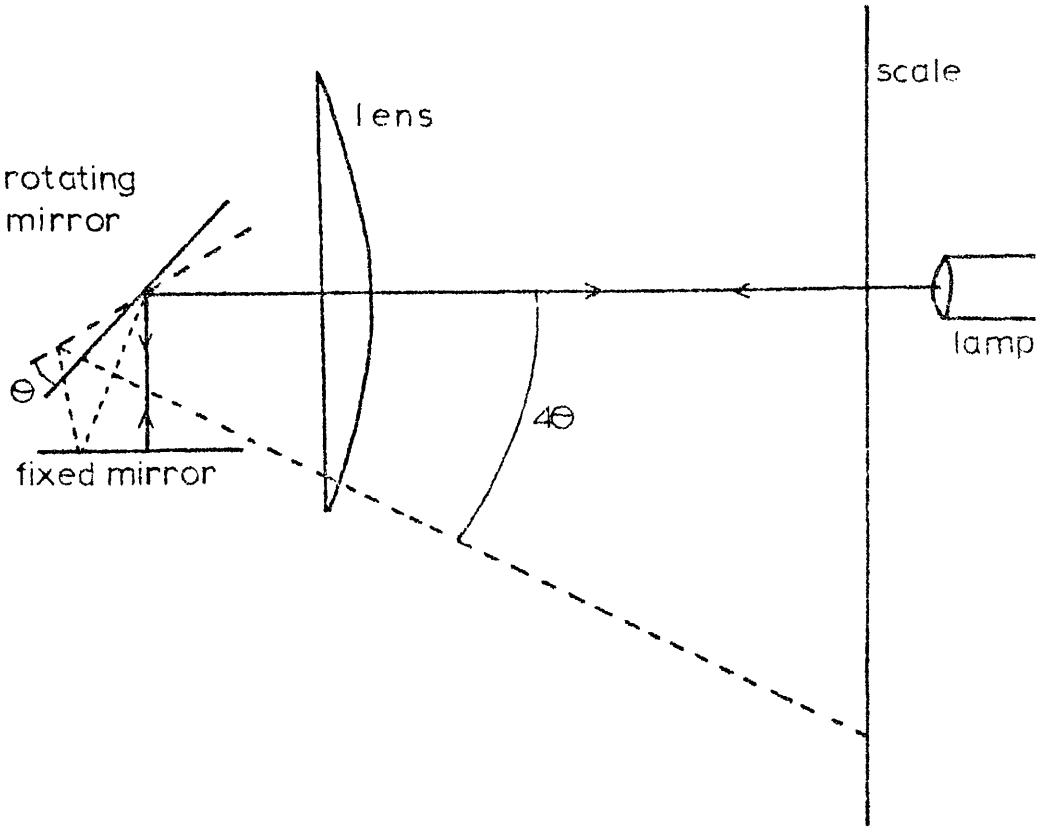

Optical lever system

(Figure 5.5)

by an electric motor. At one point, the rotating disc intersected a plane polarized beam from a separate source, a 4.5 v tungsten pea-lamp. The modulated beam was detected by a photo-diode and the output transmitted as a reference signal to the phase sensitive detector. The light from the rotating Glan Thompson prism was brought to a partial focus on the cathode of a photomultiplier. The focussing was only partial in order to make fuller use of the available cathode area, and to avoid local saturation effects.

5.5 The electromagnet

The electromagnet used in measuring the Faraday rotation was that designed, built and calibrated for similar experiments by Miller (1962). The same magnet was used for the Voigt effect measurements, with different pole pieces arranged so that the field was in the plane of the specimen, that is, transverse to the optic axis of the polarimeter. The calibration curves for the two cases are shown in Figure 5.6.

The pole pieces of the electromagnet were in both instances made of mild steel. For the Faraday rotation, the pole-pieces had semi-angle of 45° and pole face diameter 2.0 cm with a $\frac{3}{16}$" diameter hole bored through them. For the Voigt rotation the pole-pieces had semi-angle 60° and face diameter 2 cm. Brass formers wound with 1000 turns each of 16 s.w.g. double Lewcomax covered and

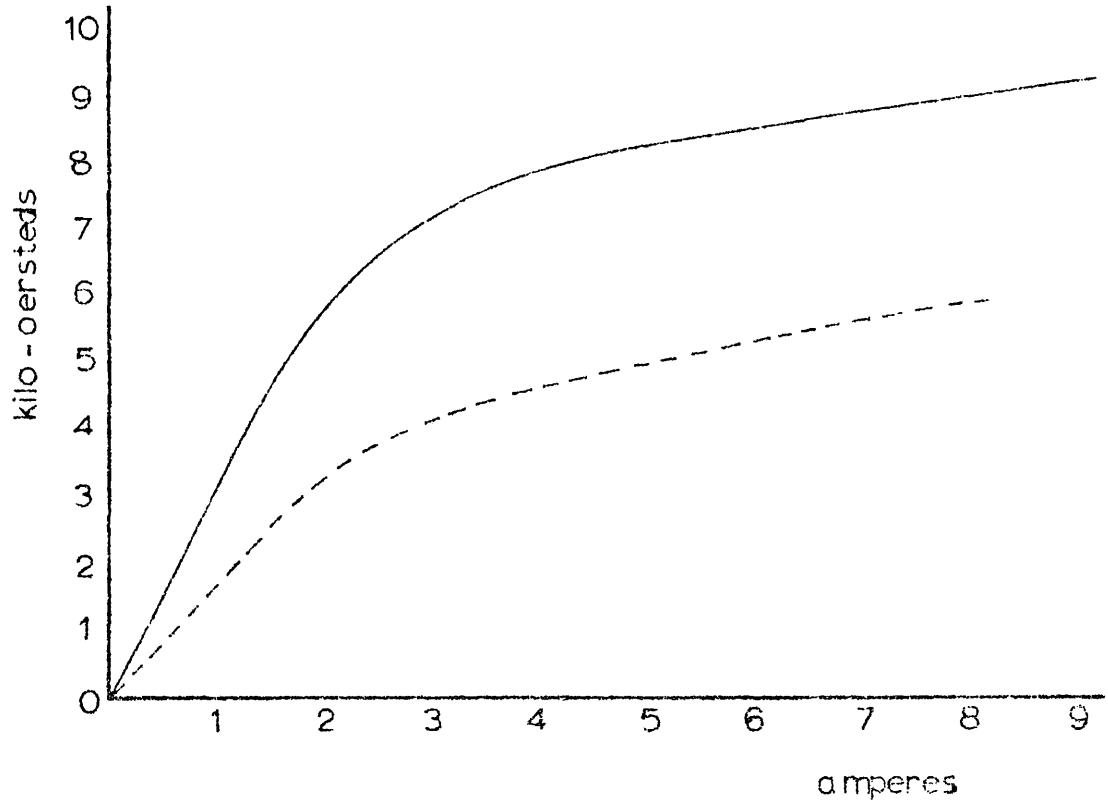

—— Faraday orientation

--- Voigt orientation

Calibration curves for the electromagnet

(Figure 5.6)

enamelled copper wire were arranged vertically above the pole pieces in order to reduce the space occupied by the magnet in the optical path. The electromagnet was held in a Dexion frame, and the pole piece bore accurately aligned to coincide with the optic axis, for the Faraday rotation measurements. The pole piece separation was 0.65 cm for the Faraday experiments and 2.0 cm for the Voigt measurements. Lamp black was applied to the inside of the bore and to the pole pieces themselves to reduce undesirable reflections.

The electrical circuit for the electromagnet is shown in Figure 5.7. The coils were arranged electrically in parallel and the current, supplied from a Farnell stabilized power supply, was controlled by variable series resistances. The coils could alternatively be connected to a Variac transformer, so that the core could be demagnetized. This ensured that on subsequently switching on the energizing current, an accurately known field was obtained.

The specimens were placed between the pole pieces of the magnet on a carriage constructed so that measurements were made with each specimen at the same point in the magnetic field. The carriage was a vertical brass strip, with a circular hole in it, attached to a horizontal brass block which could be inserted between the pole pieces until it came up against a horizontal brass stop on a table levelled on the optical bench. The specimen carriage was levelled in position and held in place by phosphor bronze springs. A diagram of the specimen carriage is shown in Figure 5.8.

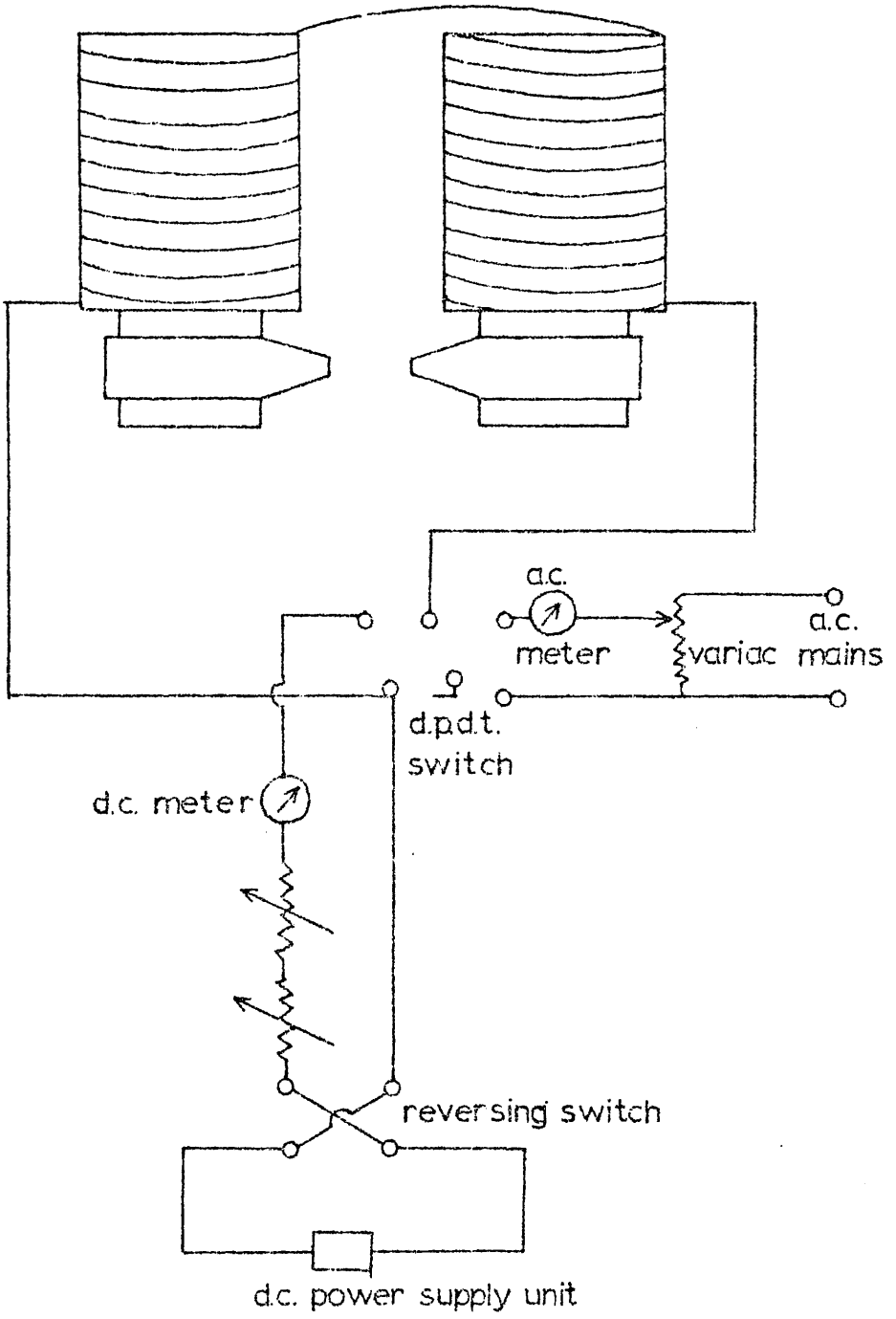

Electromagnet circuit

(Figure 5.7)

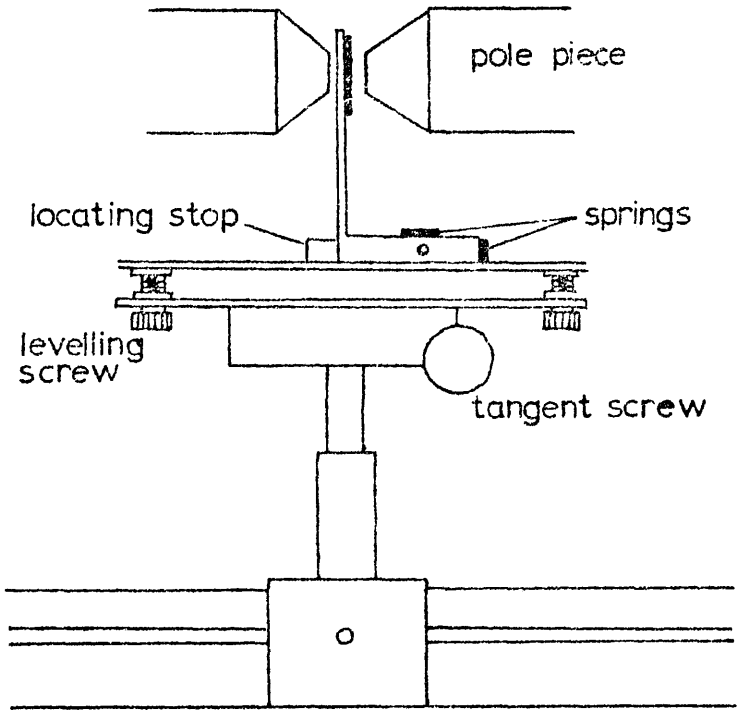

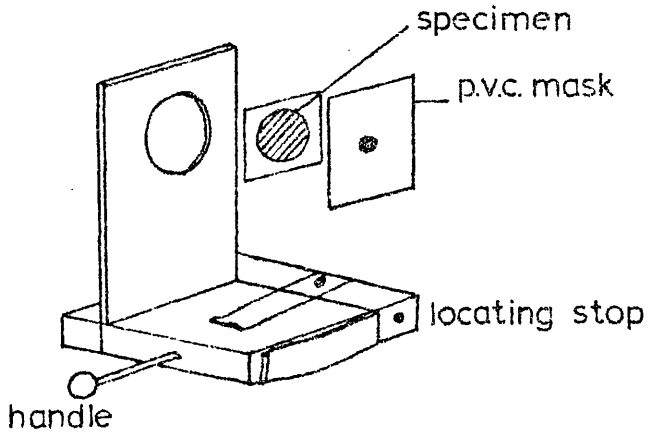

Specimen carriage

(Figure 5.8)

5.6 The photomultiplier

Two different photomultipliers were used. An E.M.I. 9558 with a quartz window was used for the ultra-violet and visible region, and an R.C.A. 7102 for the infra-red. Spectral response curves for the two photomultipliers are shown in Figure 5.9.

The 9558 was an eleven stage tube with a tri-alkali cathode, low dark current (2×10^{-9} amps) and high photosensitivity in the required region. The 7102 was a ten-stage tube with S-1 spectral response. This was not ideal for the measurements since it had quite a high dark current (1×10^{-7} amps) and relatively low photosensitivity, however, it was the best commercial photomultiplier available at the time. The photomultiplier in use was mounted in a cylindrical brass can with adjustable screws so that the photocathode could be aligned to receive light normally from the optical system. The whole was contained in an earthed mu-metal shield to guard against stray fields. Even so, the photomultipliers had to be moved some distance ($\sim$ 1 m) from the magnet to reduce interference to an acceptable level.

The Wollaston prism, rotor, reference system and photomultiplier were covered by a light-tight box while measurements were being made.

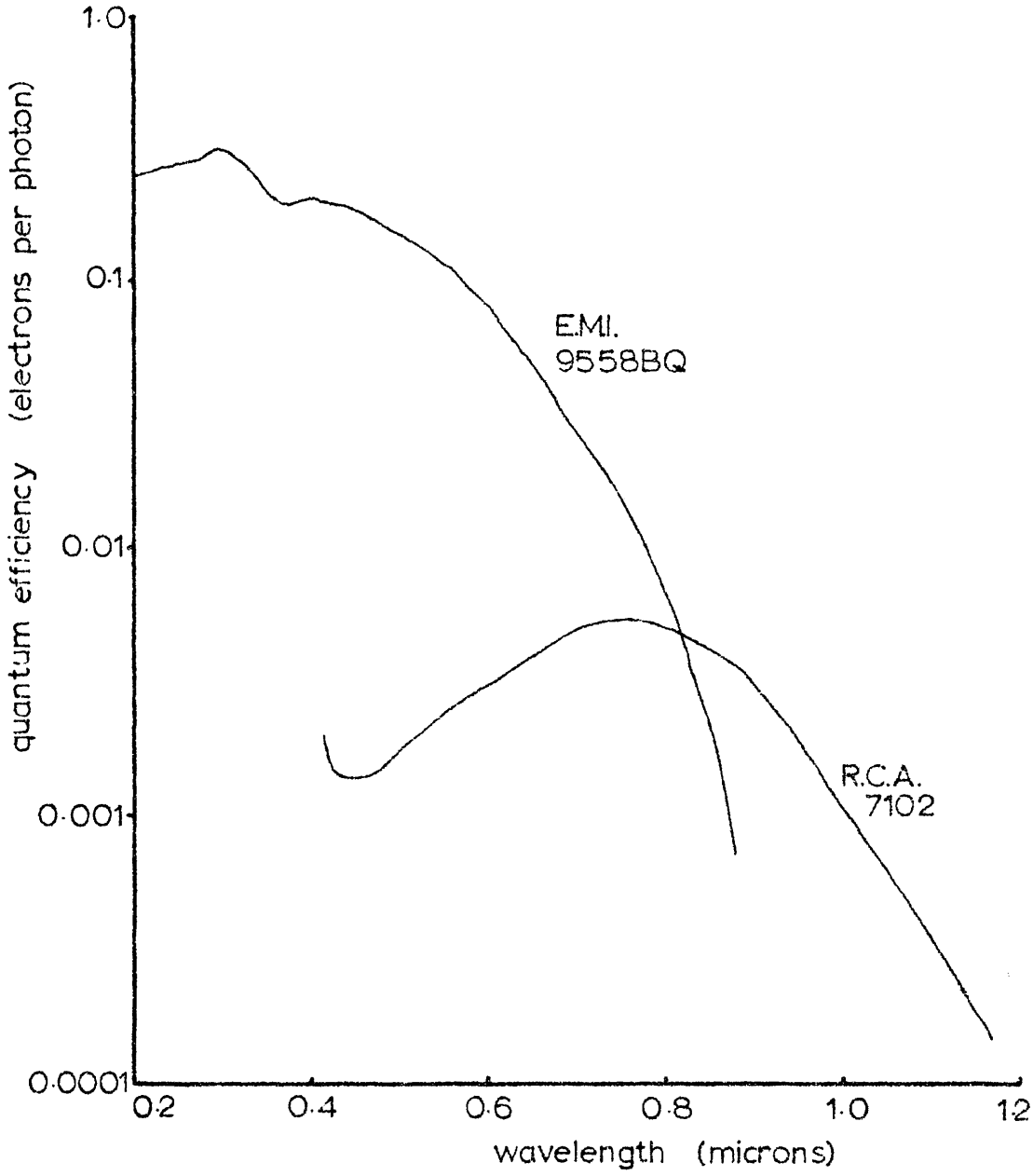

Specimen response curves for photomultipliers

(Figure 5.9)

5.7 Electrical system

A block diagram of the electrical system is shown in Figure 5.10.

The signal from the photomultiplier passed via a cathode follower to a Muirhead narrow band twin-T filter (No. 55 A). The filter was designed to pass signals at the frequency of the rotating analyser, i.e. 38.25 cycles per second (± 5%). This removed most of the random noise, mains pick-up, etc., from the signal, thereby rendering observation of the rectified signal easier, and preventing saturation of the amplifier input stage. The filter output was fed into a low frequency amplifier (Brookdeal LA635) and then into a phase sensitive detector (Brookdeal PD629), where it was coherently rectified and smoothed. The signal was then monitored on a Brookdeal MU947 meter unit.

A resistance chain of 100 K ohm high stability resistors provided the dynode potentials for the 9558 photomultiplier, with 200 K ohm between the anode and the first dynode, and between the last dynode and cathode. For the 7102, the dynode chain consisted of 50 K ohm high stability resistors with 33K ohm between the anode and first dynode and 100 K ohm between the last dynode and cathode. The anode current from the 9558 photomultiplier was monitored by a moving coil meter in a screened soft iron box with screened leads. IDL stabilized H.T. power supplies were used for the photomultipliers

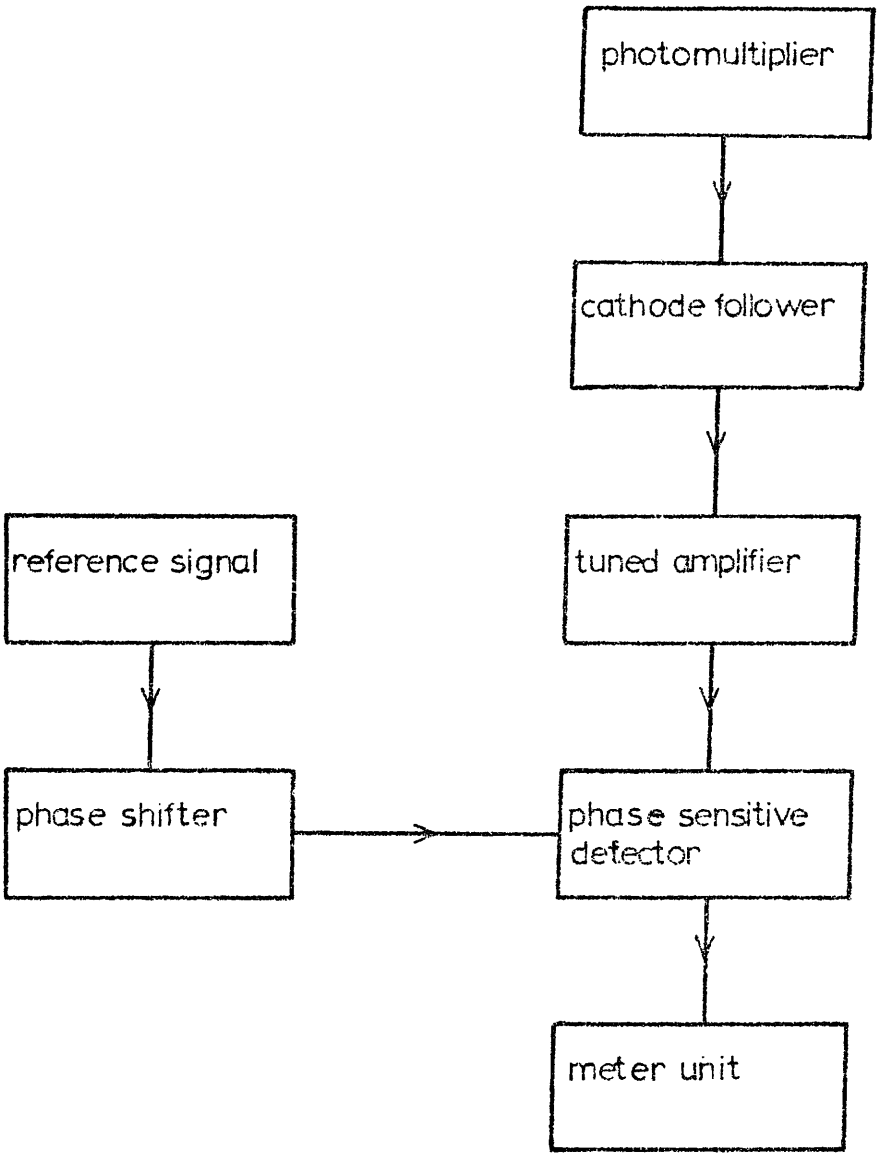

Block diagram of electrical system

(Figure 5.10)

and the cathode follower H.T. was provided by a Siemens-Ediswan stabilized power unit (Type R2160).

The reference signal was fed into a phase shifter (Brookdeal Model PS946) before injection into the phase sensitive detector with the photomultiplier signal. The rectified and smoothed signal was displayed on the meter.

The phase shifter, low frequency amplifier, phase sensitive detector, and meter unit were designed by Brookdeal to be used in conjunction with each other.

5.8 Method of measurement

Part of the specimen was examined by electron microscopy to ascertain that it was a single crystal and suitable for the experiment. The disc of film on the quartz cover slip was also examined in transmission under a bench microscope at a magnification of x50 and only used if free from holes. Pieces of black adhesive P.V.C. tape were punched with holes ranging from 1 mm to 3 mm in diameter. The largest hole-free region of the film was chosen under the microscope and the corresponding aperture stuck on the reverse side of the cover slip. The cover slip was then fastened against the vertical flat brass strip of the specimen carriage by means of the adhesive P.V.C. tape. Light was therefore transmitted firstly by the film and then by the cover slip. Measurements were also made

with the light transmitted initially by the cover slip and then by the nickel. No difference was noticed in the observed rotation in the nickel after the usual corrections for the quartz rotation had been made.

The room in which the polarimeter was situated was blacked out and only a small d.c. lamp was used to read the meter. The polarimeter was aligned with all the components accurately placed to allow maximum transmission of the monochromated light beam. The specimen carriage was put into position with a blank cover slip in place. The electrical components were switched on and allowed to stabilize. The magnet was brought into a cyclic state by passing current from the Variac through the coils, and then reducing this current to zero. The monochromator was adjusted to transmit the required wavelength. The electromagnet was then actuated so that the cover slip was in a known magnetic field. With no light allowed into the photomultiplier the zero on the meter was adjusted. Light was then allowed to pass through the system into the photomultiplier and the polarizer was rotated until the meter again read zero. The position of the spot on the optical lever scale was noted. The electromagnet was demagnetized again and the same energising current passed through the coils in the opposite direction so that the magnetic field at the specimen was now reversed. The new balance position was found and the reading on the scale of the optical lever again noted.

From the readings on the scale the double rotation produced by the quartz was found for the known field. This process was repeated for different magnetic fields and different wavelengths of light.

Variation of rotation with incident azimuth of polarization was measured in the same way but with the polarizer tilted and the Wollaston prism placed on calibrated wedges so that the incident azimuth of polarization was known.

The specimen of nickel was mounted on the calibrated cover slip and all the measurements were repeated. Hence the Faraday rotation of nickel was found for different magnetic fields, different wavelengths and different incident azimuths of polarization with respect to the crystallographic axes.

The Voigt measurements were made in the same way with the magnet perpendicular to the optic axis.

The measurements were repeated for nine specimens in the Faraday effect and five in the Voigt effect. Many more specimens were actually prepared (approximately 70), but only those fulfilling the required standards of crystal perfection, homogeneity and continuity were used. The results are presented in Chapter 7.

CHAPTER 6

Determination of film thickness

6.1 Introduction

To determine the specific rotation, i.e. the saturation rotation per cm, and hence Kundt's constant, it was necessary to accurately measure the thicknesses of the specimens. In 1955, Heavens reviewed and described the various methods available for measuring the thickness of thin films. One of the methods frequently used by earlier workers in magneto-optics (Du Bois, 1887; Konig, 1946, 48) was to determine the mass per unit area by weighing, and using the value for bulk density, to calculate the thickness. This method assumed that the film was a compact uniform layer of pure material, an assumption which lead to errors as the specimens were likely to be aggregated, granular or contaminated with occluded gases and oxidised materials. This fact probably accounts, at least in part, for the discrepancies between the results of earlier workers.

Another method was to measure optical absorption in the films, which required accurate knowledge of the optical parameters involved. However, these methods were also liable to large errors, since the optical constants of absorbing films differed in an often

unpredictable manner from those of the bulk material, owing to the effects of oxidation and structure variations.

Miller (1962) used a variation of the weighing method, developed by Heavens (1959). The films were grown epitaxially on various faces of rock salt and the masses were determined by a microchemical colorimetric method, the area of the film being measured directly. The assumption of bulk density was justified, in this case, because of the purity, good crystalline order and continuity of the films. Heavens, Brown and Hinton (1959) verified this assumption by measurements on epitaxially grown iron films.

A method which was capable of giving the actual thickness of films with smooth surfaces with high accuracy was that developed by Tolansky (1948a). This was the multiple beam Fizeau fringe technique which was chosen as being most suitable for this present work.

6.2 The multiple beam Fizeau fringe technique

When a wedge formed between silvered surfaces is illuminated normally with monochromatic light, dark fringes of constant thickness are formed by the reflected light. If part of one of the plates is covered by a film the fringes are displaced in crossing the edge. From measurements of the displacement and fringe separation a value for the thickness of the film is obtained.

$$\text{Film thickness} = \frac{\delta\lambda}{2s}$$

where

δ = displacement of the fringe on crossing the step

s = fringe separation

λ = wavelength of light used.

Tolansky (1948b) has examined the conditions for obtaining sharp fringes and accurate measurements. The most important of these are:

1. The surfaces must be coated with a highly reflecting film of minimal absorption.
2. This film must contour the surface exactly and be of uniform thickness.
3. Monochromatic light, or at most a few widely spaced monochromatic wavelengths must be used.
4. The interfering surfaces must be separated by at most a few wavelengths of light.
5. A parallel beam should be used (with 1° - 3° tolerance).
6. The incidence should preferably be normal.

6.3 Measurement of film thickness

The nickel films, prepared for the thickness measurement, on their glass substrates, and the optical flats, were silvered to a thickness of about 1000 Å in an evaporation chamber at 10^{-5} torr. The apparatus used for measuring the thickness is shown in Figure 6.1. A plate camera was used to take photographs of the fringe patterns (Figure 6.2).

Direct measurements were also made on the fringe systems by means of a varian Å-scope Interferometer. This used exactly the same principles as described above and had the advantage that it was simpler and quicker to use. In this case the reference plate of the interferometer was a multilayer filter. The nickel film and its glass substrate were silvered as above and placed on the specimen table which was raised into position. After focussing and alignment of the specimen, the fringe pattern was visible. Measurement of the thickness was made using a micrometer eyepiece.

Both methods of measurement, with reasonable precautions could be used to give values of the thickness with less than a 3% error within the range used (280 Å - 460 Å).

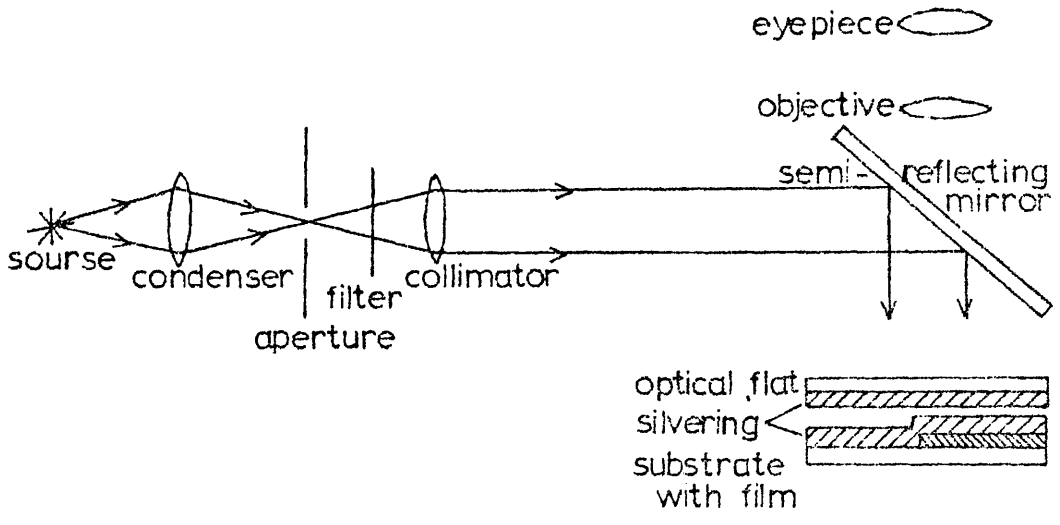

Apparatus to measure thickness

(Figure 6.1)

Typical interferogram showing fringe displacement at specimen

(Figure 6.2)

CHAPTER 7

Results and discussion

7.1 Introduction

The Faraday and Voigt effects have been measured, in monocrystalline (110) nickel films, in the wavelength range 2500 Å to 10,000 Å and 4000 Å to 6500 Å respectively, as a function of thickness. The variation in magneto-optical rotation with polarization azimuth of the incident light has been investigated and measured.

It is shown that the Voigt rotation, due to the initial magnetization in the film plane, may be calculated from the saturation values of Faraday rotation observed for each of the applied field directions normal to the specimen.

The saturation, dispersion and azimuthal behaviour of the Faraday and Voigt effects are discussed and compared with available theory.

7.2 Faraday rotation in quartz

Before the nickel film was mounted, the quartz cover slip was calibrated using the method described in Chapter 5. The double

rotation produced by the cover slip was found for different values of the magnetic field up to 8.2 kOe. For each cover slip the readings were repeated for different wavelengths and for a series of known incident azimuths of polarization. A graph of the Faraday rotation in quartz against wavelength is shown in Figure 7.1. Good agreement is obtained with the results of Sivaramakrishnan (1956) over the visible and near ultra-violet region.

7.3 Faraday rotation in nickel

The single crystal films were mounted in a known orientation on the calibrated cover slips. The double rotation due to the specimen and the quartz was found for different values of the applied magnetic field. A typical table of observations is shown in Figure 7.2. From this table a graph is drawn as in Figure 7.3 where curve (a) shows the rotation due to the nickel and quartz, (b) that due to the quartz, and (c) the rotation from the nickel alone. The applied field for saturation rotation is approximately 6kOe which agrees with the figure given by Bozorth (1955). Figure 7.4 shows the variation of specific rotation with film thickness. There is no significant variation of rotation with thickness down to 200 Å, confirming the indications of earlier work (Miller 1962). The measurements were repeated at different wavelengths of incident light. The graph in Figure 7.5 shows the variation in specific rotation at saturation

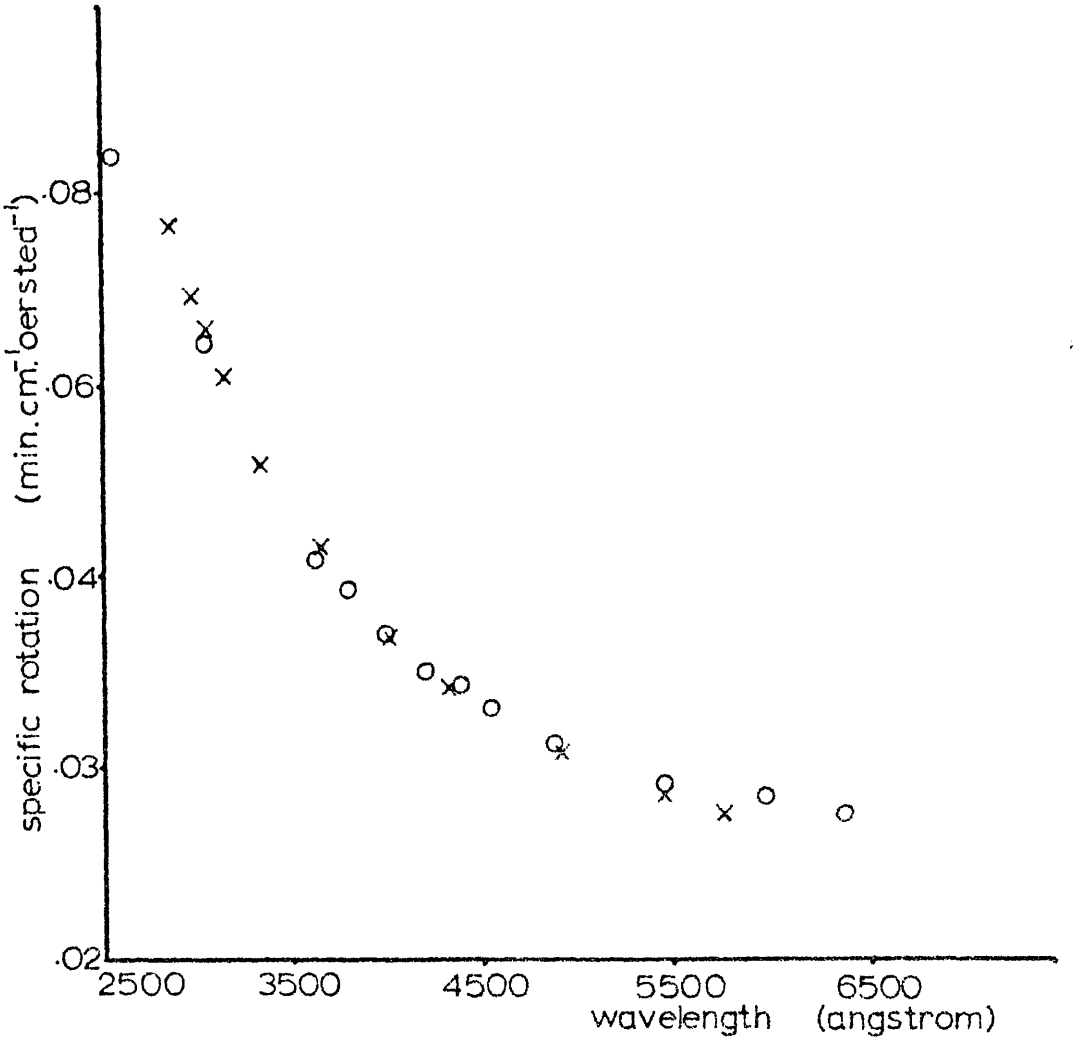

o present experimental results

x Sivaramakrishnan's results

Faraday rotation in quartz

(Figure 7.1)

coil current I amp.	applied magnetic field H koe.	scale reading of optical lever in mm.			b - a	double rotation $2\Theta = \frac{b-a}{3}$ min.
		a +H	O	b -H		
·625	2·1	345·5	361	380	34·5	11·5
·875	2·95	340		385	45	15
1·375	4·4	332·5		392·5	60	20
2·0	6·02	328·5	361	397·5	69	23
2·25	6·42	328·5		398	69·5	23·2
2·75	7·0	327·5		398	70·5	23·5
3·5	7·6	327·5		388·5	71	23·7
4·5	8·2	326·5	361	388·5	72	24

Rotation results for a monocrystalline nickel film of thickness 550Å and (110) orientation

Specimen table

(Figure 7.2)

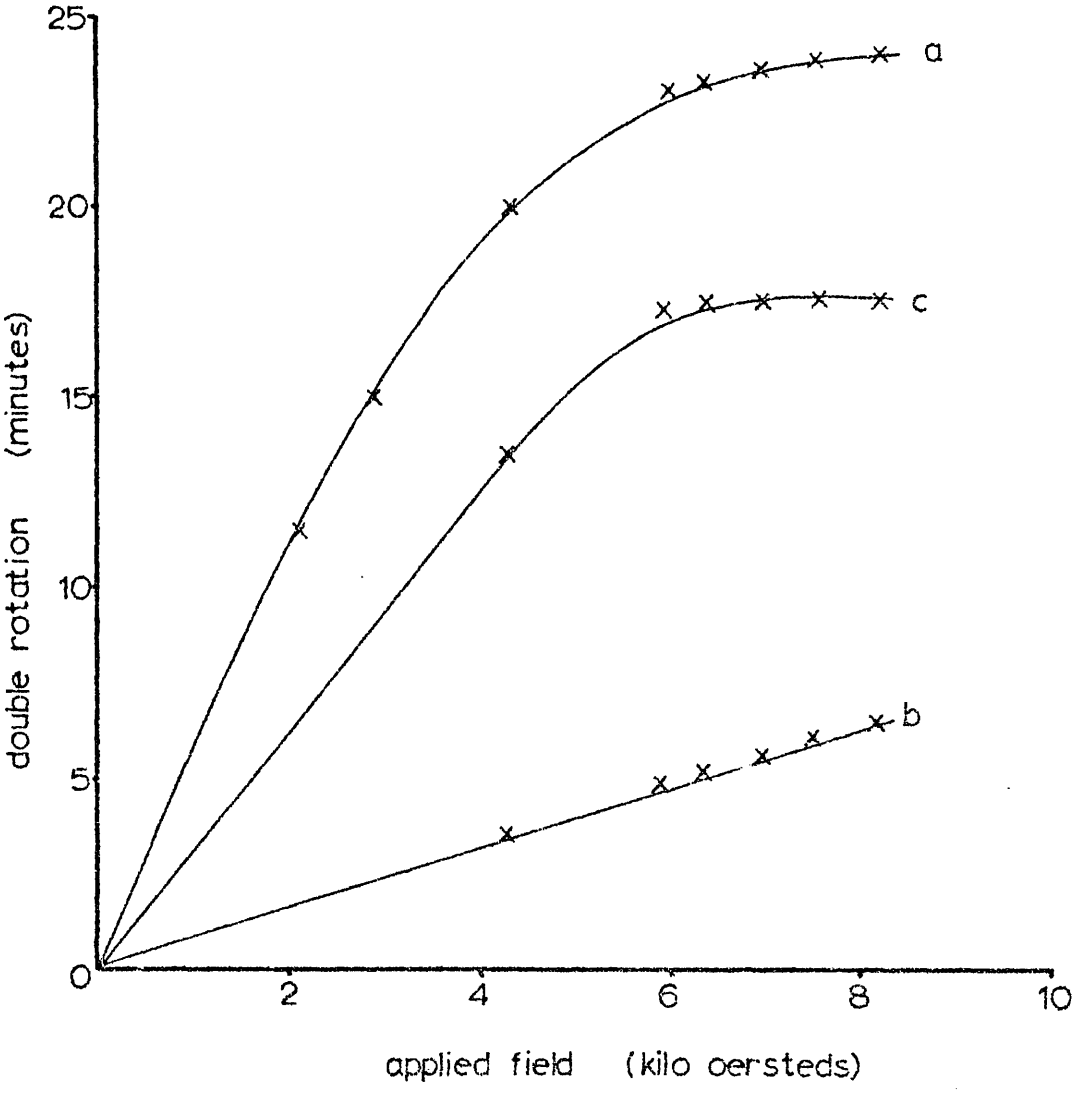

a quartz + film

b quartz

c corrected curve for film

Example graph

(Figure 7.3)

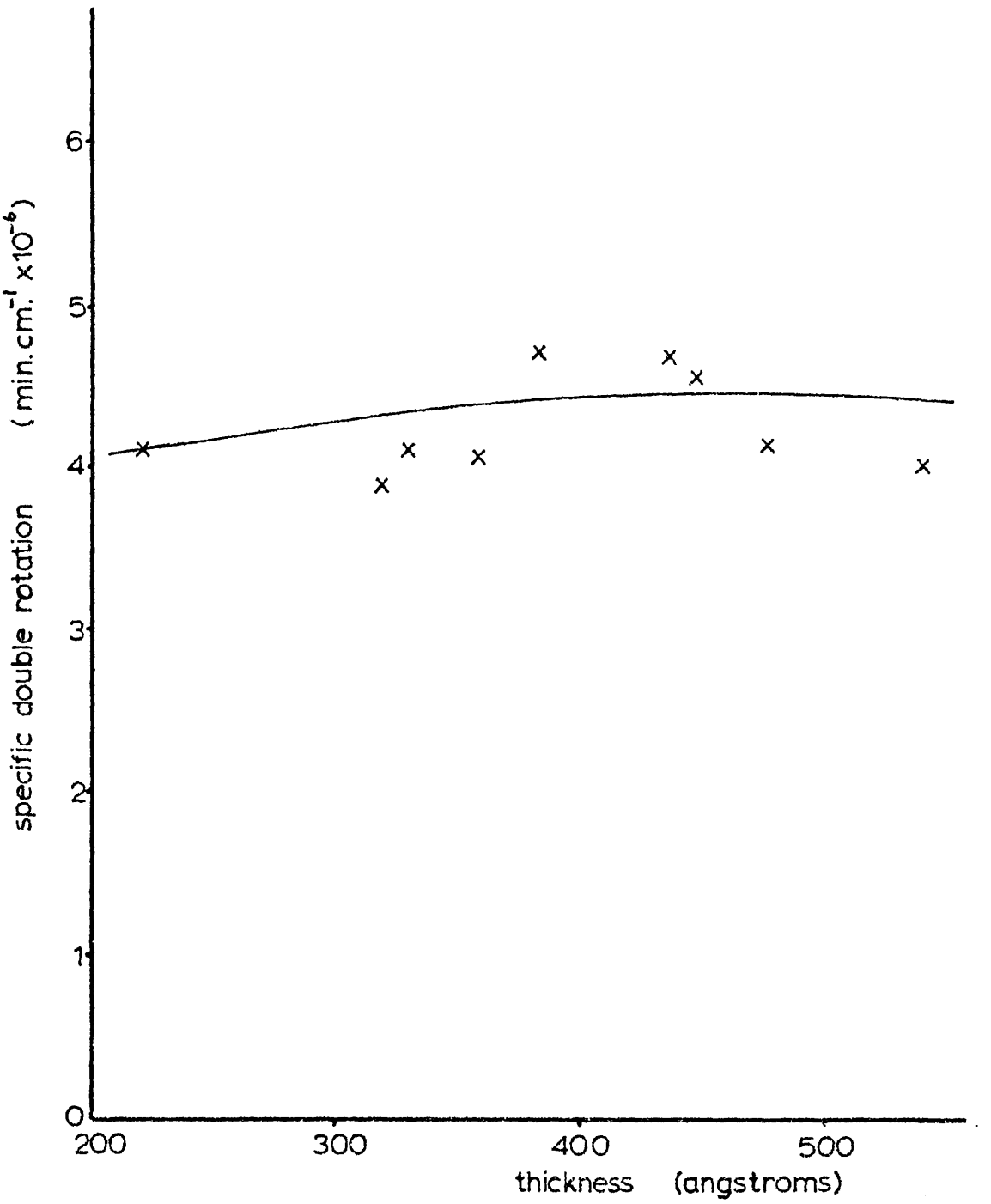

Specific double rotation against thickness

(Figure 7.4)

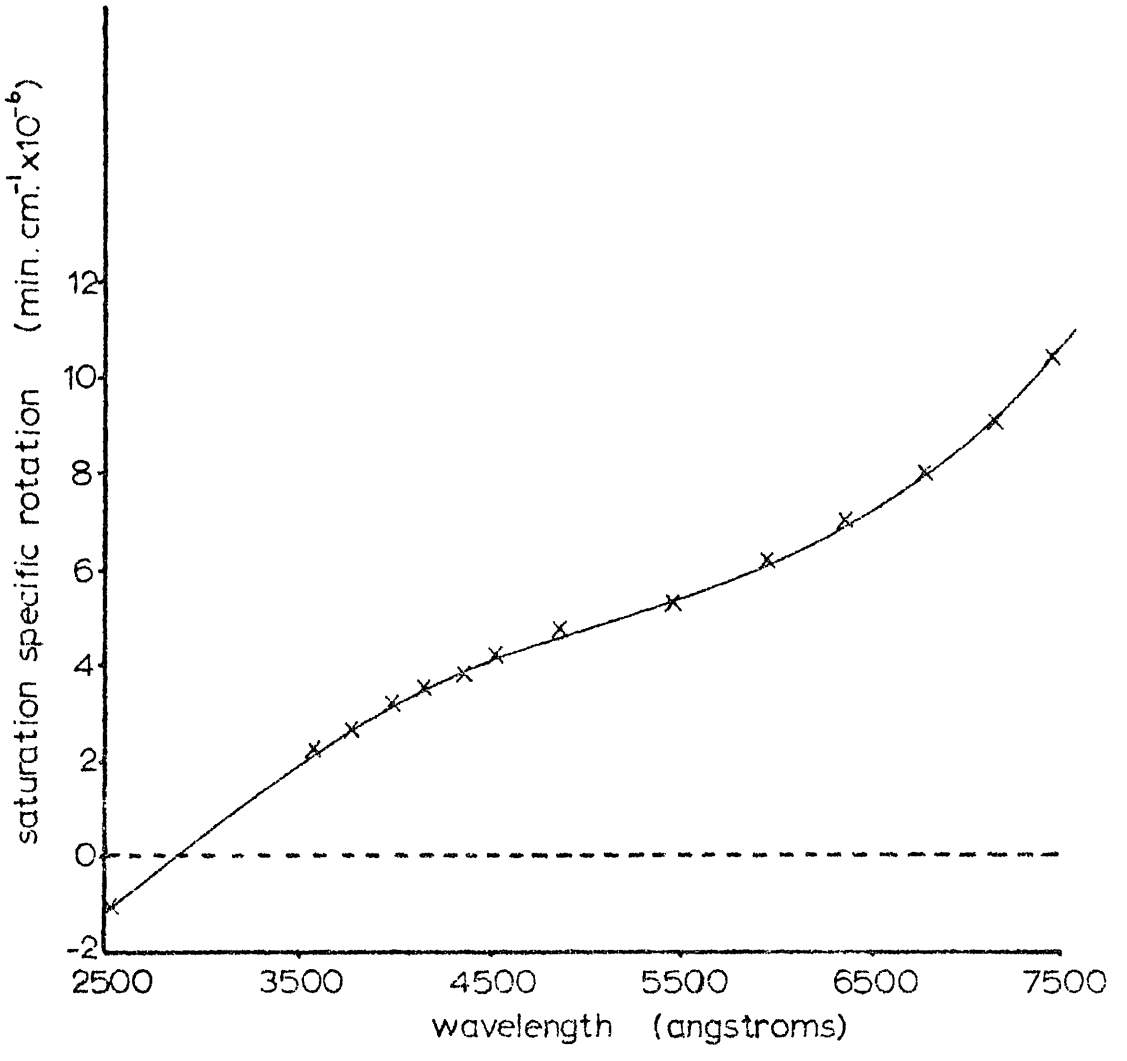

Dispersion curve for 448Å nickel film

(Figure 7.5)

for one specimen over the wavelength range 2500 Å to 7500 Å. The dispersion results for all specimens measured are shown in Figure 7.6 and compared with the results of earlier workers in Figure 7.7.

7.4 Discussion on dispersion

The principal features of Figures 7.6 and 7.7 may be summarized as follows:

(a) The curve for monocrystalline (110) films is similar in shape to those obtained by other workers for polycrystalline films and passes roughly through the middle of the spread of previous results.

(b) In the spectral range examined, a single maximum is observed at 9200 Å. (Clemens and Jaumann (1963) found indications of a maximum in the region of 10,000Å.) Many more experimental points were obtained in this work in order to trace the dispersion curve more accurately. No additional maxima or minima were detected in this range.

(c) The Faraday rotation is observed to change sign in the region of 3000 Å.

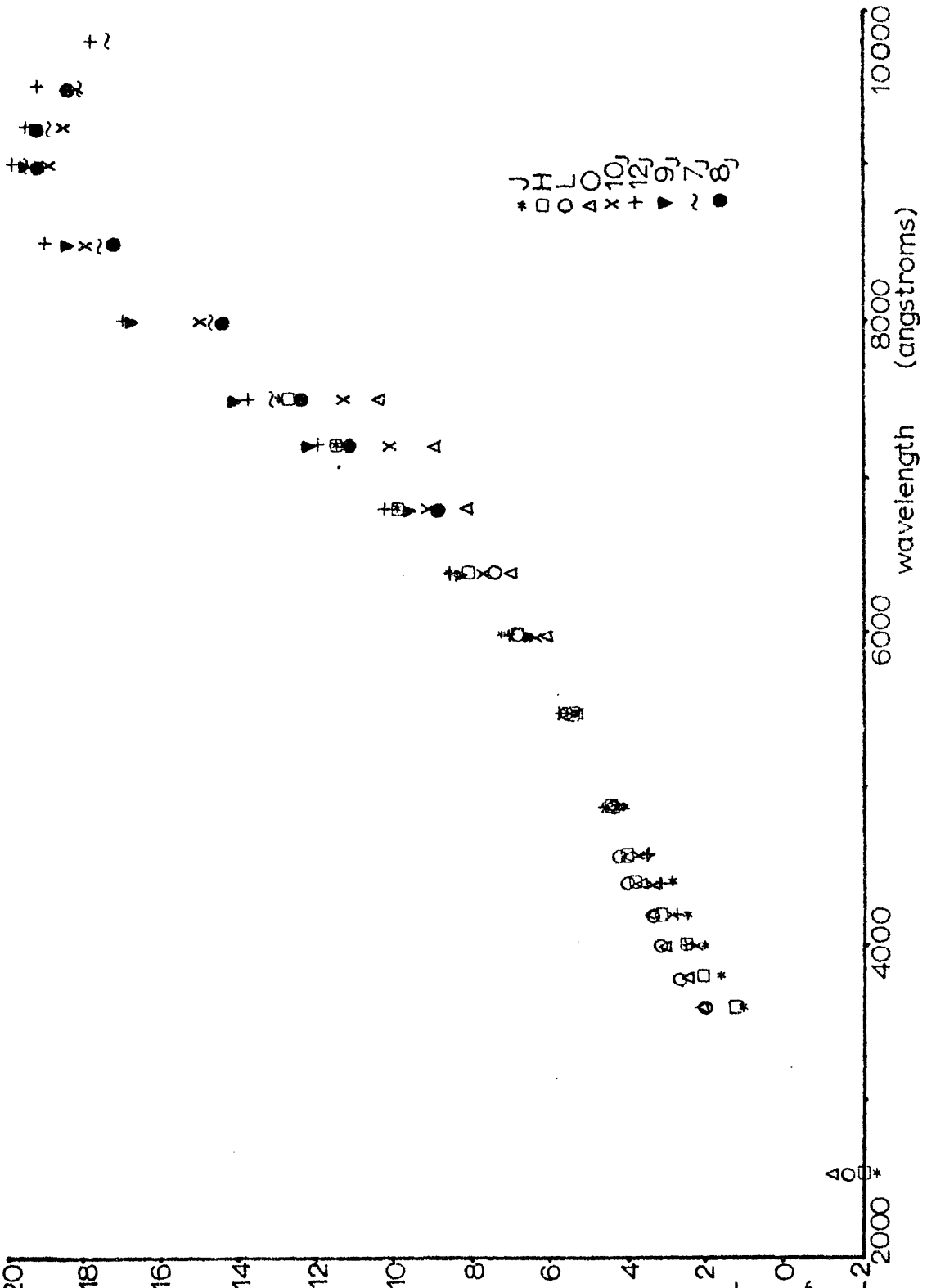
wavelength (angstroms)
10000
8000
6000
4000
2000
saturation specific rotation (min.cm.$^{-1}$ x10^{-6})
20
18
16
14
12
10
8
6
4
2
0
-2

(Figure 7.6)

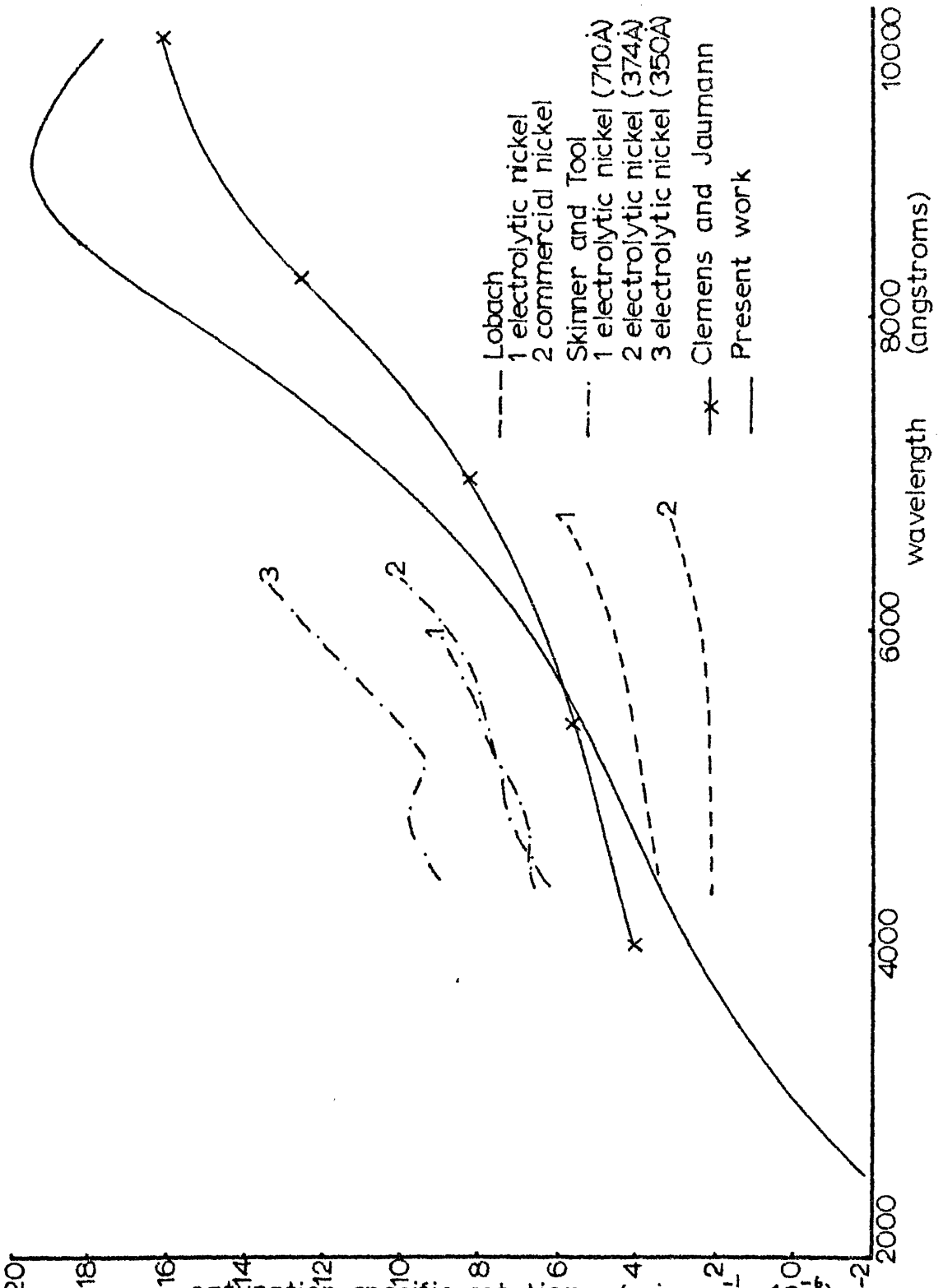
Lobach
1 electrolytic nickel
2 commercial nickel
Skinner and Tool
1 electrolytic nickel (710Å)
2 electrolytic nickel (374Å)
3 electrolytic nickel (350Å)
Clemens and Jaumann
Present work
1
2
3
1
2
20
18
16
14
12
10
8
6
4
2
0
-2
2000
4000
6000
8000
10000
wavelength (angstroms)
saturation specific rotation (min.cm.$^{-1}$ x10^{-6})

(Figure 7.7)

It is interesting to consider these new results in relation to existing theoretical work, especially as Argyres (1955) in fact predicted a change in sign of the Faraday rotation in nickel. Equation (1.18) gave an expression for the polarizability tensor

$$\sigma_1 = -\frac{4ec}{m}\left[\sum_{m>n}\left(\frac{Q_{mn}}{\omega_{mn}^2 - \omega^2}\right)_{av}\right] J$$

which after further approximations as to the structure of the wave functions and energy bands, may be expressed as

$$|\sigma_1| \sim \frac{1.0 \times 10^{11} A (E_n - E_m)(E_\ell - E_m)}{\Delta E\,[(E_m - E_n)^2 - \hbar\omega^2]} J \qquad (7.1)$$

Argyres used values, given by Slater (1936), for

$$(E_m - E_n) \sim 4eV = 6.4 \times 10^{-12} \text{ erg}$$

$$\Delta E \sim 1eV = 1.6 \times 10^{-12} \text{ erg}$$

$$E_m - E_\ell \sim 5eV = 8.0 \times 10^{-12} \text{ erg}$$

which gives a value of

$$|\sigma_1| \sim 1.0 \times 10^{28} A J ,$$

using $\lambda = 6000$ Å and hence $\hbar\omega = 3.0 \times 10^{-12}$ erg . For a singularity

to occur

$$(E_m - E_n)^2 = \hbar^2\omega^2$$

in equation (7.1), i.e.

$$\hbar\omega = 6.4 \times 10^{-12} \text{ erg}$$

or

$$\lambda = 2800 \text{ Å} .$$

The Faraday rotation should therefore fall to zero at this wavelength. This prediction is confirmed by the experimental dispersion curve (Figure 7.7), which changes sign at 3000 Å.

Another feature of the experimental results is the maximum in Faraday rotation which occurs at 9200 Å. Clemens and Jaumann's (1963) curve indicates a maximum in the region of 10,000 Å but there are experimental points only at 8200 Å and 10,100 Å in this wavelength range.

A maximum in Faraday rotation is to be expected from the work of Argyres (1955), but it is difficult to predict quantitatively where this maximum should occur because of approximations made to the structure of the wave functions and the energy bands. A second maximum in the rotation has been found at 5μ, and this has been investigated by Krinchik and Nuralieva (1959).

7.5 Anisotropy of Faraday effect

The azimuth of the plane of polarization of the incident light was varied by changing the angle of the polarizer. The angle of the Wollaston prism was also changed by inserting wedges of various sizes underneath the prism to coincide with the angle through which the polarizer was rotated. Azimuthal angles ϕ were measured between the E vector in the incident light and the <001> direction in the plane of the film.

Again the rotation was measured for a series of different values of field, with the current through the electromagnet increasing by stages until saturation was reached. For each reading the values of the rotation for zero field and for the field in the two opposite directions were measured.

Graphs were plotted for each specimen showing the rotation for the field in one direction θ_+ and the rotation for the field in the opposite direction θ_-, as a function of ϕ. The specific rotations, derived from values of $\frac{1}{2}(\theta_+ + \theta_-)$, were also plotted against ϕ. Examples of these graphs are shown in Figures 7.8 - 7.15. These graphs will be referred to as group A. In general, $\theta_+ \neq \theta_-$, and in view of this, graphs of $(\theta_+ - \theta_-)$ against ϕ were plotted (group B). These indicated that an azimuth-dependent rotation of the incident light occurred even at zero applied field. These 'group B' curves are discussed further in the section 7.11.

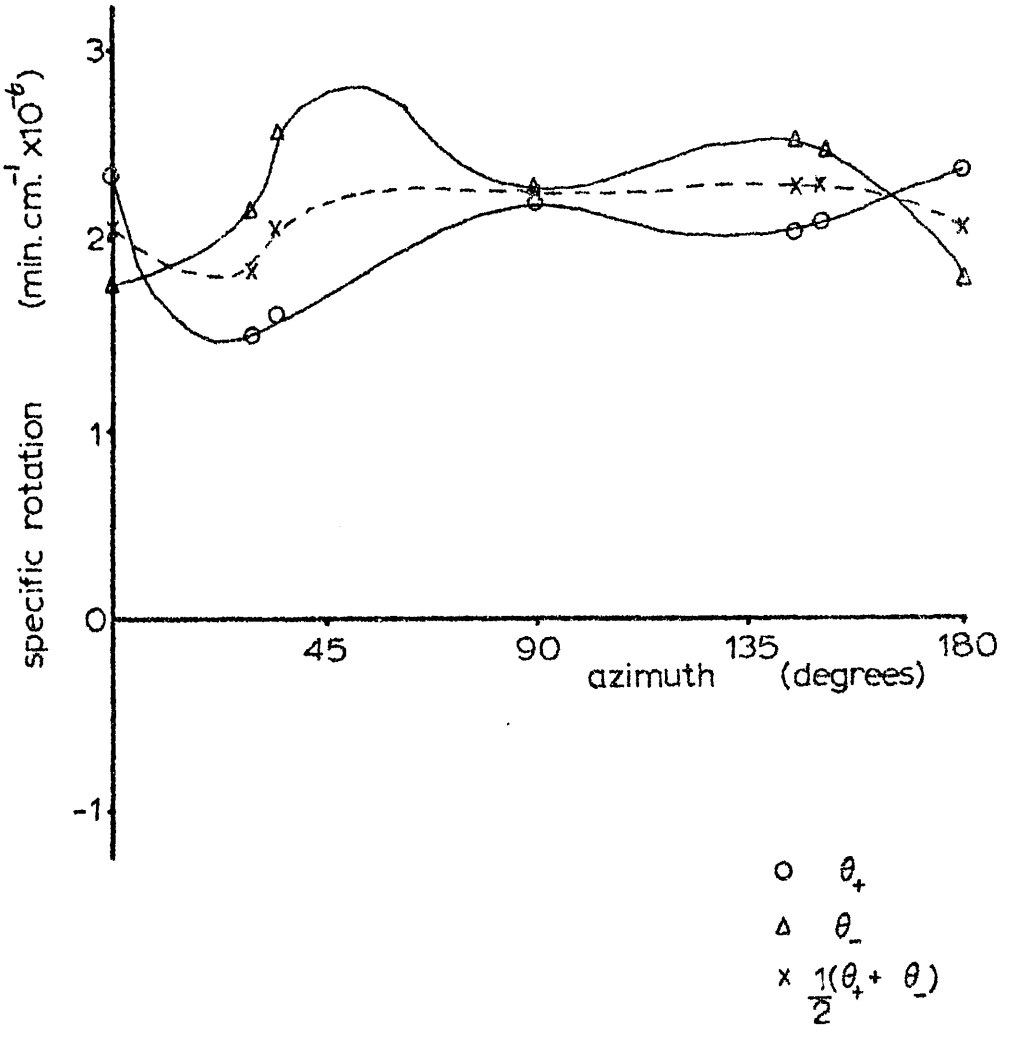

Experimental results (film 7)

(Figure 7.8)

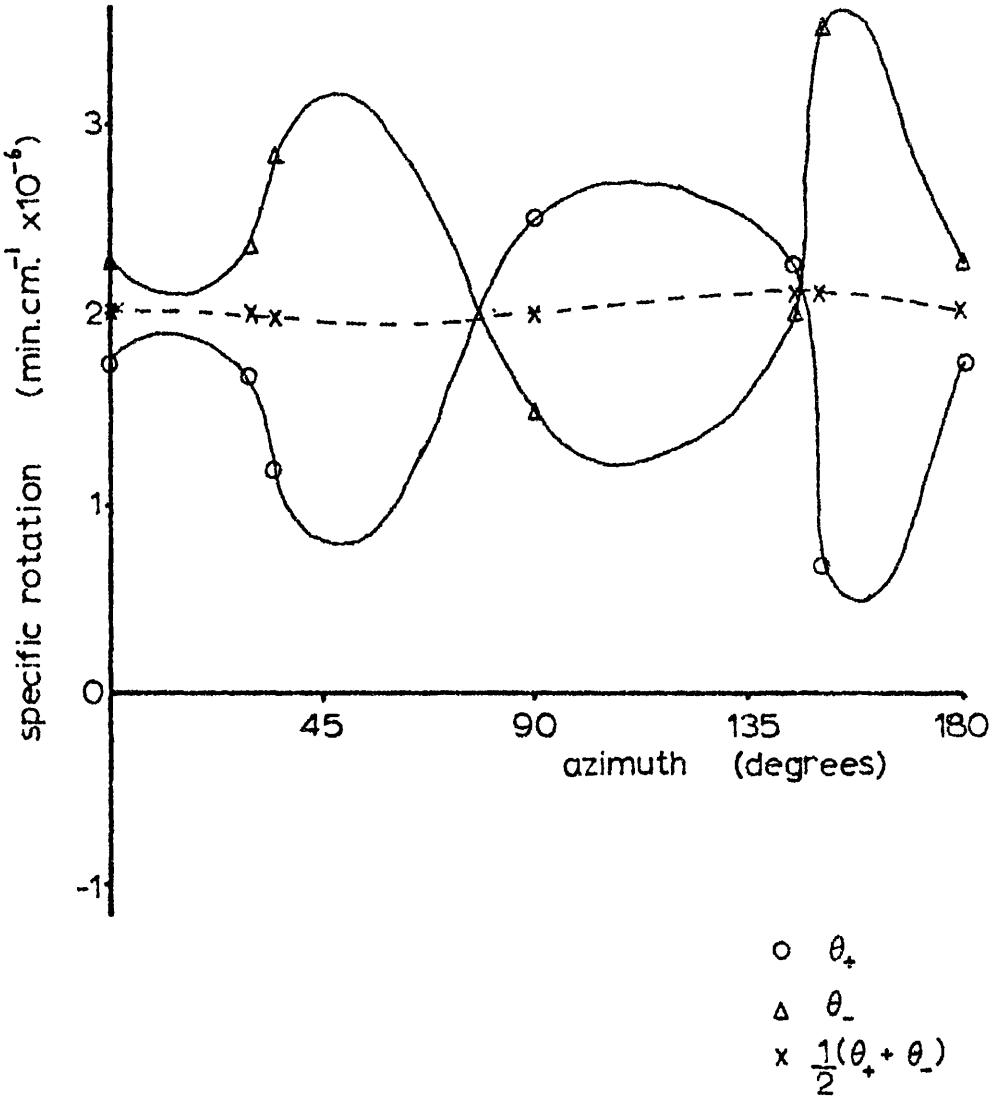

Experimental results (film 8_J)

(Figure 7.9)

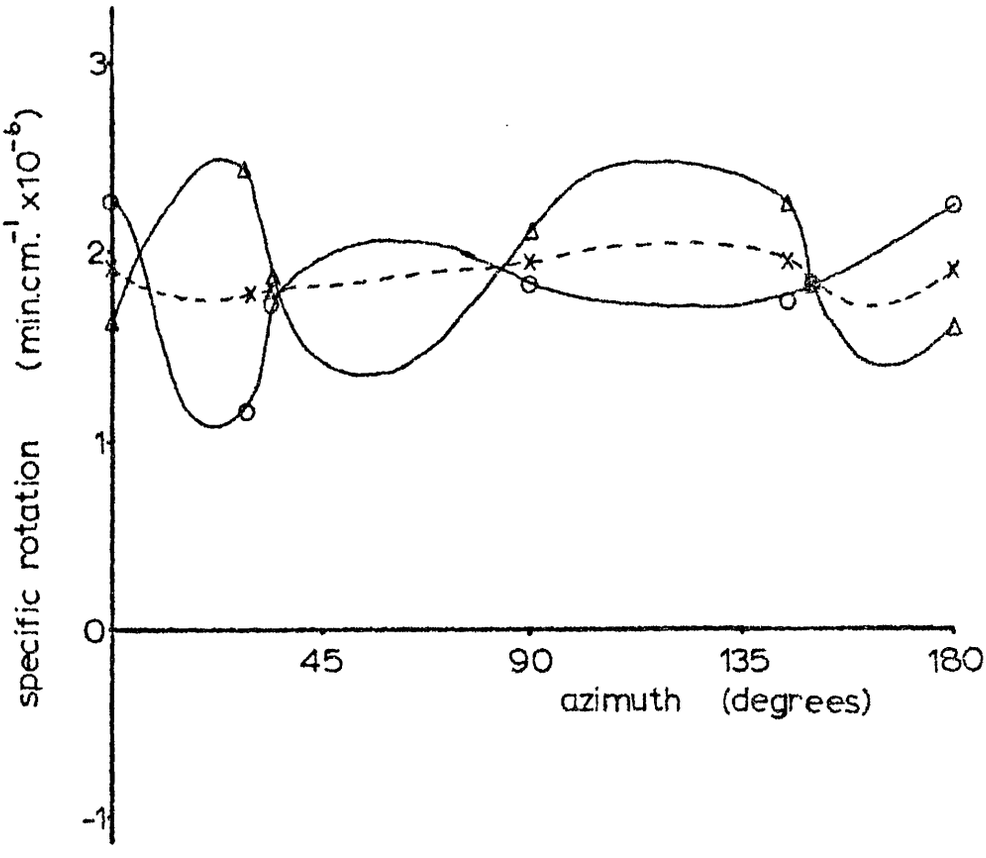

Experimental results (film 9_J)

(Figure 7.10)

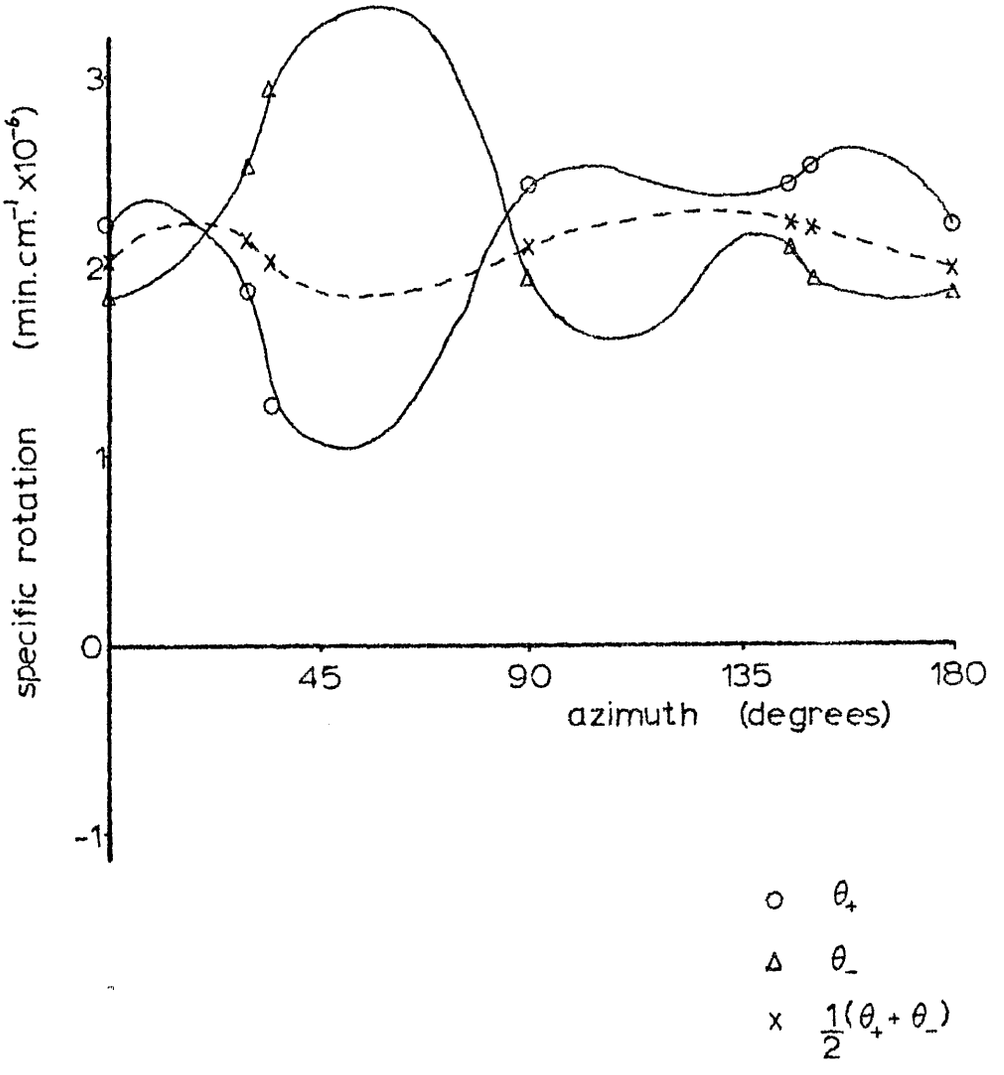

Experimental results (film 10$_j$)

(Figure 7.11)

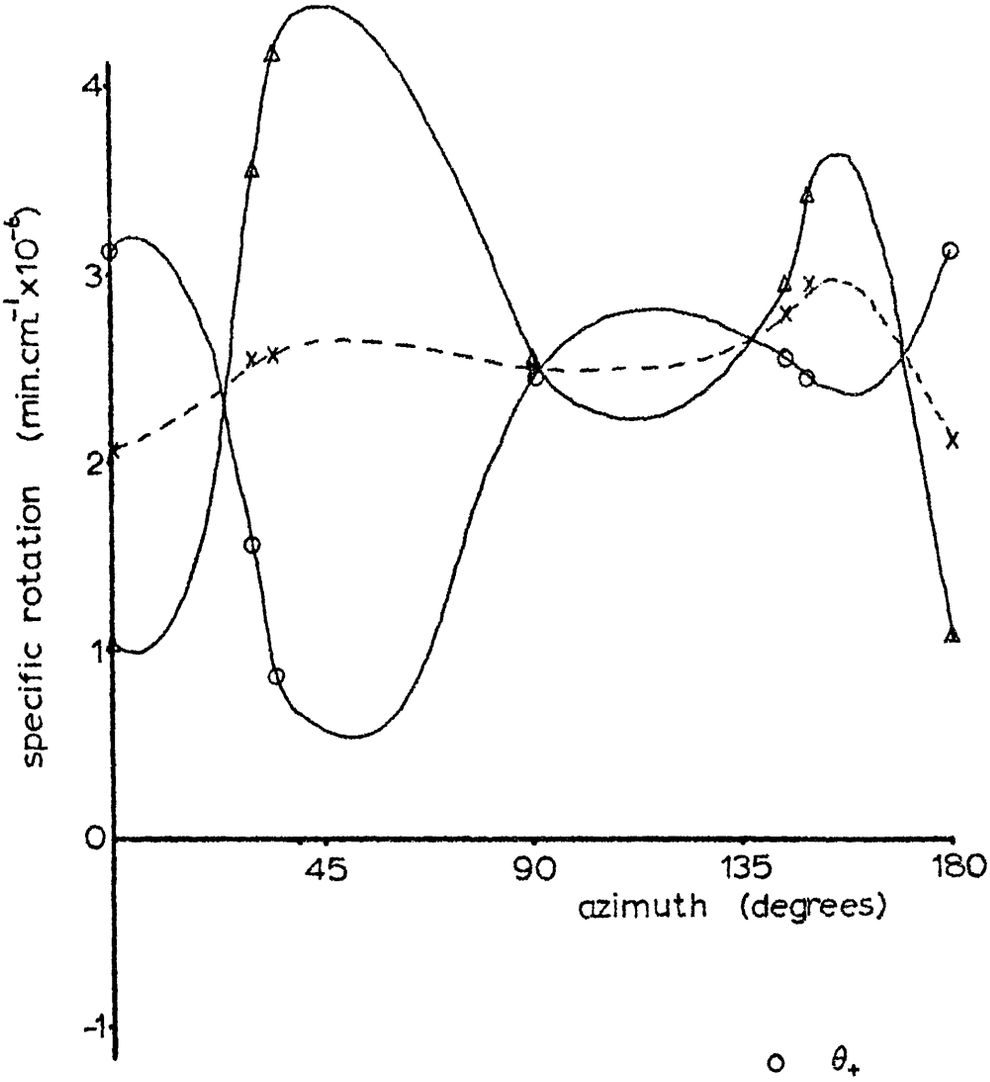

Experimental results (film 12_J)

(Figure 7.12)

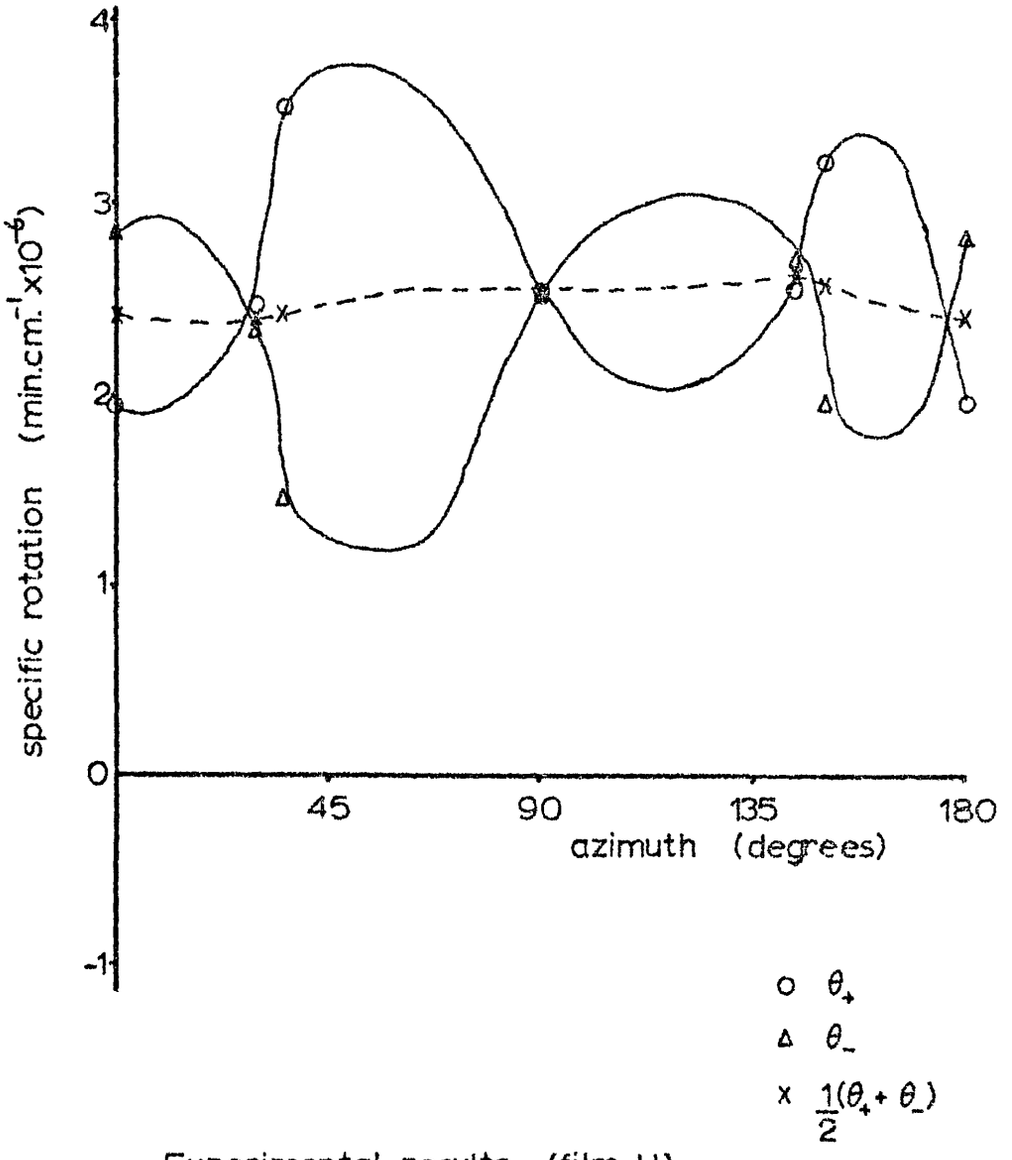

Experimental results (film H)

(Figure 7.13)

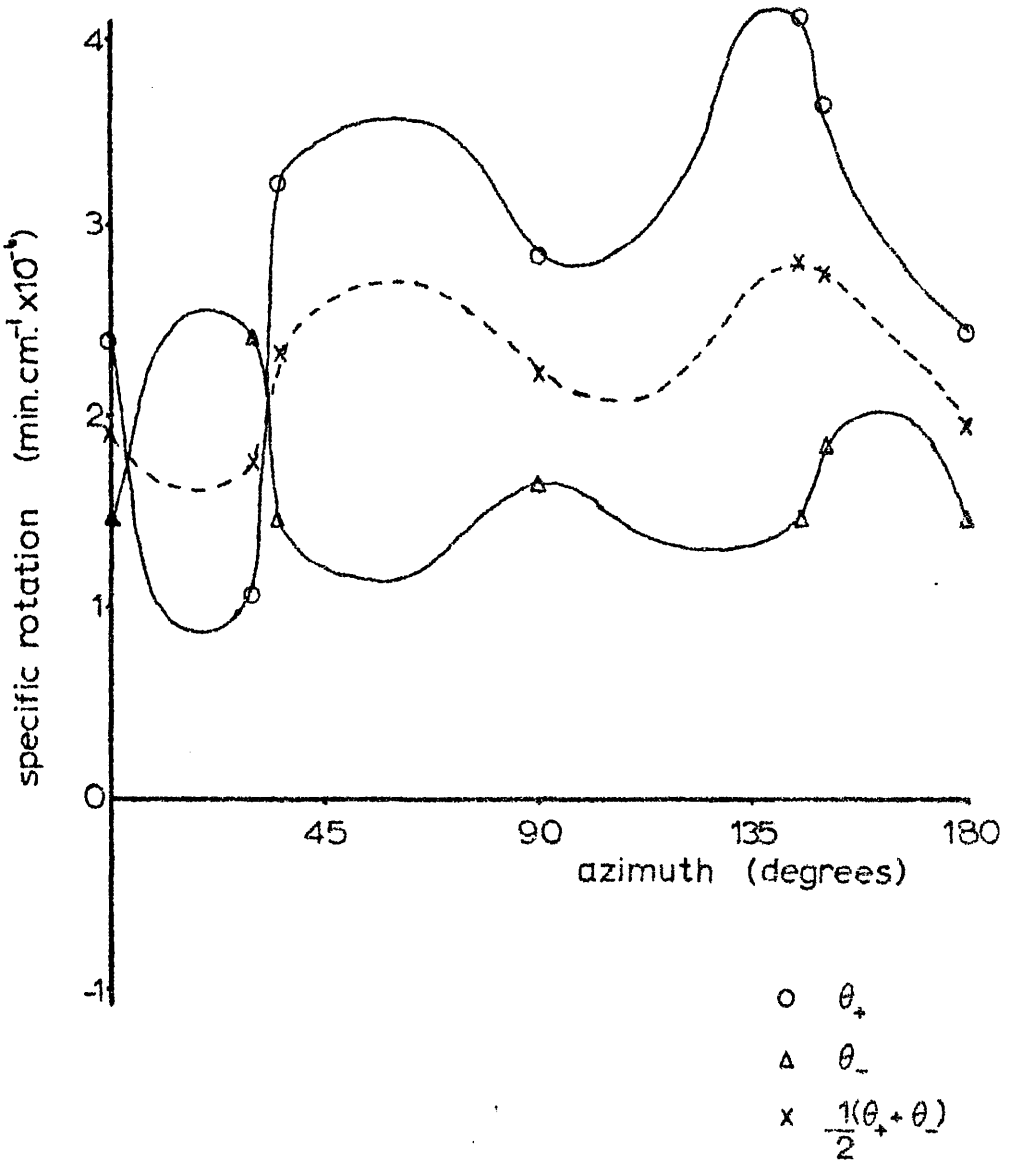

Experimental results (film J)

(Figure 7.14)

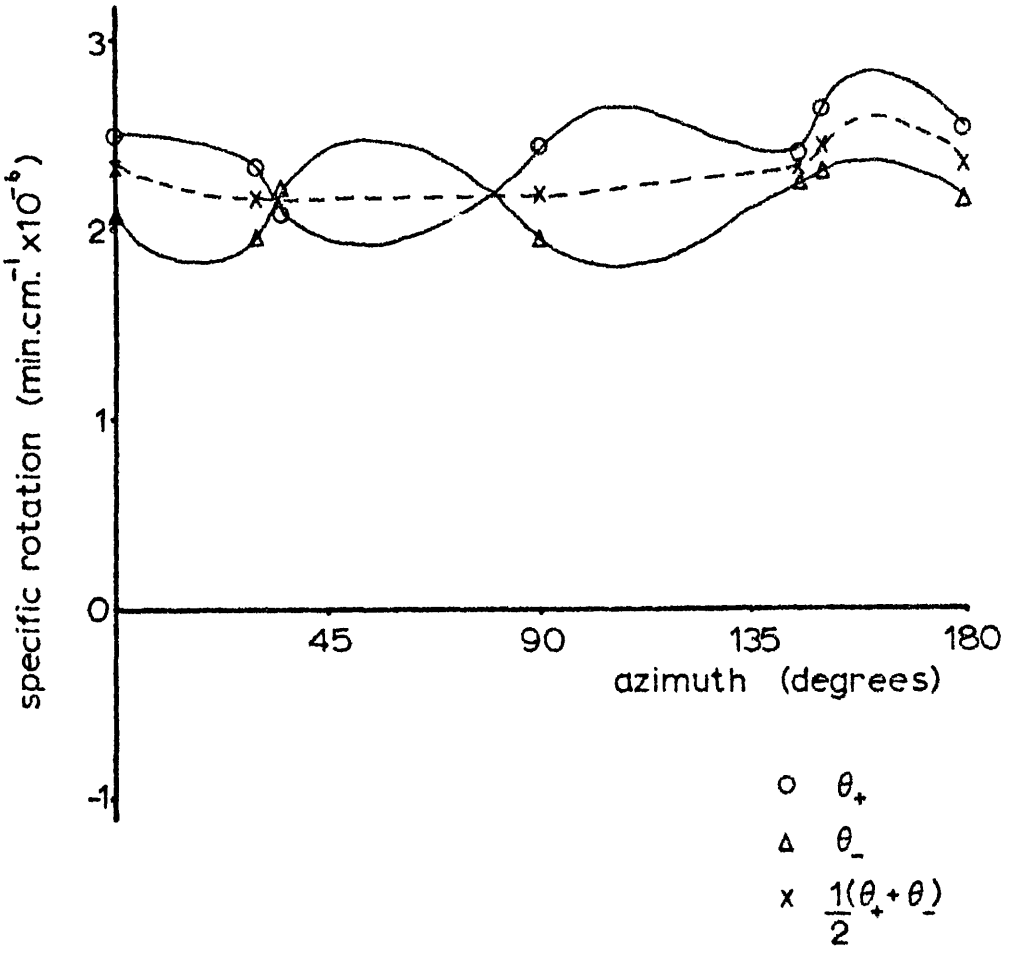

Experimental results (film L)

(Figure 7.15)

7.6 Discussion of curves in group A

According to the theory of Medcalf (1965)

$$\theta = \tfrac{1}{2}\,\tilde{\beta}\, z_o(1 - 0.05\,\beta_3 \sin 2\phi) \qquad (7.2)$$

where $\tilde{\beta}$ = numerical constant having an approximate value of $3.1 \times 10^3\ cm^{-1}$.

z_o = thickness of film

β_3 = direction of field

ϕ = azimuthal angle of polarization of incident light.

This variation of θ is shown in Figure 7.16. Curve 'a' represents the theoretical value of θ with the field in one direction, curve 'b' represents θ with the field in the opposite direction. The straight line parallel to the axis is the theoretical value of the quantity $\frac{1}{2}(\theta_+ + \theta_-)$. Equation (7.2) represents a sinusoidal variation of θ about a mean with an amplitude of about 5%, and stationary values at $\phi = \pm \frac{\pi}{4}$ and $\phi = \pm \frac{3\pi}{4}$. The theory does not indicate which sign is to be associated with the maximum and which with the minimum, since the sign of the parameters is arbitrary, but it is clear that the maximum and minimum will be interchanged by reversing the field direction $(\beta_3 = \pm 1)$. The theory therefore

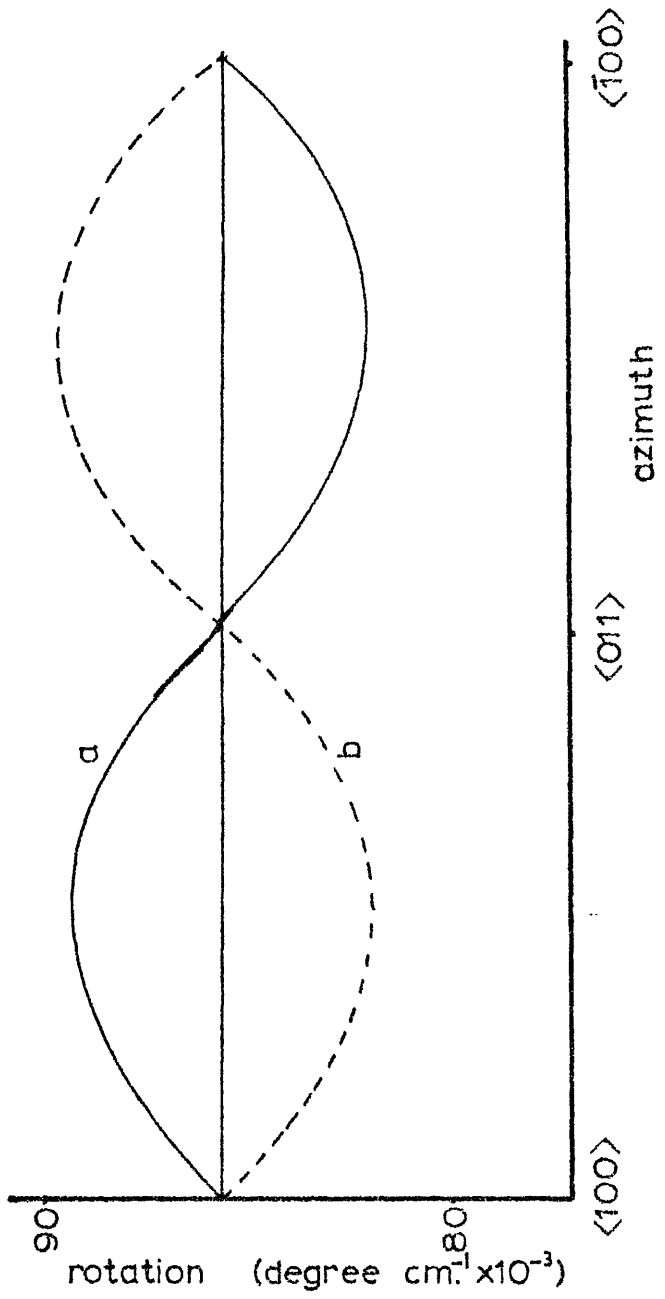

Theoretical results of Medcalf

(Figure 7.16)

predicts that $\frac{1}{2}(\theta_+ + \theta_-)$ plotted against ϕ should produce a straight line $\frac{1}{2}(\theta_+ + \theta_-) = \frac{1}{2}\bar{\beta} z_o$, independent of ϕ.

By comparing the theoretical curves with the experimental ones, it is evident that the latter are not sinusoidal, nor obviously consistent in shape, but there are nevertheless a number of similarities to Medcalf's graphs. In films 8_J, 9_J, 10_J, H and L (Figures 7.9, 7.10, 7.11 and 7.15), although lines through the values of θ_+ and θ_- do not have the same shape as the theoretical curves, they do in fact give a reasonable 'mirror image' of one another, indicating a similar variation to that proposed by Medcalf as the field direction changes sign.

In an attempt to correlate the graphs of $\frac{1}{2}(\theta_+ + \theta_-)$ against azimuth, all the curves were superimposed on one diagram (Figure 7.17). From this it was obvious that two curves were different from the rest: curves L and H. They did not show such a large variation in $\frac{1}{2}(\theta_+ + \theta_-)$ as the others, but had higher average specific rotations. Removing these two curves from the graph produced Figure 7.18 and a mean-value curve was drawn from this graph. The average curve has two peaks which fall roughly at 30° and 150° azimuthal angles. These are close to the directions in the specimen plane at which twin boundaries on (111) planes would be expected to lie. A possible correlation was therefore sought between the variation in $\frac{1}{2}(\theta_+ + \theta_-)$ and the percentage of (111) twinning in each sample.

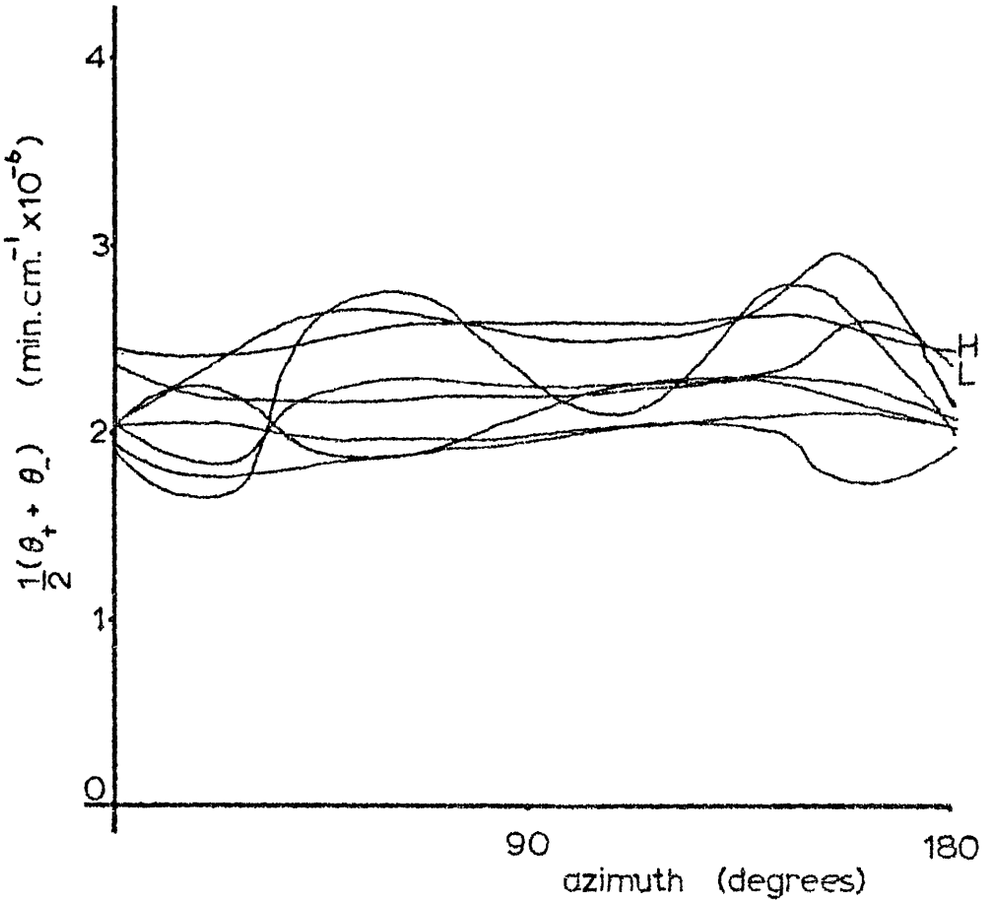

Superimposed graphs of $\frac{1}{2}(\theta_+ + \theta_-)$ against azimuth

(Figure 7.17)

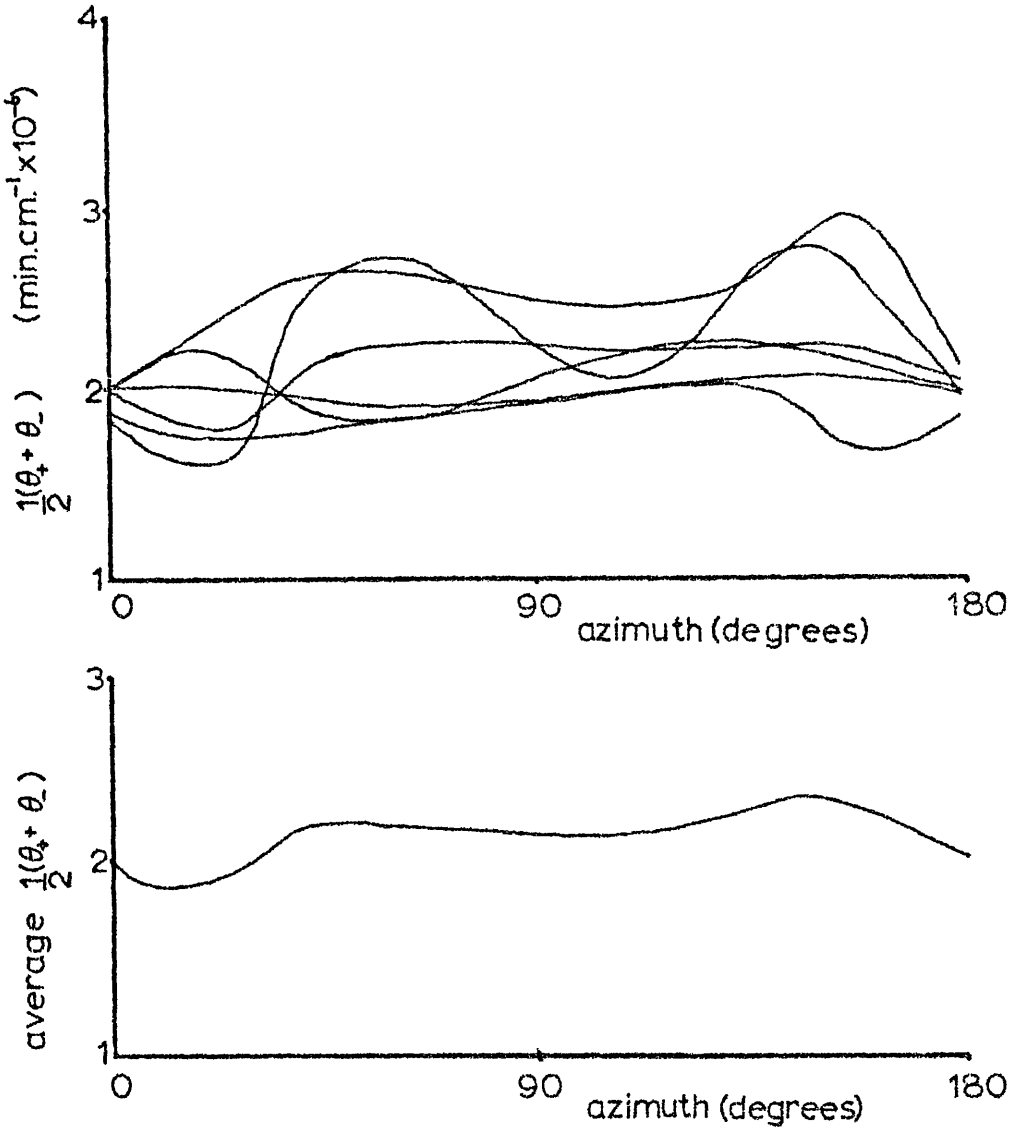

Graphs of $\frac{1}{2}(\theta_+ + \theta_-)$ against azimuth

(Figure 7.18)

A graph of variation in $\frac{1}{2}(\theta_+ + \theta_-)$ with percentage twinning is shown in Figure 7.19. It is not possible to draw any definite conclusions from the graphs owing to the wide scatter. There does appear to be a slight upward trend for the lower values of percentage twinning, sufficient to justify an investigation of the way in which twins might affect the measured rotations. A theory has been developed (M. C. Jones) which takes into account the finite thickness and the degree of twinning in the specimens.

Let (i_x, i_y) be the components of the light vector entering the specimen, and (t_x, t_y) the components of the vector emerging from the specimen. If the specimen has no twinning, the transmission tensor acting on these components is

$$\begin{pmatrix} T_{xx} & T_{xy} \\ T_{yx} & T_{yy} \end{pmatrix}$$

If the specimen is 100% twinned, the matrix has the form

$$\begin{pmatrix} {}^{T}T_{xx} & {}^{T}T_{xy} \\ {}^{T}T_{yx} & {}^{T}T_{yy} \end{pmatrix}$$

If a fraction μ of the whole area of the specimen is twinned, and the incident azimuth angle of the polarized light is $\alpha = (\theta + \frac{\pi}{4})$,

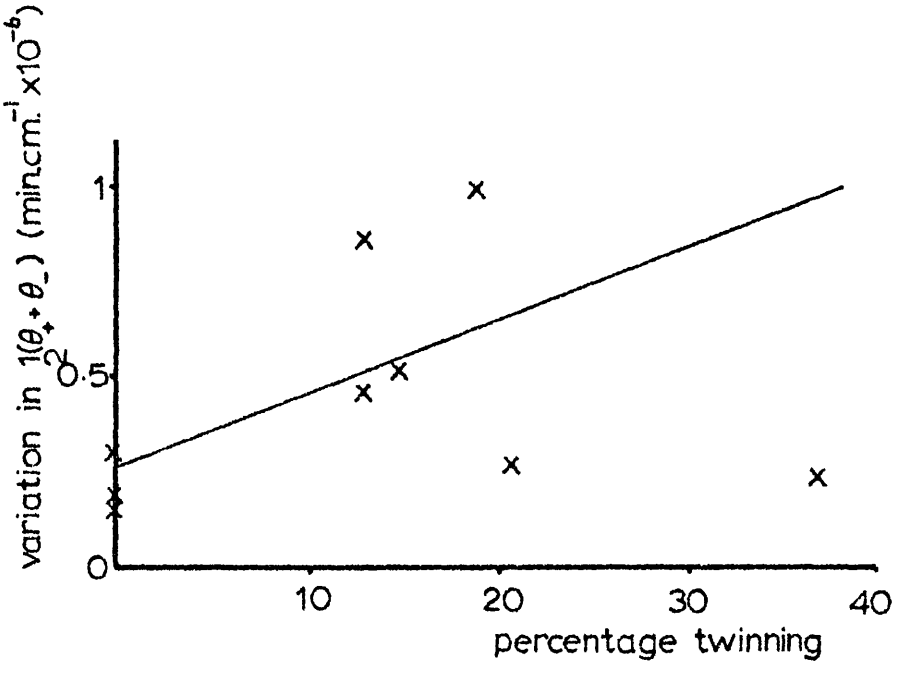

Graph of variation in $\frac{1}{2}(\theta_+ + \theta_-)$ with twinning

(Figure 7.19)

then for the polarimeter to see equal signals transmitted through the Wollaston prism, the following formula must hold

$$(1-\mu)(T_{xx}\cos\alpha + T_{xy}\sin\alpha)^2 + \mu(T^T_{xx}\cos\alpha + T^T_{xy}\sin\alpha)^2$$

$$= (1-\mu)(T_{yx}\cos\alpha + T_{yy}\sin\alpha)^2 + \mu(T^T_{yx}\cos\alpha + T^T_{yy}\sin\alpha)^2$$

This gives an expression for α (or θ) in terms of the components of the two transmission tensors. Expressions for these components may be found in Ah-Sam and Jones (1970). Examples of computed curves are given in Figures 7.20 and 7.21, with the corresponding experimental points.

According to this theory the effect of twinning is to move the position of the maxima and minima of the θ_+ and θ_- curves, but not to alter the amplitude of the rotations. Some such alteration would, in fact, be expected in view of Miller's result (1962) on Faraday rotation in films grown on different planes. Some agreement with theory was obtained for films in which there was practically no twinning (Figure 7.20) but the shift in maxima and minima predicted for twinned films could not be established from the results obtained.

We must conclude that although there is some tentative evidence (Figure 7.19) that twinning is in some way associated with the anisotropy observed in the Faraday rotation measured in the nickel films, no clear explanation emerges from this association. Other

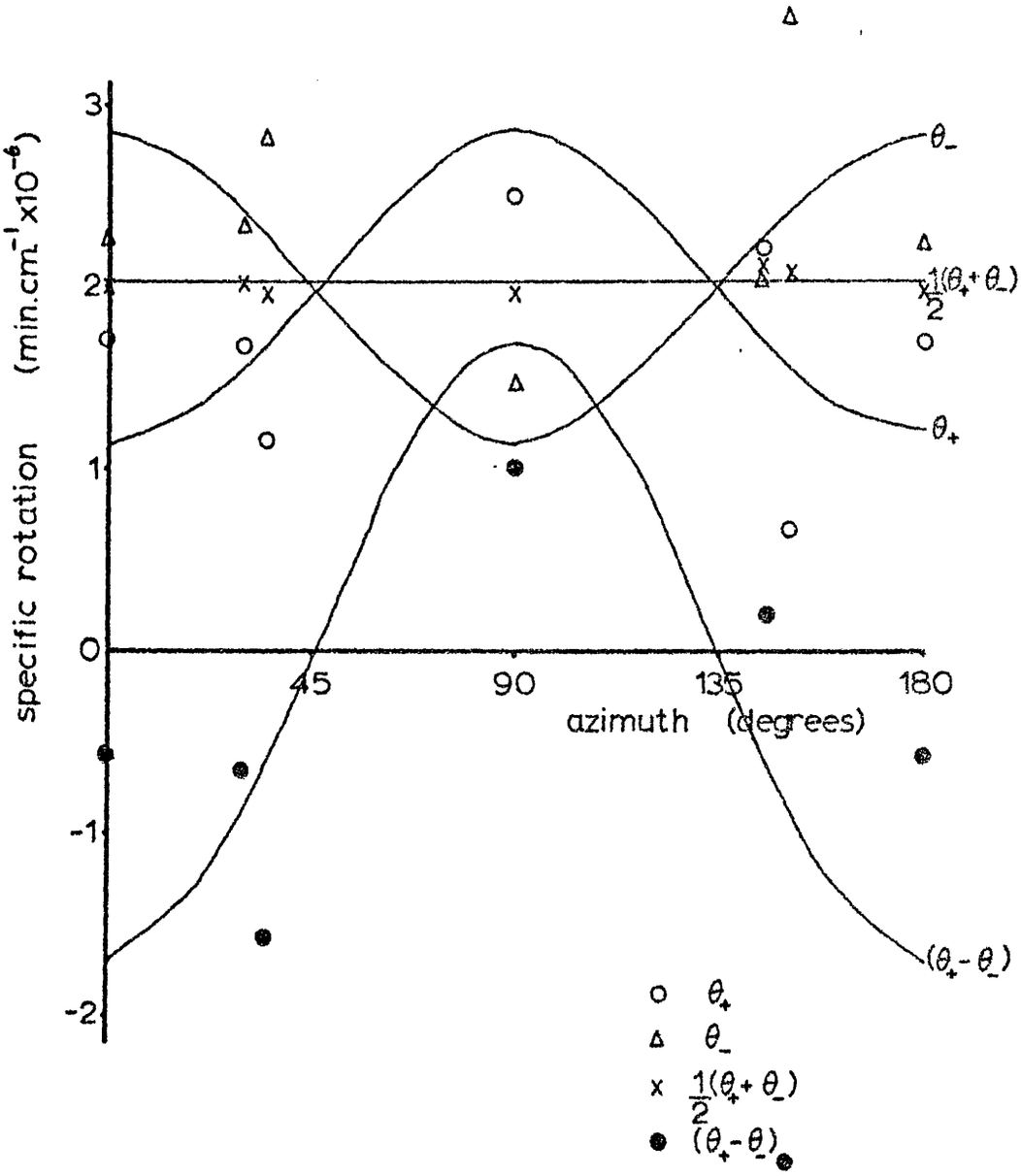

Computed and experimental results (film 8$_j$)

(Figure 7.20)

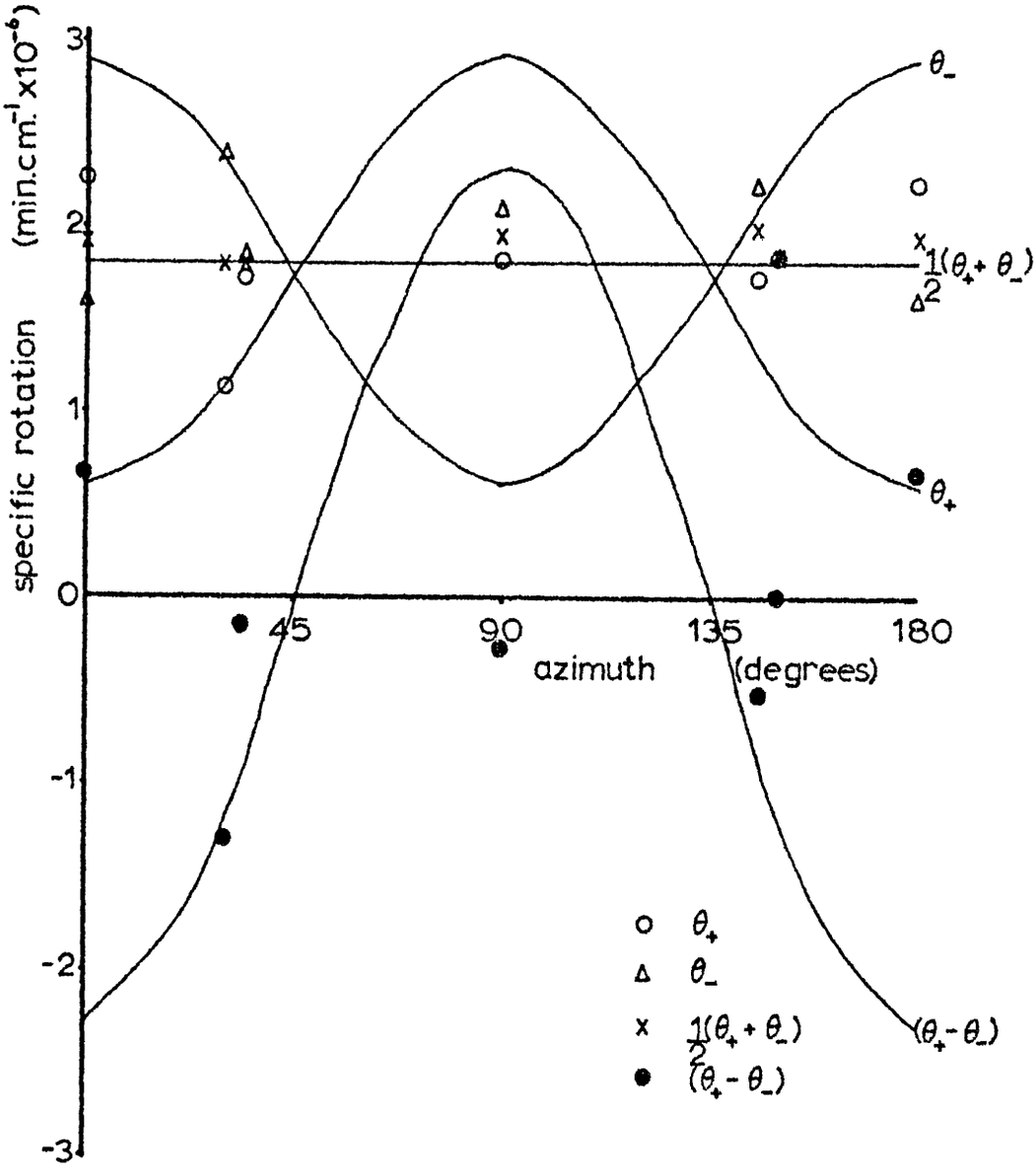

Computed and experimental results (film 9_J)

(Figure 7.21)

variable and unknown factors must also be responsible, since there are some differences in degree of anisotropy from specimen to specimen. One might speculate upon the possible effects of variable film structure, defects and local strains in the region of twin boundaries, but at present no further evidence is available.

7.7 Voigt rotation

In general, when a plane polarized electromagnetic wave is incident upon a body in a magnetic field, the transmitted wave becomes elliptically polarized with the major axis rotated with respect to the direction of polarization of the incident wave. When the magnetic field is perpendicular to the direction of propagation of the wave this phenomenon is called the Voigt effect.

7.8 Voigt effect in quartz

Quartz cover slips, of the same type used as substrates for the nickel films, were placed in position between the pole pieces of the electromagnet so that the plane of each cover slip was parallel to the magnetic field, and perpendicular to the incident light. The magnetic field, the wavelength and plane of polarization of the incident light were varied, but under no conditions was there any measurable Voigt rotation for the quartz cover slip.

7.9 Voigt effect in nickel

Medcalf (Ph.D. Thesis 1965) suggested that the Voigt rotation would be a maximum when the angle between the direction of the magnetic field and the direction of polarization of the incident light was $\frac{\pi}{4}$, and when the propagation and magnetic field directions were along <110>-type crystal directions.

The nickel film was placed between the pole pieces of the magnet such that the above conditions were obeyed. The Voigt rotation was measured for different values of the applied field, and the results from a typical specimen are shown in Figure 7.22. The measurements were repeated for different wavelengths as shown in Figure 7.23.

A graph of saturation rotation against wavelength is shown in Figure 7.24. Figure 7.25 shows the variation of specific saturation rotation with wavelength for several samples and Figure 7.26 gives the relation between specific saturation rotation and thickness at a given wavelength (λ = 5460 $\mathring{A}$).

The nickel film was placed with the angle between the directions of the magnetic field and the polarization of the incident wave at 0 and $\frac{\pi}{2}$ but no rotation was detected, thus confirming Medcalf's prediction.

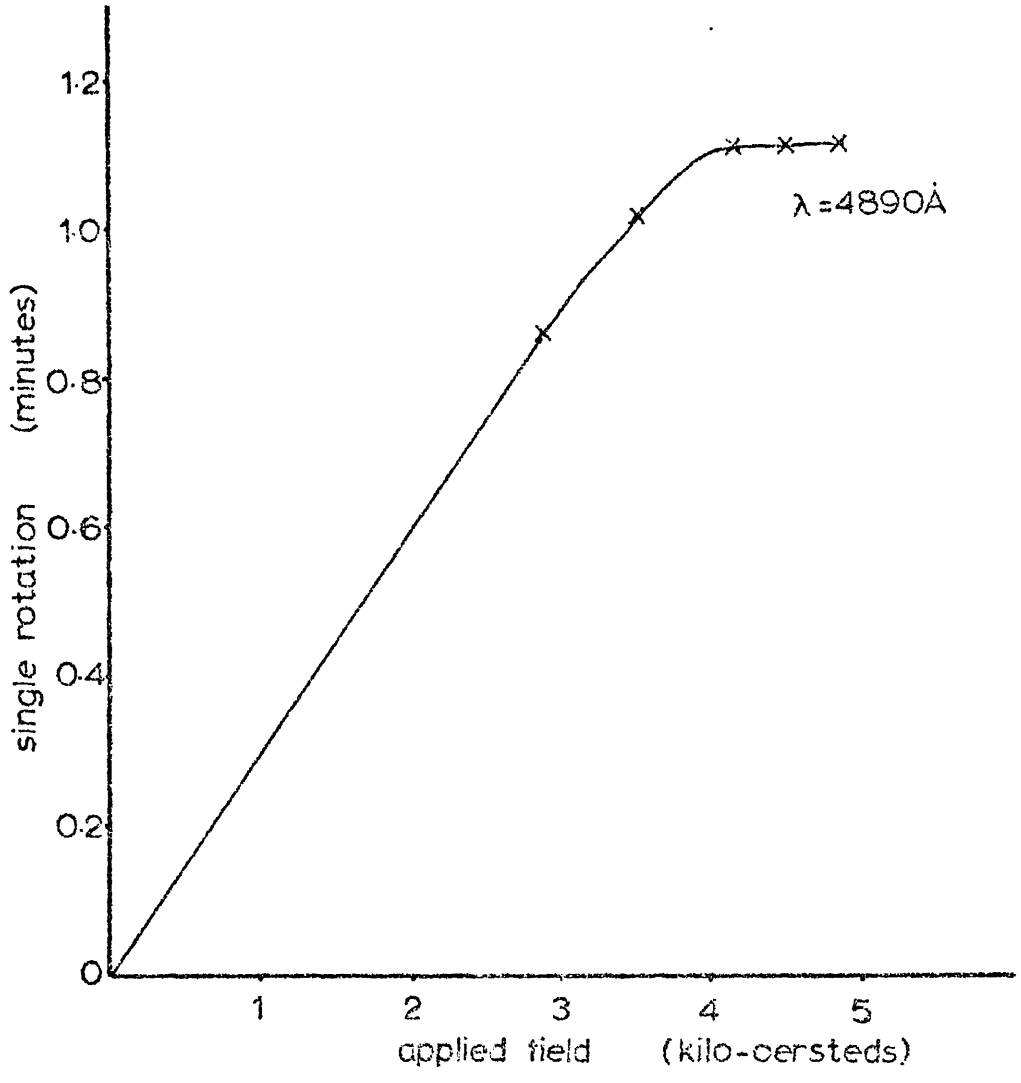

Voigt effect experimental results (film T_j 480Å)

(Figure 7.22)

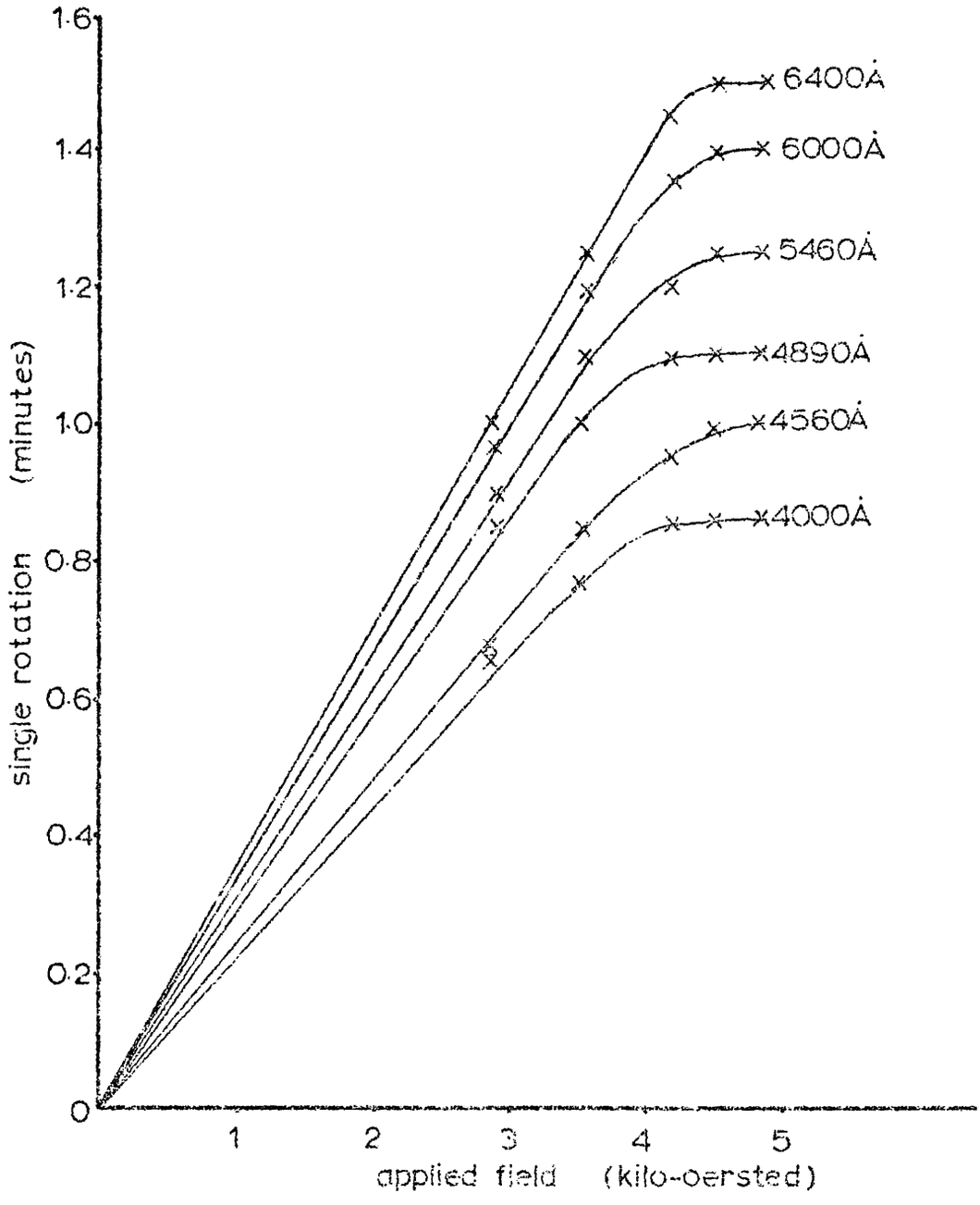

Voigt effect experimental results (film T_1 480Å)

(Figure 7.23)

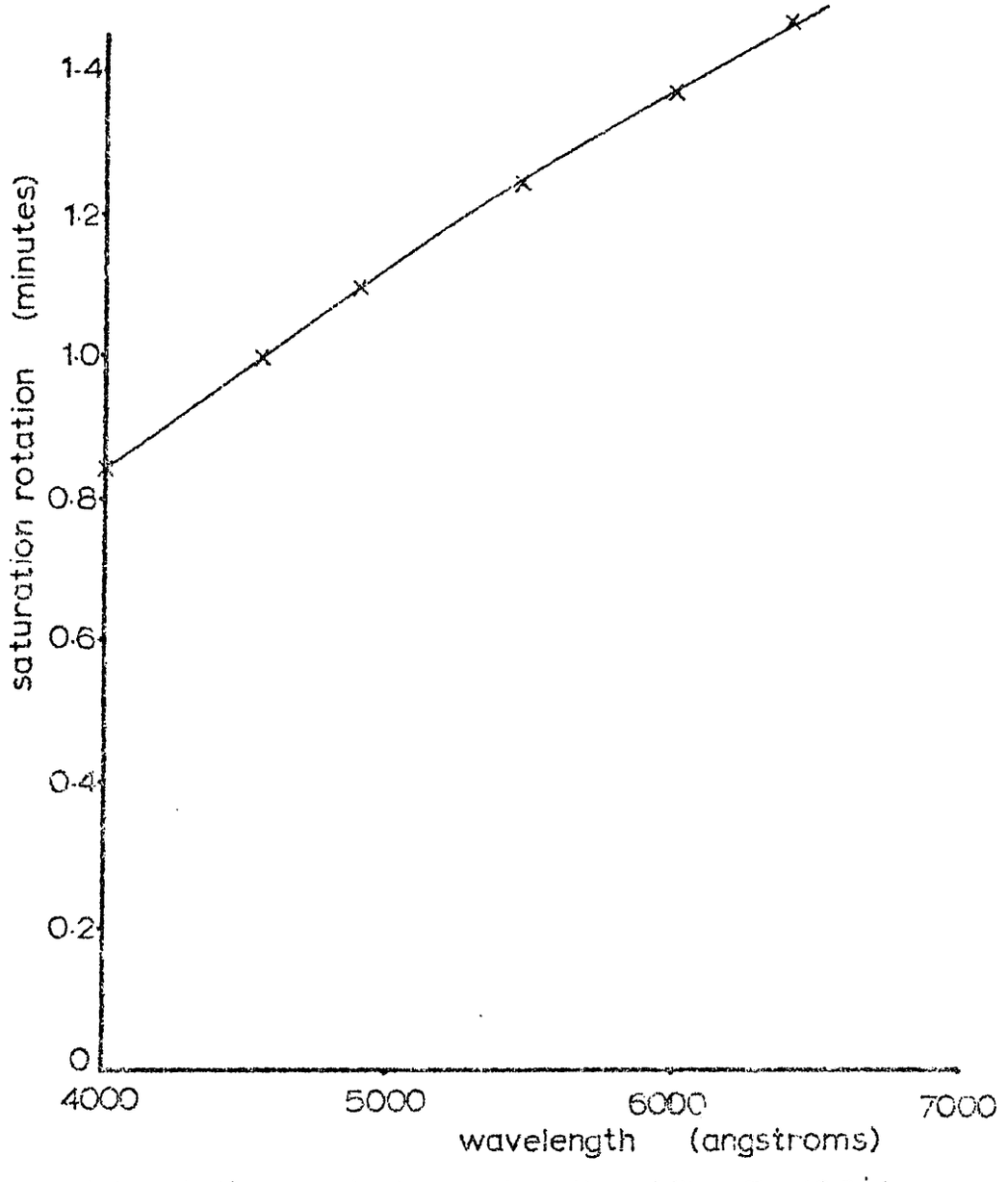

Voigt rotation against wavelength (film 7 480Å)

(Figure 7.24)

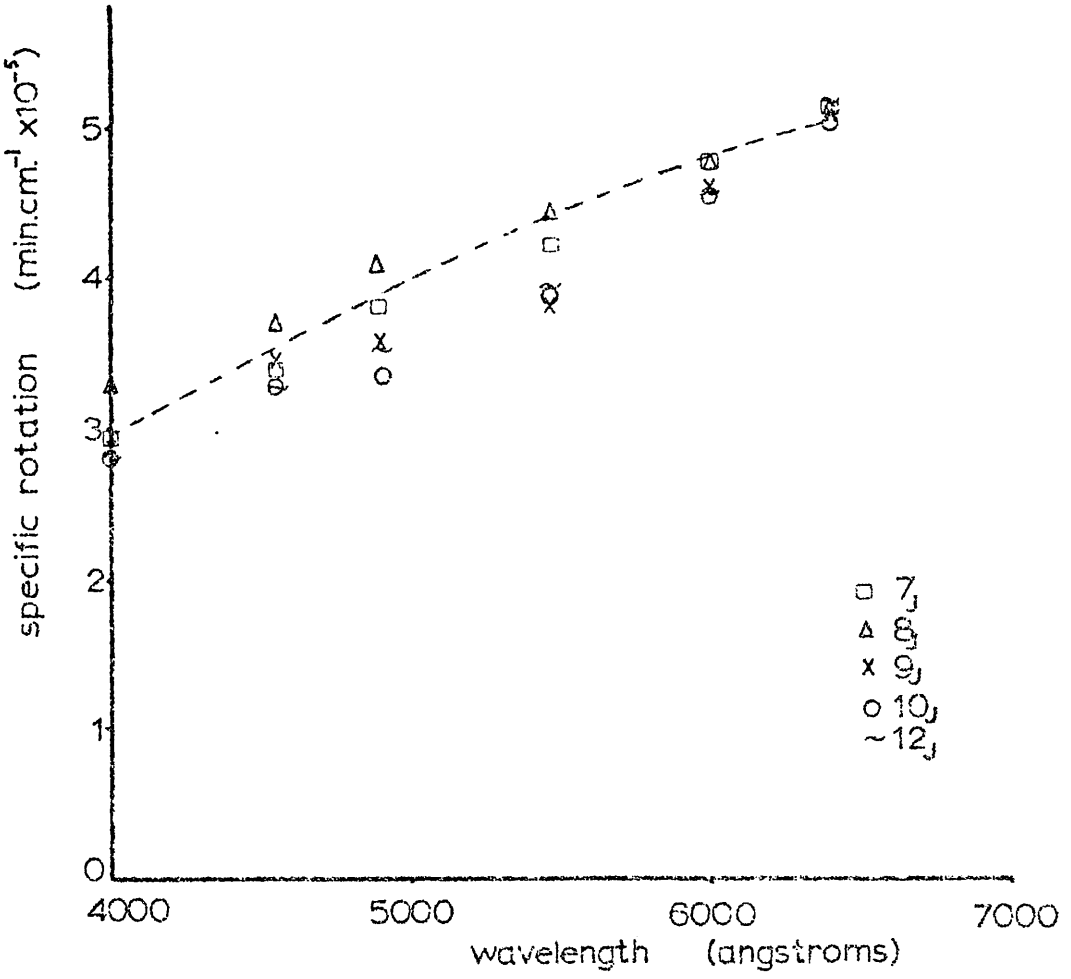

Voigt rotation against wavelength

(Figure 7.25)

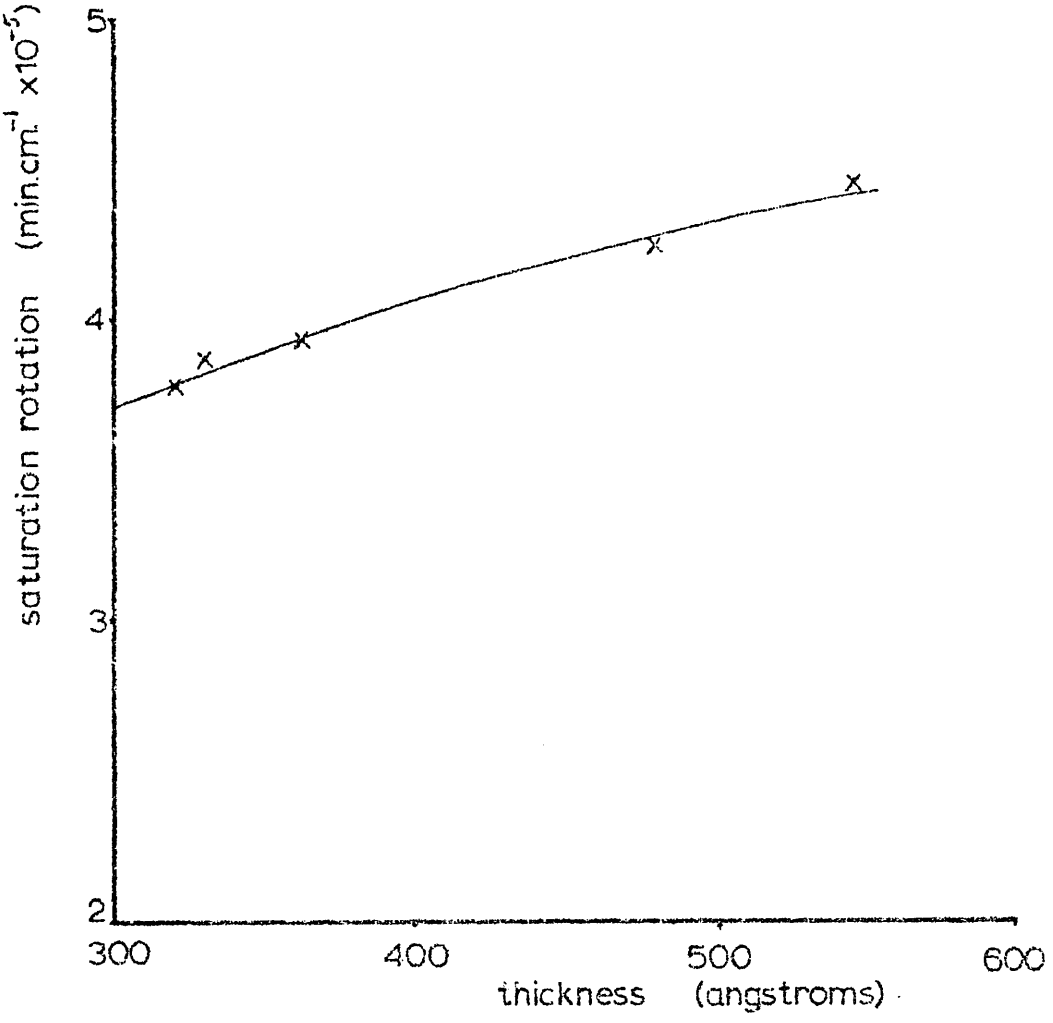

Voigt rotation against film thickness

(Figure 7.26)

7.10 Discussion on dispersion of Voigt effect

From Figure 7.22 it may be seen that the nickel films saturated at a field of about 4.5 kOe which is considerably less than the saturation field for Faraday rotation measurements (6.2 kOe), owing to the lower demagnetizing factor.

Medcalf's expression for the Voigt rotation is

$$\theta' = \tfrac{1}{2} \bar{\alpha} z_o (f_1 \sin 2\phi - f_2 \cos 2\phi)$$

In estimating the size of the effect, Medcalf put in a constant value for $\bar{\alpha}$. However, this quantity varies with wavelength, since

$$\bar{\alpha} = \mathcal{R} (n_+ - n_-)$$

where $n_\pm$ are the refractive indices for elliptically polarized light, the positive sign being associated with a clockwise rotation of the E-vector, as seen by an observer looking in the direction of propagation of the wave. The Voigt rotation should, in fact, increase with increasing wavelength. This is confirmed by the experimental results, shown in Figures 7.24 and 7.25, in the spectral region investigated in this work.

Medcalf estimated the size of the Voigt effect in the optical and ultra-violet regions. He calculated a value of 5000° cm^{-1} for

the Voigt rotation in nickel. Over the wavelength region covered in this work the value of the Voigt rotation for the given configuration varied between 3000^{o} cm^{-1} and 5000^{o} cm^{-1} which compares well with Medcalf's order of magnitude estimate.

The experimental results obtained for the Voigt rotation therefore appear to confirm Medcalf's theory in the frequency range investigated. They also confirm that the maximum and zero values of rotation occur at the predicted azimuthal angles.

7.11 The Voigt effect in zero applied magnetic field

At first sight, it would appear that the Faraday rotations θ_+ and θ_- should be equal, i.e. the quantity $(\theta_+ - \theta_-)$ should be zero. Figures 7.27 and 7.28 show that this is not the case so far as the measured values are concerned, and that the magnitude of $(\theta_+ - \theta_-)$ varies with ϕ, the incident polarization azimuth. This apparent discrepancy can be at least partly explained by considering the effect on the measured values of θ_+ and θ_-, of the Voigt rotation, in zero applied field, caused by the intrinsic magnetization in the plane of the specimen.

The magnetization M of a (110) nickel film generally lies along the <110> direction, midway between the two <111> type directions, in the plane of the film (Figure 7.29). There will be

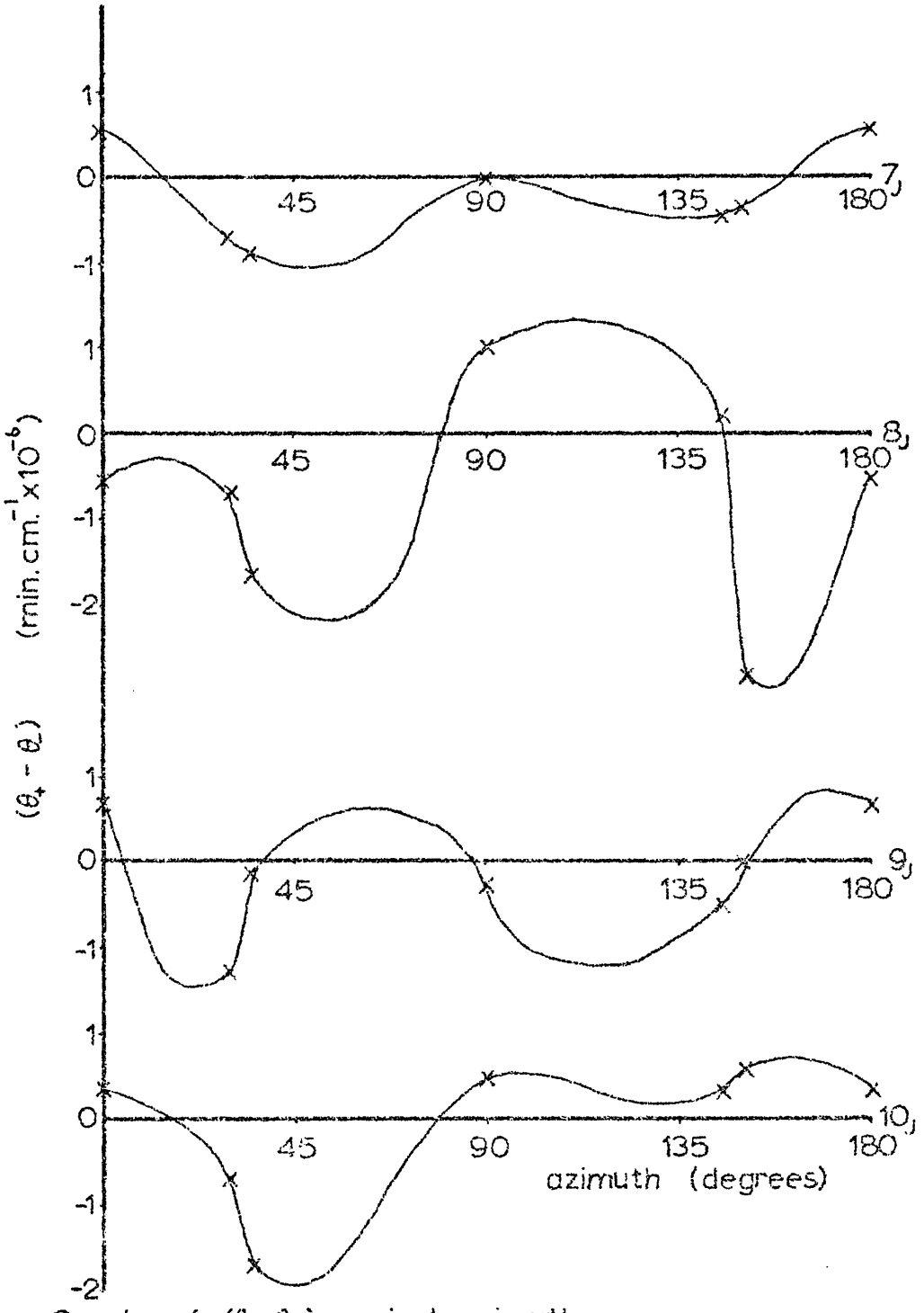

Graphs of $(\theta_+ - \theta_-)$ against azimuth

(Figure 7.27)

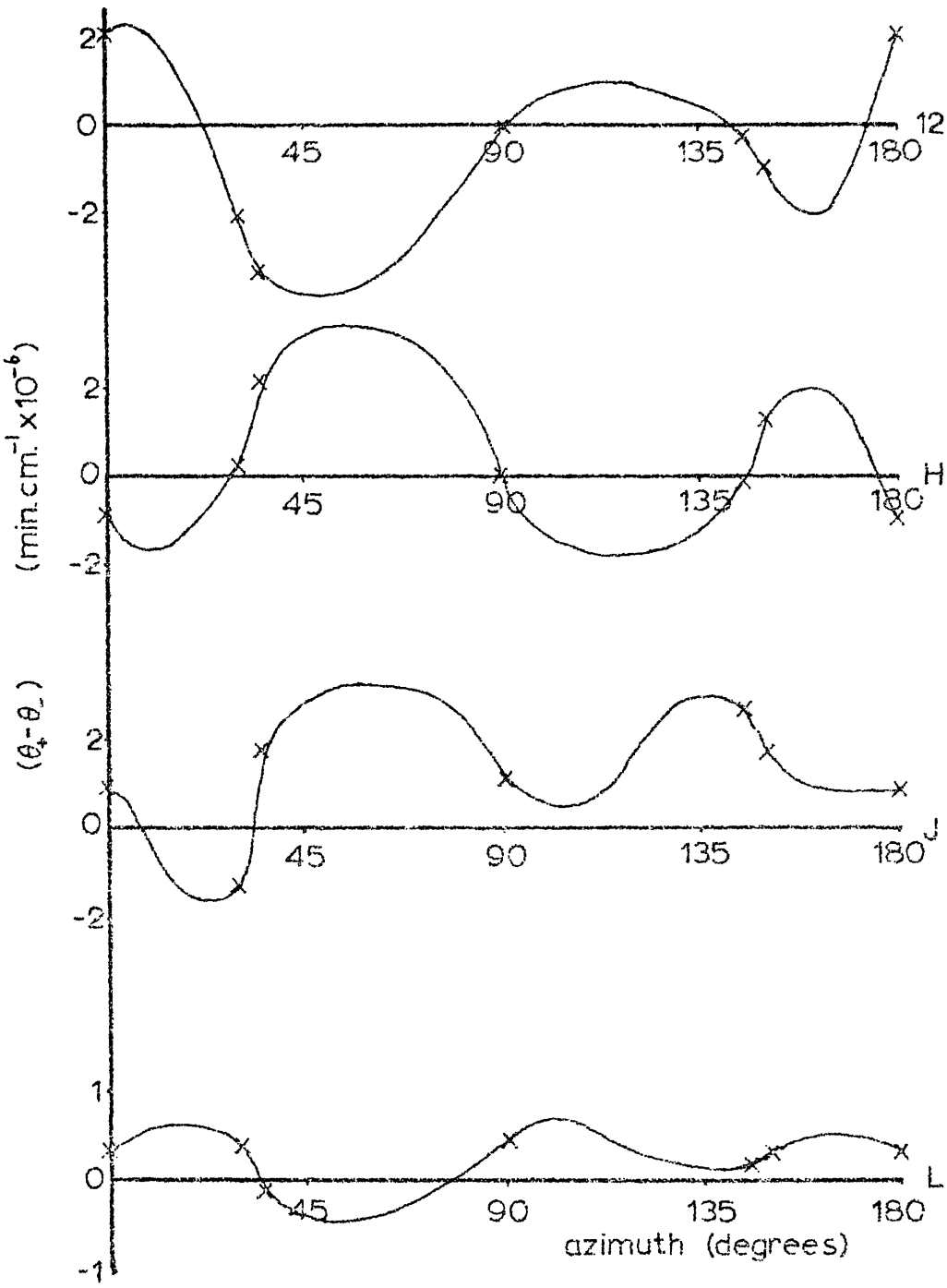

Graphs of (θ_+-θ_-) against azimuth

(Figure 7.28)

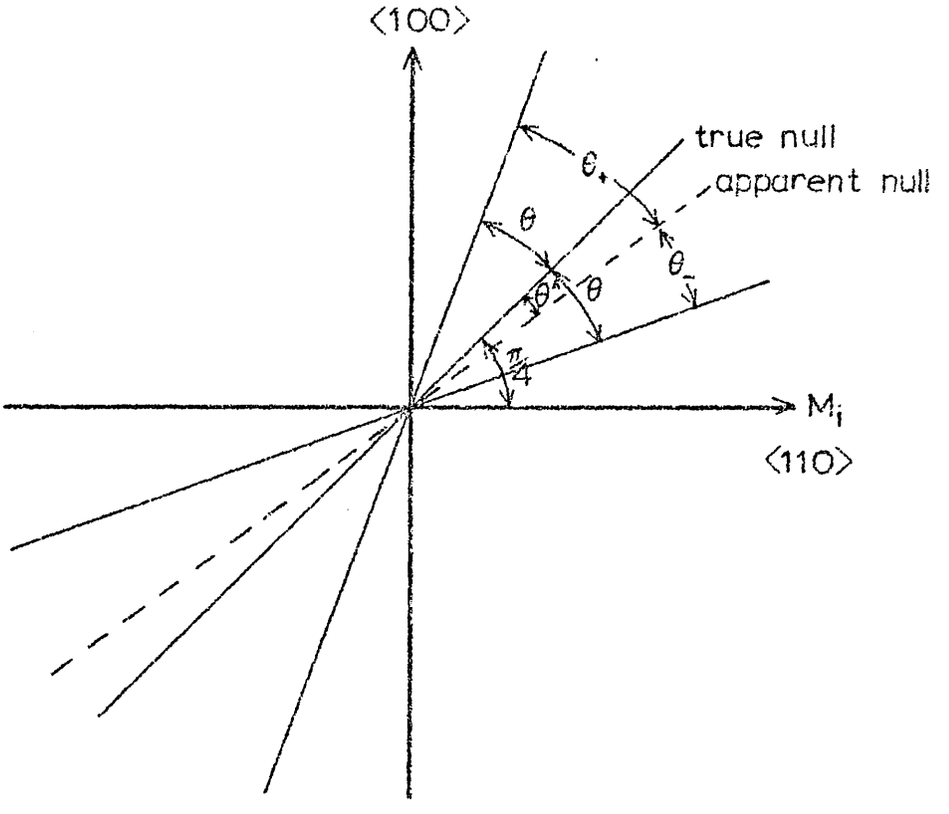

$$(\theta_+ - \theta_-) = 2\theta'$$

(Figure 7.29)

some dispersion, due to defects, strains, etc., and in some cases, a particular <111> direction may be adopted, but in general the magnetization lies along <110> .

Consider such a specimen in the Faraday rotation polarimeter. If the instrument is set to zero, with zero applied magnetic field, and the incident polarization at a 45° azimuth to the <110> direction, then a Voigt rotation θ' will be produced, causing the null position to be offset by θ' . When the saturation magnetic field is applied in the forward direction normal to the film, M rotates until parallel to the field (and propagation) direction and the Voigt effect falls to zero. The recorded rotation is then $\theta_+ = \theta + \theta'$, θ being the true Faraday rotation in the forward direction. When the field is switched off, M reverts to the original <110> direction, and the apparent zero is restored. When the applied field is reversed, the recorded rotation is $\theta_- = \theta - \theta'$. by a similar sequence of events. The quantity

$$\theta_+ - \theta_- = 2\theta'$$

i.e. twice the Voigt rotation in the specimen due to the intrinsic magnetization.

The case described above will give the maximum Voigt rotation (i.e. at 45° to <110>); for other incident orientations (or orientations of M) a smaller effect will be observed. In order to

check the foregoing reasoning, values of $(\theta_+ - \theta_-)$ from all the saturation Faraday rotation measurements were averaged, and plotted for the azimuths employed. The results were compared with Voigt measurements for different orientations (Figure 7.30) and the points shown to fit remarkably well with the expected trend of the graph, considering the disturbing effects of strain, dispersion, etc., which are likely to be present.

7.12 Final conclusions

The results for Faraday rotation in quartz are seen to agree well with existing measurements over the visible and near ultra-violet region of the spectrum.

The measurements of Faraday rotation, in monocrystalline nickel, as a function of applied field and thickness, agreed well with the previous results of Miller on single crystal films. The wavelength dispersion of the Faraday rotation in nickel has been measured more precisely, and over a wider range than previously. Moreover, these measurements have been taken on monocrystalline films of known structure, in contrast to earlier work on polycrystalline specimens. The numerical values of specific rotation in single crystal specimens lie roughly in the middle of the polycrystalline results, and confirm the general shape of the dispersion curves in the region where previous methods are available.

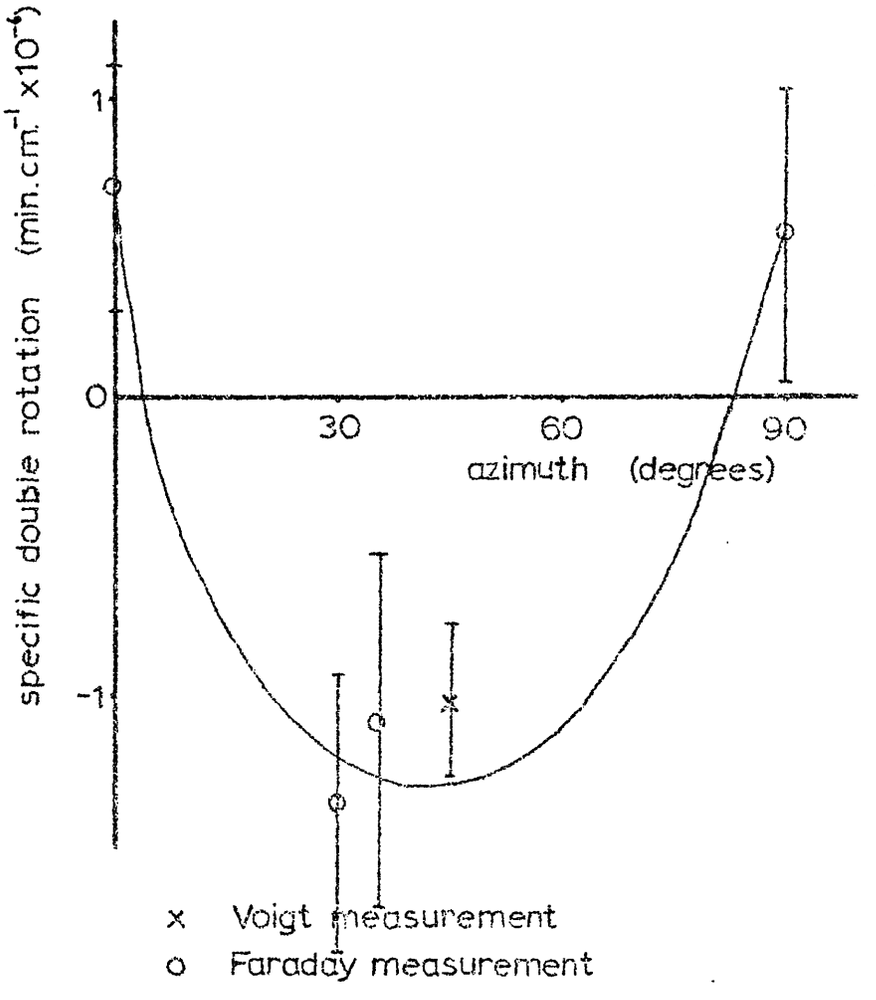
specific double rotation (min.cm^{-1} x10^{-4})
1
0
-1
30
60
90
azimuth (degrees)
x Voigt measurement
o Faraday measurement

(Figure 7.30)

Another feature of the dispersion results is the precise location of a maximum at 9200 Å of which earlier indications had been given from polycrystalline film data.

A third principal result is the observation, for the first time, of the change in sign of the rotation in nickel about 3000 Å, which had been predicted in the theoretical work associated with this subject. The dispersion measurements therefore extend previous experimental work and provide confirmation of existing theory.

The results of the anisotropic variations in Faraday rotation are rather more difficult to characterize and explain, as there is no record of this type of experimental work on ferromagnetics for comparison, and only very tentative theoretical approaches have been made to date. An attempt has been made to investigate a possible correlation with one of the variables, crystallographic twinning, which occurs in the specimens, and although the eye of faith might discern some tentative evidence for such a link, the possible mechanisms involved are not clearly ascertainable.

The final group of experimental results which were presented are those concerning the measurement of the Voigt rotation in nickel. There is no previous experimental work on the Voigt effect in feromagnetics, so no comparison may be drawn with earlier results. Such theoretical work as exists appears to be confirmed by the experimental results presented in this thesis.

7.13 Suggestions for further work

It would seem that there is a great deal of work still to be done in magneto-optical measurements on ferromagnetic materials. With the advent of better techniques for preparing monocrystalline specimens and improvements in methods of structure analysis, a more precise knowledge of the state of the material being used may be gained. More accurate polarimetry is desirable, also, in view of the small magnitude of some of the effects involved, especially the Voigt effect.

Although considerable difficulties face the theoreticians in this field, more realistic theoretical models are required, especially involving the defects in specimens, e.g. twinning, since the experimentalist must make his measurements on real, i.e. non-ideal, systems.

References

Ah-Sam L. E. G. and Jones M. C. (1970) Phys. Rev. B, 1, 3896.

Argyres P. N. (1955) Phys. Rev., 97, 334.

Becquerel A. H. (1879) C.R. Acad. Sci., Paris, 88, 334.

Bozorth R. M. (1951) Ferromagnetism (New York: Van Nostrand).

Brace D. B. (1901) Phil. Mag., 1, 464.

Breuer W. and Jaumann J. (1963) Zeit. für Physik, 173, (1) 117.

Cau M. (1929) Ann. Phys., 10, 354.

Clemens K. H. and Jaumann J. (1963) Zeit. für Physik, 173 (1) 135.

Coren R. L. and Francombe M. H. (1964) Journal de Phys., 25, 233.

Darwin C. G. (1935) Proc. Roy. Soc., A, 151, 512.

Donovan B. and Medcalf T. (1964) Brit. J. Appl. Phys., 15, 1139.

Drude P. (1912) Optik, (Leipzig), 407.

Du Bois H. (1887) Wied. Ann., 31, 941.

Faraday M. (1846) Phil. Trans., Part 1.

Fresnel A. J. (1825) Ann. de Chim., 28, 147.

Hall E. H. (1881) Phil. Mag., 12, 171.

Harris W. D. (1907) Phys. Rev., 24, 337.

Heavens O. S. (1955) Optical Properties of Thin Solid Films (Butterworths, London), 96.

Heavens O. S. (1959) Lab. Practice, 8, 203.

Heavens O. S., Brown M. M. and Hinton V. (1959) Vacuum, 1, 17.

Heavens O. S. and Miller R. F. (1962) Proc. Roy. Soc., A, 266, 547.

Heavens O. S. Miller R. F., Moss G. L. and Anderson J. C. (1961) Proc. Phys. Soc. 78, 33.

Heisenberg W. (1928) Zeit. Physik, 49, 619.

Hellenthal W. (1959) Zeit. für Physik, 156, 573.

Hirsch E. H. (1893) Ann. Phys., 48, 456.

Hirsch P. B., Horne R. W. and Whelan M. J. (1956) Phil. Mag., 1, 677.

Hirsch P. B., Howie A. and Whelan M. J. (1960) Phil. Trans., A, 252, 499.

Holmes J. R., Rosen A and McLung F. (1958) 5th Nat. Symp. on Vac. Tech. Trans., 76.

Hulme H. R. (1932) Proc. Roy. Soc., A, 135, 237.

Ingersoll L. R. (1909) Phil. Mag., 18, 74.

Ingersoll L. R. (1924) J.O.S.A., 8, 493.

Ingersoll L. R. (1953) Rev. Sci. Instrum., 24, 23.

Jones M. C. (1971) private communication.

Kittel C. (1951) Phys. Rev., 83, 208 (Abstract).

König H. (1946) Naturwiss, 3, 71.

König H. (1948) Optik, 3, 101.

Krinchik G. S. and Nuralieva R. D. (1959) J.E.T.P., 36, 724.

Kundt A. (1884) Phil. Mag., 18, 308.

Kundt A. and Röntgen W. K. (1879) Wied. Ann., 6, 332.

Lobach W. (1890) Wied. Ann., 39, 347.

Medcalf T. (1965) Ph.D. Thesis (London University).

Miller R. F. (1962) Ph.D. Thesis (London University).

Miller R. F. (1965) Brit. J. Appl. Phys. 16, 1353.

Poritsky H. (1926) J.O.S.A., 12, 458.

Righi A. (1878) Nuovo Cim., 3.

Rudolph H. (1955) J.O.S.A., 45, 50.

Schütz W. (1936) Handbuch der Experimentalphysik, 16.

Sivaramakrishnan V. (1956) Proc. Ind. Acad. Sci., 44A, 206.

Skinner C. A. and Tool A. Q. (1907) Ann. Phys. Soc. Chicago.

Skinner C. A. and Tool A. Q. (1908) Phil. Mag., 16, 833.

Slater J. C. (1936) Phys. Rev., 49, 537, 931.

Smith D. O. (1964) Proc. Int. Conf. Mag. (Nottingham) 854.

Stoner E. C. (1926) Magnetism and Atomic Structure (Methuen, London).

Strong J.(1938) Modern Physical Laboratory Practice, Chapter 2 (Blackie, London).

Tolansky S. (1948a) Multiple Beam Interferometry (Oxford University Press), p.147.

Tolansky S. (1948b) Multiple Beam Interferometry (Oxford University Press), p.21.

Verdet M. E. (1854) Ann. de Chim. Phys., 41, 370.

Voigt W. (1908) Magneto-und Electro-optik (Teubner, Leipzig) 289.

Wannier G. H. (1947) Phys. Rev., 72, 304.